CHALMERS
UNIVERSITY OF TECHNOLOGY

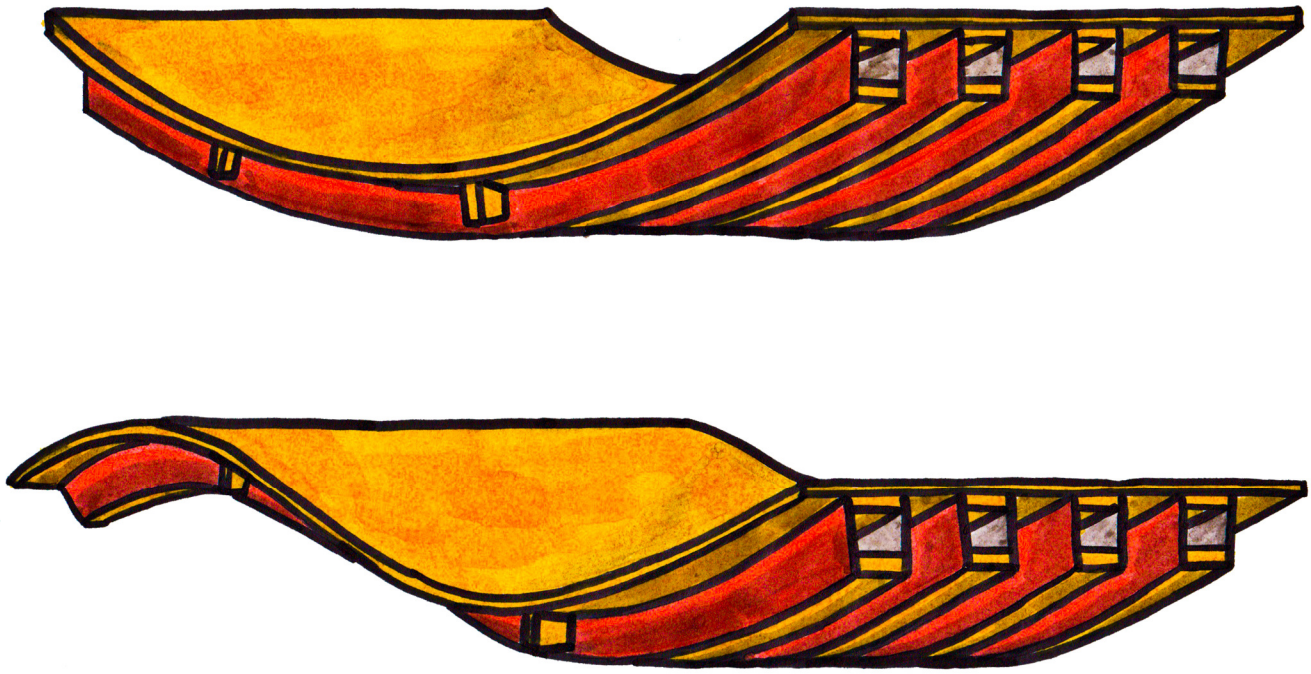

Dynamic response of timber floors – criteria, performance and design for acceptability

Master's Thesis in the Master's Programme Structural Engineering and Building Technology

Jakob Brandin
Andreas Oscarsson

Department of Civil and Environmental Engineering
Division of Structural Engineering
Steel and Timber Structures
CHALMERS UNIVERSITY OF TECHNOLOGY
Gothenburg, Sweden, 2015
Master's Thesis 2015:134

MASTER'S THESIS 2015:134

Dynamic response of timber floors –

criteria, performance and design for acceptability

Master's Thesis in the Master's Programme Structural Engineering and Building Technology

Jakob Brandin

Andreas Oscarsson

Department of Civil and Environmental Engineering
Division of Structural Engineering
Steel and Timber Structures
CHALMERS UNIVERSITY OF TECHNOLOGY
Göteborg, Sweden, 2015

Dynamic response of timber floors –
criteria, performance and design for acceptability

Master's Thesis in the Master's Programme Structural Engineering and Building Technology

Jakob Brandin

Andreas Oscarsson

Examensarbete 2015:134/ Institutionen för bygg- och miljöteknik,
Chalmers tekniska högskola 2015

Department of Civil and Environmental Engineering
Division of Structural Engineering
Steel and Timber Structures
Chalmers University of Technology
SE-412 96 Göteborg
Sweden
Telephone: + 46 (0)31-772 1000

Department of Civil and Environmental Engineering, Göteborg, Sweden, 2015

Dynamic response of timber floors –

criteria, performance and design for acceptability

Master's thesis in the Master's Programme Structural Engineering and Building Technology

Jakob Brandin
Andreas Oscarsson
Department of Civil and Environmental Engineering
Division of Structural Engineering
Steel and Timber Structures
Chalmers University of Technology

ABSTRACT

Traditionally, timber has been one of the leading building materials for single-family houses in Sweden. Today the use of timber in multi-family houses is increasing and there is a need to develop better performing timber floors in order to increase the comfort of the residents.

The purpose of this project is to design and evaluate promising concepts for a timber floor structure that are well performing with regard to the vibration response.

In the first part new design criteria, based on research from the last fifteen years, were formulated. It was found that the parameters traditionally used; the deflection due to a 1kN point load and the first eigenfrequency, are still relevant. However, a new relationship between those two was introduced.

The evaluation of a benchmark floor showed that, even though fulfilling the criteria of Eurocode 5, it failed to be accepted by the new design criteria. A full-scale experiment showed that both analytical and numerical calculations overestimate the stiffness of this benchmark floor. The fault was probably due to the slip in the connections between parts. A parametric study of the benchmark floor showed that, with small alterations, an acceptable dynamic behaviour could be achieved.

New timber floor concepts were generated comprising both one-way and two-way action alternatives. The process resulted in some promising concepts, one of which was evaluated further. This concept, called "fat beam", has a very material-effective cross-section that enables the use of low-quality material where it is possible and high-quality material where it is crucial. In addition, it has an open cross-section with good accessibility for installations and very good possibilities to make holes in the web, used for example to insert a strongback.

Key words: timber floor, design criteria, first eigenfrequency, design process, two-way action, EMA

Dynamisk respons i träbjälklag –
kriterier och design för ett acceptabelt verkningssätt

Examensarbete inom masterprogrammet Structural Engineering and Building Technology

Jakob Brandin
Andreas Oscarsson
Institutionen för bygg- och miljöteknik
Avdelningen för Konstruktionsteknik
Stål- och träkonstruktioner
Chalmers tekniska högskola

SAMMANFATTNING

Trä har traditionellt sett varit ett av de främsta byggmaterialen för enfamiljshus i Sverige. Idag ökar användandet av trä i flerfamiljshus och det finns ett behov av att utveckla bättre presterande träbjälklag för att tillfredsställa de boendes krav på ökad komfort.

Syftet med detta projek är att designa och utvärdera koncept för träbjälklag som anses lovande med avseende på dynamisk respons.

Ett nytt kriterium för bedömning av träbjälklag, baserat på de senaste årens forskning inom subjektiv upplevelse av vibrationer i träbjälklag, formulerades. Det visade sig att de parametrar som traditionellt sett använts för bedömning fortfarande är relevanta; nedböjningen vid 1 kN punktlast och den första egenfrekvensen. En ny relation mellan dessa etablerades.

Utvärderingen av ett referensbjälklag visade att även om detta uppfyllde de krav som ställs av Eurocode 5, med avseende på vibrationer, så lyckades det inte uppfylla kraven enligt det nya bedömningskriteriet. Ett experiment i fullskala visade att både analytiska och numeriska beräkningar överskattade styvheten i referensbjälklaget. Detta beror antagligen på en överskattad samverkan mellan bjälklagets delar. En parameterstudie visade att med små förändringar så kunde en acceptabel dynamisk respons uppnås.

Nya koncept för träbjälklag, med både en- och tvåvägsbärnings alternativ, genererades. Detta resulterade i några lovande koncept varav ett utvärderades ytterligare. Detta koncept, kallat fat-beam, har ett väldigt materialeffektivt tvärsnitt som utnyttjar lågkvalitativt material där det går och högkvalitativt material där det behövs. Dessutom har det god tillgänglighet för installationer och möjlighet för håltagning i livet som kan användas för kontinuerliga tvärbalkar och installationer.

Nyckelord: träbjälklag, dimensioneringskriterier, första egenfrekvensen, design process, tvåvägsbärning, EMA

Contents

Preface

After nine semesters of theoretical studies time had finally come for us to use our knowledge to produce a master's thesis. As the final semester approached we found each other and our shared interest for timber structures. Being able to build structures with a grown material is just incredible.

There exists plenty of interesting research areas to address within timber structures so to find a specific appealing problem was as challenging as attempting to find a solution to it. The work began in January 2015 and was finished in June the same year at the office of Ramböll and at the Division of Structural Engineering at Chalmers University of Technology, both situated in Gothenburg. We hope that the findings in this master's thesis can contribute to building multi-family timber houses of even better quality than today.

Plenty of people have been important to be able to complete this master's thesis, and we would like to use this opportunity to thank some of them. Apart from the authors who´s works we refer to in the thesis, we would like to thank our examiner Robert Kliger, for his inspiration and for all interesting discussions about everything under the sun. Next, we would like to thank our supervisors, Niklas Johansson at Ramböll, who has given us valuable advice throughout the process, and Tobias Persson at A-hus, without whom it would have been impossible to get the full-scale experiment to work.

We would also like to thank Anders T. Johansson, assistant professor at Chalmers University of Technology, for teaching us how to perform experimental modal analyses as well as assisting us with our full-scale experiment. And finally we would like to thank our opponents and friends Altaf Ashraf and Waleed Hasan.

Göteborg, August 2015

Notations

Roman upper case letters

C_{ij}	System transfer function between input DOF j and response DOF i
C	Compliance (m/N)
B	Span width (m)
$(EI)_B$	Flexural rigidity in transversal direction (Nm^2/m)
$(EI)_L$	Flexural rigidity in longitudinal direction (Nm^2/m)
$(EI)_L/m$	Flexural rigidity per surface-area mass in longitudinal direction (Nm^4/mkg)
L	Span length (m)
X_j	System input at DOF j
Y_j	System response at DOF i

Roman lower case letters

a_{rms}	Root mean square acceleration due to a 1 Ns impulse (m/s^2)
a_{peak}	Peak acceleration due to a 1 Ns impulse (m/s^2)
c	Damping (Ns/m)
c_{cr}	Critical damping (Ns/m)
f	Frequency (Hz)
f_1	First eigenfrequency (Hz)
f_n	Eigenfrequency or Natural frequency (Hz)
h	Cross-section height (mm)
h'	Impulse velocity response (m/s)
h'_{max}	Unit impulse velocity response (m/s)
k_{amp}	Shear deformation amplification factor
k_{dist}	Distribution factor
k_{strut}	Transversal stiffness factor
m	Mass per surface area (kg/m^2)
s	Joist spacing (mm)
t	Cross-section thickness (mm)
v'	Fictitious velocity (m/s)
v'_0	Fictitious initial velocity (m/s)
v	Unit impulse velocity response (m/s)
v'_{max}	Maximum unit impulse velocity response (m/s)
v'_{rms}	Root mean square unit velocity response (m/s)
w_{1kN}	Deflection under a 1 kN point load (mm)

Greek letters

ω	Angular frequency (rad/s)
ω_n	Natural angular frequency (rad/s)
σ_0	Damping coefficient (Hz)
ζ	Damping ratio (%)

Syllabus

CLT	Cross laminated timber
High-frequency floor	A floor structure with its first eigenfrequency above 8 Hz
Low frequency noise	Noise with frequency range 10-200 Hz
Low frequency vibration	Vibration in the range 0-8 Hz
Light-weight floor	If added mass and damping from a human body significantly change the modal properties of a floor it will be considered as a light-weight floor
LVL	Laminated veneer lumber
RMS	Root mean square
Strongback	A continuous transversal beam used to connect longitudinal joists. Used to introduce transversal stiffness without making the cross-section deeper or decreasing longitudinal stiffness.

1 Introduction

Timber is a promising building material in many ways. It has a high strength-to-weight ratio and it possesses some environmental benefits, among other being a carbon dioxide trap during the service life of the building. As the need for our society to take a new direction towards a sustainable development more and more initiatives are taken to introduce timber as a potential building material for multi-story buildings.

1.1 Background

Historically timber has been one of the primary building materials in Sweden, but as fires occasionally spread within the densely populated areas during the 19th century the use of timber in buildings higher than two stories was banned. It would take just until 1994 till this ban was eventually revoked. Due to this timber has mainly been used for single-family houses during the 20th century.

After 1994 the use of timber for multi-family houses has been increasing. The user experience has however not always been fully satisfying. Particularly timber floors in multi-family houses are very susceptible to annoying vibration caused by human activities. This is due to the low mass and relatively low stiffness of timber, compared to for example concrete. The vibration response is also dependent on the damping properties of the structure. It has been shown that damping is a key factor for the human perception of the vibration response, and thus annoyance (Lenzen 1966).

Due to the susceptibility to annoying vibrations a well performing timber floor requires a larger construction height than a comparable concrete floor, for example a standard hollow-core concrete slab. Especially if a longer distance, like that of an office building, is to be spanned. The construction height is important since regulations of the municipality limit the height of new buildings, not the number of stories. Thus, sometimes concrete and/or steel buildings can be built with more stories than timber buildings on the same site. If the construction height of timber floors could be reduced then the number of stories could potentially be increased according to regulations making timber houses further competitive.

The attitude towards timber amongst developers is still somewhat mild as concrete is seen as a more durable and robust choice. In order to change this attitude and promote a further use of timber as a construction material the floor systems has to be further developed. This is also important if timber should be able to gain market shares among commercial buildings.

The European building regulations for timber structures, Eurocode 5, provide some guidelines for how to design timber floors to give a sufficiently good experience for the users. However, these threshold values do not always manage to single out problematic floors (Negreira et al. 2015). Ongoing research is trying to relate the subjective and individual human experience to vibrations with some possible measurable values. This is very important in order to be able to design a floor that is not only acceptable according to Eurocode 5 but in relation subjective rating to modern timber floors.

1.2 Principle objective

The principal objective of this project is to design and evaluate promising concepts for timber floor structures that are well performing with regard to the dynamic response. The project will result in one or several promising concepts than can be worth further developing. Furthermore, the report will in itself be an example of a design process for achieving such concepts.

1.3 Aims

To fulfil the principal objective a literature study with aim to investigate the perception of vibration response in floors is conducted. This is done in order to find design guidelines that better match the subjective rating of modern timber floors than the guidelines available in Eurocode 5.

An existing solution for a timber floor, a benchmark floor, will be evaluated in a full-scale experiment considering the dynamic parameters of interest in order to understand how a modern timber floor performs regarding vibration response.

Furthermore, improvements to this benchmark floor will be tested aiming to improve the performance of the benchmark floor as well as the knowledge of how to design such a product.

Finally new concepts will be generated aiming to find concepts that could be further developed to a well performing solution of a timber floor.

1.4 Limitations

The project focuses on high frequency floor structures, meaning that footfall loading can be regarded by a transient approach instead of steady state. The scope of the project does not include synchronised loading from many people like loading on the floor of a gymnasium during an aerobics session. Instead the conclusions are applicable to residential buildings and office buildings.

The acoustic performance, which is very important, especially regarding low-frequency noise, is not considered in this project.

Only technical aspects will be considered, economic aspects will be disregarded.

1.5 Method

The method used is based on gaining knowledge and experience along the project that can be used when generating new concepts. It can basically be summed up in the following steps:

1. Define evaluation criteria
2. Evaluate the benchmark timber floor
3. Compare the benchmark floor to other products
4. Improve the benchmark floor

5. Generate new concepts
6. Evaluate one or more promising concepts

First of all papers of the most prominent researchers within vibrations of timber floors and in particular the human perception and subjective rating were reviewed. These researchers have all tried to correlate the subjective rating of vibration in floors to limits of certain dynamic parameters that can be used as design guidelines or criteria. The results obtained by these researchers were compiled and evaluated with the goal of finding design criteria that could be used throughout this project. The design criteria should better correlate to the subjective rating of modern timber floors than the guidelines available in Eurocode 5.

This Master´s thesis project was carried out in collaboration with A-hus who produces multi-storey timber houses, and their timber floor was evaluated as a part of the project. This timber floor is referred to as the benchmark floor. Two full-scale test specimens were produced by A-hus for the purpose of this project. These were assessed by a full-scale experiment including an experimental modal analysis (EMA) and a static deflection test, see Appendix A. The results from this full-scale experiment were compared to analytic and numerical predictions in order to understand how the prediction methods commonly used correlate to reality.

The following formulas were used to analytically evaluate timber floor concepts:

1. For a simply supported rectangular timber floor with a span length L and width B the first eigenfrequency was calculated with the following analytical formula based on Euler-Bernoulli beam theory:

$$f_1 = \frac{\pi}{2L^2}\sqrt{\frac{(EI)_L}{m}} \tag{1.1}$$

   If the floor is resting on flexible supports, i.e. a primary beam the first eigenfrequency of the whole system needs to be considered. The Southwell-Dunkerly approximation (Jacobsen & Ayre, 1958) says that a lower limit for the first eigenfrequency of the system can be calculated as

$$\frac{1}{f_1^2} = \frac{1}{f_{1,A}^2} + \frac{1}{f_{1,B}^2} + \cdots + \frac{1}{f_{1,N}^2} \tag{1.2}$$

   where $f_{1,A}$ is the first eigenfrequency of the first sub-system in the system, i.e. the primary beam, $f_{1,B}$ the second sub-system etc.

   It should be noted that Euler-Bernoulli beam theory does not take shear deformation into account. The first eigenfrequency might thus be overestimated, which means that there is a risk of accepting a floor that in reality should have been rejected. In this project the analytical formula will be used as a guiding tool. Concepts worth investigating further will be evaluated numerically.

2. The deflection at mid-span due to a 1 kN point load was investigated and reasonable criteria were proposed. For more information about how the deflection was calculated see Chapter 2.5.6.

A literature study on timber floor products available on the Swedish and European market was conducted aiming to find products that are competitive to the benchmark floor. The products of interest were evaluated using the design criteria suggested in this project. The results were compared to the benchmark floor, in order to understand how well the benchmark floor performs in relation to other products. These products were then used as an inspiration for improvements to the benchmark floor. Some improvements were formulated and evaluated using the design criteria suggested in this project.

From the experience and knowledge gained during the project new concepts were generated. This was done through some fundamental theoretical ideas and by building scale-models in an iterative fashion. The forms established were evaluated with some different materials using the design criteria.

One of the concepts was chosen for further evaluation establishing limits to span lengths and shear capacity. Finally a numerical analysis was carried out considering this concept for a case study.

2 Perception of vibration in floors

Vibrations in floors, that some people feel are annoying, another person might find barely perceptible. The subjective feeling is hard to translate to a number easy to use in the design of structures. Nonetheless, many attempts have been made to statistically determine what properties should be fulfilled for an acceptable floor. The research is not unambiguous but certain conclusions can still be drawn. The purpose of this chapter is to give an introduction to the problem of vibrations in floor structures, in particular high frequency timber floors, and to develop easy-to-use design criteria.

A very basic introduction on the subject of structural dynamics is presented in Chapter 2.1. For a more thorough guidance through the theory of structural dynamics the reader is directed to Craig Jr & Kurdila (2006) and Ewins (2000).

2.1 Basic structural dynamics of floors

When a floor is subjected to dynamic loading (i.e. a load that varies with time) it will start to vibrate. This is called a vibration response. The vibration response of a floor depends both on the load it is subjected to and the dynamic properties of the floor (i.e. stiffness, mass and damping).

A floor structure can be illustrated with a free undamped single degree of freedom (SDOF) system consisting of a mass m connected to a spring with stiffness k. The equation of motion for the system can be obtained by applying Newton's second law;

$$m\ddot{u}(t) + ku(t) = 0 \tag{2.1}$$

or

$$\ddot{u}(t) + \omega_n^2 u(t) = 0 \tag{2.2}$$

where $\omega_n = \sqrt{k/m}$ is the angular natural frequency (rad/s). The natural frequency is easily obtained as:

$$f_n = \frac{\omega_n}{2\pi} = \frac{1}{2\pi}\sqrt{\frac{k}{m}} \text{ Hz} \tag{2.3}$$

Stiffness and mass obviously plays an important role considering the natural frequency or eigenfrequency of a structure.

Furthermore, damping describes the rate of decay of the vibration response. There exist some different models for describing damping, e.g. viscous damping and hysteretic damping, see Ewins (2000). In general the damping of a structure is a dynamic property that causes an induced mechanical vibration to decline and, in the end, stop. Damping causes the mechanical vibration energy to dissipate by transforming it into for example thermal energy. Theoretically, if no damping is present in a system it could continue to vibrate forever. The damping of a structure is dependent on the material damping, design of connections and joints etc. It is very difficult to estimate, in comparison to mass and stiffness that are much more easily predicted.

The damping of a structure is, using the viscous damping model, easily described by:

$$\zeta = c/c_{cr} \tag{2.4}$$

Where c is the damping and c_{cr} the critical damping. The critical damping is the minimum level of damping that stops a system from oscillating, i.e. after an applied displacement the system returns to equilibrium without oscillation.

When considering a multiple degree of freedom (MDOF) system, there exist more than one natural frequency or eigenfrequency – one for each DOF. Each eigenfrequency is connected to a specific mode shape that describes the form of the vibration for that eigenfrequency. The physical parameters mass and stiffness of a MDOF system together with the geometry and boundary conditions define the modal properties; eigenfrequencies, mode shapes, modal mass and modal damping. Figure 2.1 shows three examples of typical mode shapes of a two-sided simply supported floor structure.

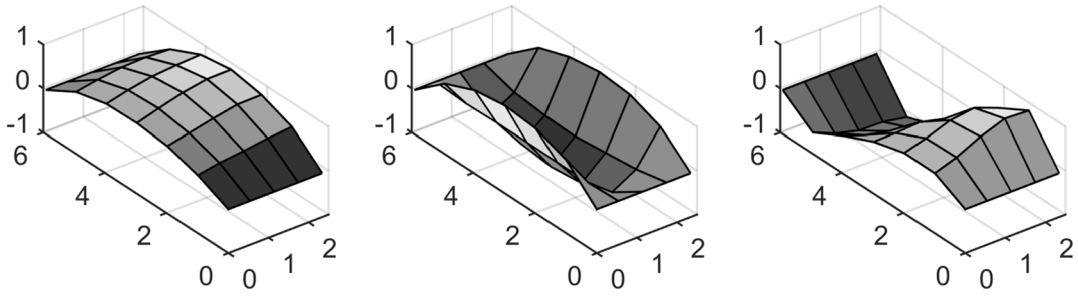

Figure 2.1 Examples of mode shapes of the timber floor structure tested in this project. From the left; the first longitudinal bending mode, the first transversal bending mode, the second longitudinal bending mode.

2.2 Human tolerance to vibrations

The human organs are very sensitive to low-frequency vibrations. Many investigations, aiming to establish measures of human sensitivity to vibrations, have been carried out and have resulted in an international standard ISO 2631:1978. The basis of this standard is an acceleration-frequency curve which defines the limit for human perception of vibrations, see Figure 2.2. The most sensitive area lies between 4 and 8 Hz which corresponds to the eigenfrequencies of some of the organs of the human body. This is recognised by Eurocode 5 as the lower limit of the first eigenfrequency for timber floors is 8 Hz.

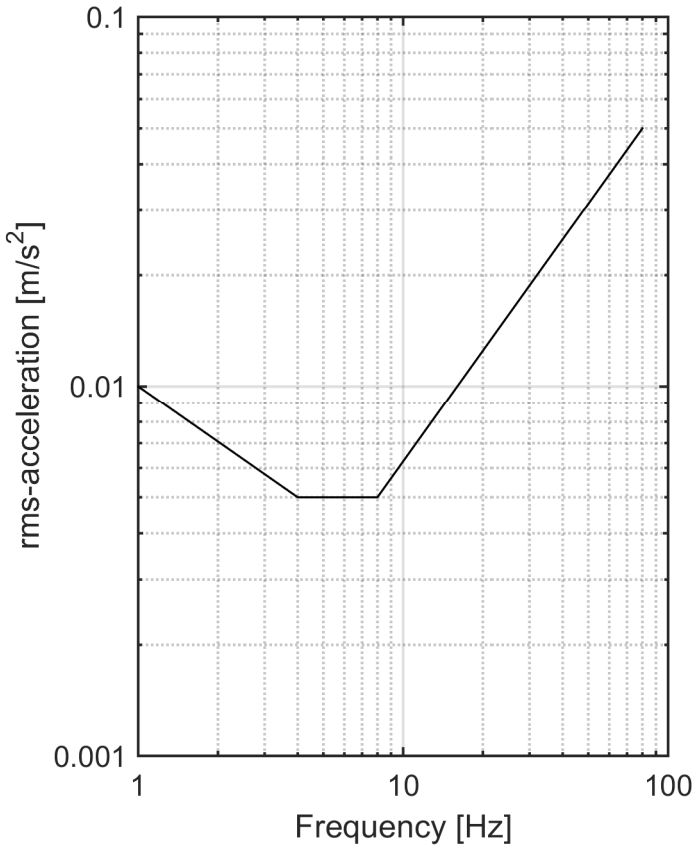

Figure 2.2 Base curve of acceleration threshold of perception for whole-body vibrations in the frequency range of 1-80 Hz, based on ISO 2631:1978.

2.3 Footfall-load causing vibration

Floor structures can be put in motion by a multiple of different types of loading, such as human activity, machinery, vehicles etc. There are basically two types of dynamic loads: continuous loading and transient loading. Continuous loading will not be treated in this project. As this project focuses on dynamic response of timber floors for residential or office use the most likely dynamic load will be caused by human activity.

The impact load of a footstep, i.e. a footfall load, can be characterised by a force-frequency function with its main components around 0-2 Hz but with essential contributions up to 40 Hz (Ohlsson 1988). An ordinary floor structure usually has at least one of its eigenfrequencies in the range 0-40 Hz. Excitation of the floor at a frequency close to its eigenfrequency might cause excessive vibration. In other words, the mobility (m/s^{2}N) of the floor around its eigenfrequencies is high. Figure 2.3 shows an example of a footfall load, a mobility function of a floor and the corresponding vibration velocity caused by the footfall load on the floor – all in the frequency domain. It is obvious that even though the components of the footfall load are minimal at around 20 Hz where the floor exhibits its first eigenfrequency the resulting vibration velocity is high.

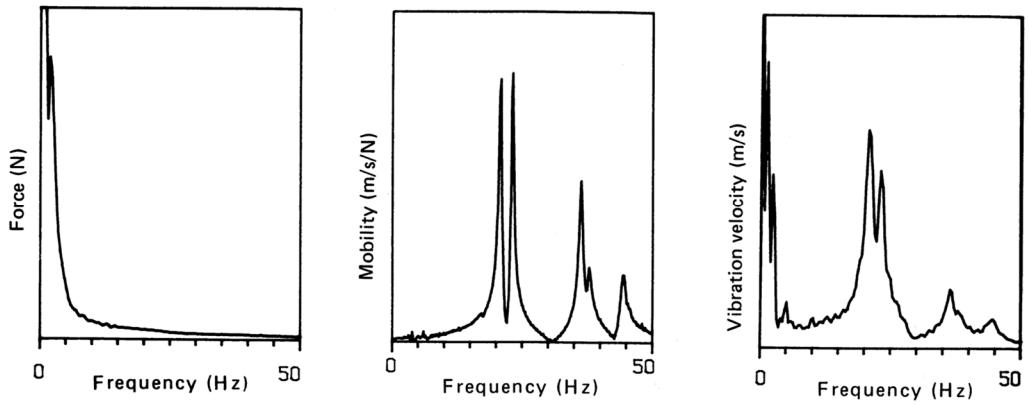

Figure 2.3 Footstep force of a walking person, mobility of the structure and the resulting vibration velocity in the frequency domain (Ohlsson 1988).

The mass of the floor plays an essential role in the amplitude of the vibration velocity response. A higher mass reduces the response to both transient and continuous loading – the floor is more difficult to set in motion. However an increase of mass causes a decrease of the first eigenfrequency that could in fact increase the vibration velocity response. In general it is favourable for a floor to have a high mass and a high stiffness-to-mass ratio. The stiffness-to-mass ratio governs the eigenfrequency according to equation (1.1).

2.4 Vibration problems in modern timber floors

The way a person experience a floor vibration can be divided into two main areas distinguishing between vibrations that are felt through the balance organs respective through sight or hearing:

1. The floor vibrations make people on the floor vibrate and they experience discomfort (Ohlsson 1988).

2. The floor vibrations cause loose things on the floor or in the ceiling to rattle, shake or swing, or make the structure squeak, which causes discomfort (Smith 2003). Also direct audible response from the footfall, a drum-like response of the floor, might feel disturbing (Bernard 2008).

In order to simplify the discussion about vibrations that are felt through the balance organs Ohlsson (1988) makes the following distinction about the source and the sensor:

1a. Springiness of a floor is the sensation of self-generated floor vibrations from a single footstep, i.e. the sensor is also the source of the vibration.

1b. Footfall induced vibrations are vibrations generated by other walking persons (sources). Such vibrations are experienced by a person (sensor) who is standing, sitting or lying on the floor.

The feeling of springiness has not been the main cause of complaints in recent studies as the laboratory tests of new timber floors show that they have a high structural rigidity and a relatively high first eigenfrequency (Bernard 2008). In addition,

springiness is connected to the vibration of the human body, which has its most critical values at low frequencies, 4-8 Hz (Jarnerö et al. 2014). This indicates that it is a larger problem at low-frequency floors, which is beyond the scope of this project.

Even though the problem of springiness is less in newer timber floors than in older, footfall induced vibrations still cause annoyance. Different types of source have an impact on how sensitive people are for footfall induced vibrations. Ohlsson (1988) takes the example of a parent sitting next to his joyfully jumping child. The parent is more tolerant for the resulting floor vibrations than a person in another room who feels the same vibrations. The time range of loading and the activity of the disturbed person are also of great importance; a person sitting still reading will experience more discomfort than someone in motion. This makes the subjective grading even more difficult.

The rate of decay of the vibrations is very important for the perception of the floor. This rate is governed by the damping of the structure that is easily expressed as a damping ratio $\zeta = c/c_{cr}$. The damping ratio of a structure depends on plenty of components such as the material, the joints in the structure, the boundary conditions, etc. and is quite difficult to predict. Ohlsson (1982) introduces the damping coefficient $\sigma_0 = \zeta f$ with the limit of $\sigma_0 \approx 0.4$ (Hz) as a way to distinguish between lightly and heavily damped vibrations, see Figure 2.4.

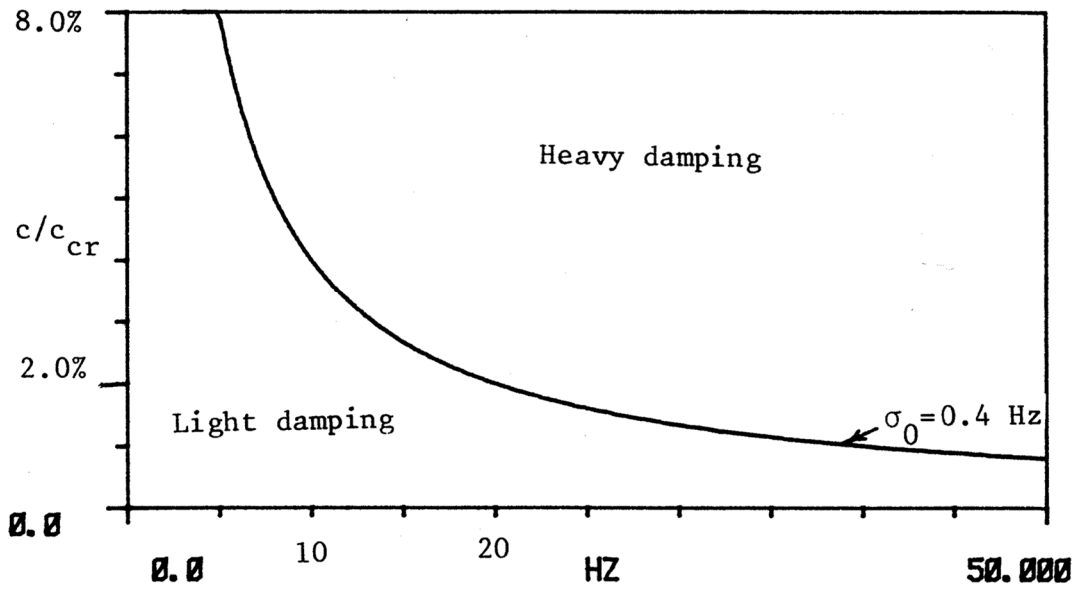

Figure 2.4 *Relation between the damping ratio c/c_{cr} and the frequency of vibration for the limit damping coefficient $\sigma_0 = 0.4$ Hz, after* (Ohlsson 1982).

From the diagram it is clear that the demands of damping on lower frequencies to be considered as heavily damped are much higher than on higher frequencies. This means that vibration frequencies below 5 Hz will almost never become heavily damped but, on the other hand, frequencies above 40 Hz will be heavily damped in most cases. A high eigenfrequency of a floor could thus be beneficial to decrease the need for damping.

Today Eurocode 5 comprises limits on several parameters regarding vibration of timber floors. The criteria were, however, derived in a time when timber floors mostly were used in single family houses and before the rise of engineered wood products like laminated veneer lumber (LVL) and cross-laminated timber (CLT). In several articles it is suggested that these new products need to be addressed with new criteria on the design for vibration serviceability (Hu et al. 2001). A survey made by the Swedish research program AkuLite has shown that people living in buildings with a light-weight structure are more annoyed by structural vibrations than residents in concrete buildings (Negreira et al. 2015). Hamm et al. (2010) has also stated that, even if the criteria of Eurocode 5 are fulfilled, there are problems with floor vibrations. Her conclusion is that the limits of Eurocode 5 are not sufficient – there is thus a need to further develop pertinent design criteria.

2.5 Historical and present design criteria

The efforts of correlating the subjective perception to numbers easily used for design guidelines have historically been focusing on several different parameters such as; first eigenfrequency, number of eigenfrequencies below 40 Hz, damping, mean acceleration, peak acceleration, velocity, and deflection under a static load.

The design of floor systems for serviceability was for a long time based on limiting the deflection under a static design load. By engineers this was believed to also limit the effects of vibrations due to human activity on the floor. Traditionally, in North America, floors have been designed using a deflection limit of L/360 of the bare joist under a uniform load of 1.914 kN/m^2 (Al-Foqaha'a 1997). Also, a minimum span-to-depth ratio has been used. The British Standard from 1984 had a value of maximum deflection, under design load, of L/333 or 14 mm, whichever smallest. The Swedish Building Code from 1980 includes two alternative criteria that can be used; either that the maximum deflection of a point load of 1 kN at mid-span should be less than 1.5 mm or that the deflection under live load only should be below L/600.

These criteria were, however, found to be insufficient to limit vibrations due to dynamic loading. Some floor structures that were designed using these criteria exhibited excessive vibrations (Ohlsson 1988), this called for a further development in both Europe and North America of design criteria during the 1980s in order to be able to design acceptable floors regarding vibrations.

2.5.1 European work and Eurocode 5

In Europe the works of Ohlsson, which are also the basis for the Eurocode 5, have been very important. Ohlsson (1982) tested floors made of steel and timber to develop design criteria. He made subjective tests both in laboratory, to which people were invited, and field studies where the resident and the test manager rated the floors. The dynamic responses of floors were also measured under transient and continuous loading. The conclusions in his doctoral dissertation are that a design criteria need to consider limits to the following parameters:

1. The weighted maximum frequency transformed compliance (m/N) of the floor.

$$|C|_{max}^{weight} = |C|_{max}(1 + \frac{n}{2}) \tag{2.5}$$

Where n is the number of other peaks larger than $1/2\ |C|_{max}$. An example can be seen in Figure 2.5.

2. The fictitious initial velocity v_0' as defined by Figure 2.6 and evaluated from the impulse velocity response $h'(t)$ for the first 0.6 s after a 100 Ns impulse. The impulse velocity response curve should be inserted into an envelope formed by the curve

$$v' = v_0' \cdot \mathrm{e}^{-2\pi\sigma_0 t} \tag{2.6}$$

where $\sigma_0 = 0.4$ Hz. This is based on the assumption that the human response is governed by the maximum peak velocity and the rate of decay of the vibration.

The first parameter above is for limiting the effect of continuous loading and the second for transient loading.

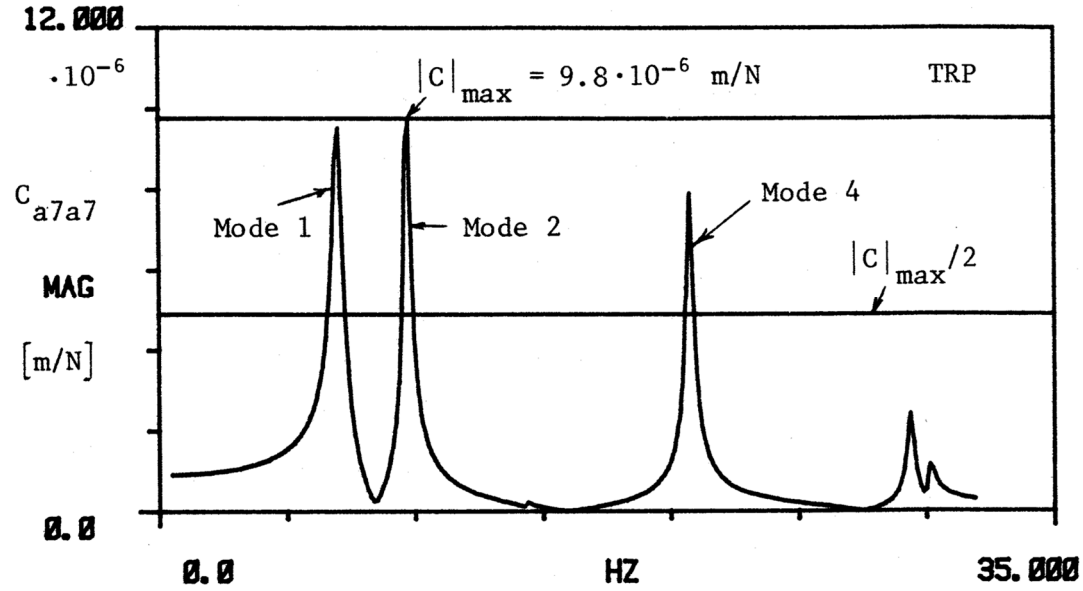

Figure 2.5 Example of a point compliance function (Ohlsson 1982).

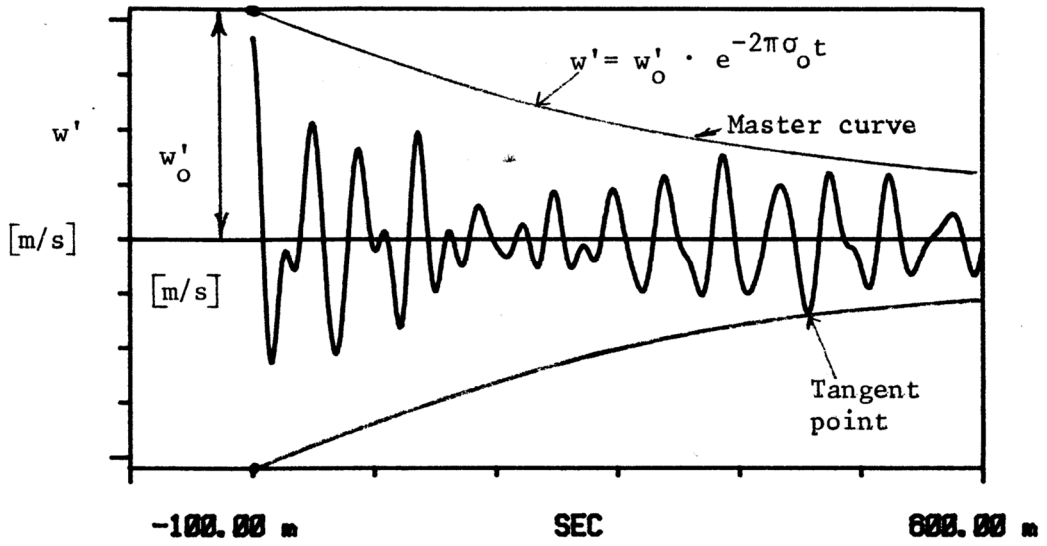

Figure 2.6 *Example of the evaluation of the fictitious initial velocity* (Ohlsson 1982).

Ohlsson also suggested that the spacing between adjacent natural frequencies should be at least 5 Hz. This suggestion is based on his belief that the presence of closely spaced vibration modes is especially annoying.

Ohlsson produced a design guide (1988) where he suggested slightly more developed criteria for design. In this guide he further developed a way of classifying the response of a floor to an impact load by using the maximum unit impulse velocity response h'_{max} and the damping coefficient σ_o, see Figure 2.7. However, regarding continuous loading the frequency transformed compliance was replaced by a limit to the RMS value of the vibration velocity v'_{RMS}. As for the impulse load, he neglected the contribution from frequencies above 40 Hz. Since the continuous loading conditions for floors would be very different depending on the use, Ohlsson did not put forth any limit value for the acceleration, but rather used his calculations to compare with existing, well-performing, floors.

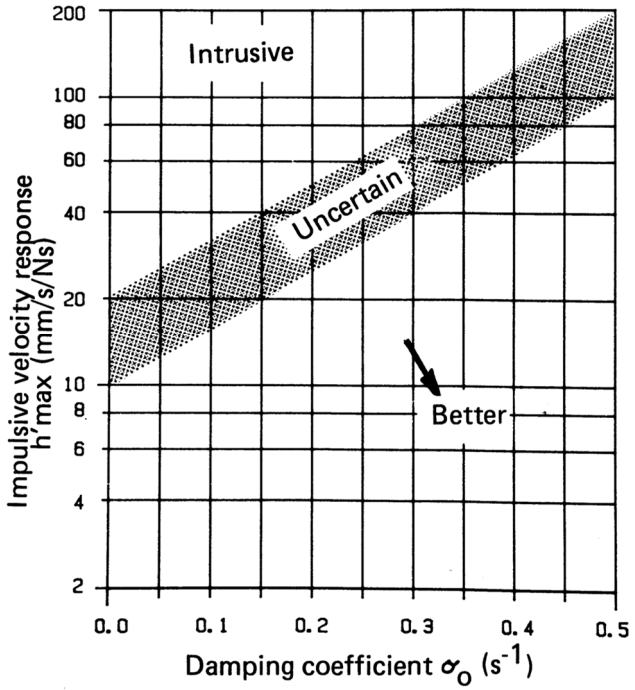

Figure 2.7 *Chart for classification of a floor subject to an impact load* (Ohlsson 1988).

He also suggested that the deflection under a 1 kN point load should be limited to 1.5 mm when the load is put on the most flexible point of the floor, as in the Swedish Building Code from 1980.

2.5.1.1 Present Eurocode 5 guidelines

Design criteria based on the maximum unit impulse velocity response h'_{max} and the 1 kN point load deflection was later adapted to Eurocode 5 while the RMS value of the vibration velocity was omitted. Today Eurocode 5, with the Swedish National Annex, considers the following limits on pertinent parameters:

1. The first eigenfrequency should be higher than 8 Hz. If not, a special investigation should be made, considering the ISO 2631 base curve.

$$f_1 > 8 \text{ Hz} \tag{2.7}$$

2. The maximum instantaneous deflection under a 1 kN point load applied at any point of the floor taking account of load distribution is limited to:

$$w_{1kN} \leq 1.5 \text{ mm} \tag{2.8}$$

3. The unit impulse velocity response, i.e. the maximum initial value of the vertical floor vibration velocity (m/s) caused by an ideal unit impulse (1 Ns) applied at any point of the floor giving maximum response (disregarding components above 40 Hz) is limited to:

$$v \leq 100^{(f_1 \zeta - 1)} \text{ m/s} \tag{2.9}$$

Where the modal damping ratio is 0.01, unless other values are proven more appropriate.

2.5.1.2 National modifications of Eurocode 5

Because of regional differences in the way people perceive structures and the differences in construction methods in different parts of Europe, the National Annexes to the Eurocode can specify certain parameters for their specific country. The most notable differences for design of timber floors throughout Europe are:

1. Most countries use the formula for a simply supported beam to calculate the first eigenfrequency, even for a four-side supported floor. In Austria and Finland multiplication factors taking the transversal stiffness into account are also used.

2. The limit of the point load deflection for a 6 m span differs between 0.5 mm (Finland) and 1.7 mm (Denmark).

3. The way of calculating the load distribution from the point load is not specified in Eurocode 5 but Austria, Finland, UK and Ireland have their own formulas in their respective National Annex.

For a more thorough explanation of the regional differences see Zhang (et al. 2013).

2.5.2 North American work

Onysko (1985) made a study of timber floors in Canada through a survey among residents and testing of floors in existing houses. He found that the traditional North American criterion of deflection under a uniformly distributed load was not well correlated to acceptability among residents. The deflection under a 1 kN point load was better correlated. He also found that the span length should be included in the criterion. The correlation to the duration of a transient vibration also had a good correlation to acceptability, but since the effect of damping is difficult to estimate this could not be included in a design criterion. He says, however, that if the damping could be reliably estimated a criterion based on the transient vibration response would be the best one. Much of Onysko´s work has been implemented in the National Building Code of Canada.

Chui (1987) did laboratory testing as well as an in situ investigation on timber floors and found that the RMS value of the acceleration together with the first eigenfrequency were the most suitable parameters for predicting the subjective perception. A design method based on these two parameters was also developed. He stated, contradictory to Ohlsson, that the parameters of static deflection, peak velocity, and peak acceleration are not as good correlated to the perception of the floor as the two former mentioned parameters.

2.5.3 **Recent studies**

Dolan et al. (1999) suggested in his study of timber floors that the first eigenfrequency should be kept above 15 Hz and 14 Hz for unoccupied and occupied floors respectively.

The three North American researchers Hu, Chui, and Onysko summed up their work in an article from 2001 (Hu et al. 2001) where they agree that frequency components, magnitude of response and damping are the most important factors. Hu (2002) continued with field testing of timber floors and developed five different criteria through the statistical technique logistic regression:

$$f_1 \frac{1}{w_{1kN}^{0.39}} \geq 15.3 \tag{2.10}$$

$$f_1 \frac{m^{0.27}}{w_{1kN}^{0.22}} \geq 37.1 \tag{2.11}$$

$$f_1 \frac{L^{0.35}}{v_{1Ns}^{0.21}} \geq 17.5 \tag{2.12}$$

$$f_1 \frac{L^{0.38}}{a_{RMS}^{0.19}} \geq 10.3 \tag{2.13}$$

$$f_1 \frac{L^{0.49}}{a_{peak}^{0.14}} \geq 10.7 \tag{2.14}$$

All of the criteria could in a good way predict if the floor is acceptable or not. Equation (2.10) containing first eigenfrequency and point load deflection was chosen, since these parameters are the easiest to predict accurately. After development of designer useable formulas the criterion was somewhat modified (Hu & Chui 2004); the analytical formulas overestimated the first eigenfrequency. The formulas are based on the ribbed-plate theory of Timoshenko and Woinowsky-Krieger (Chui 2002). The field tests of Hu (2002) as well as the criteria are shown in Figure 2.8.

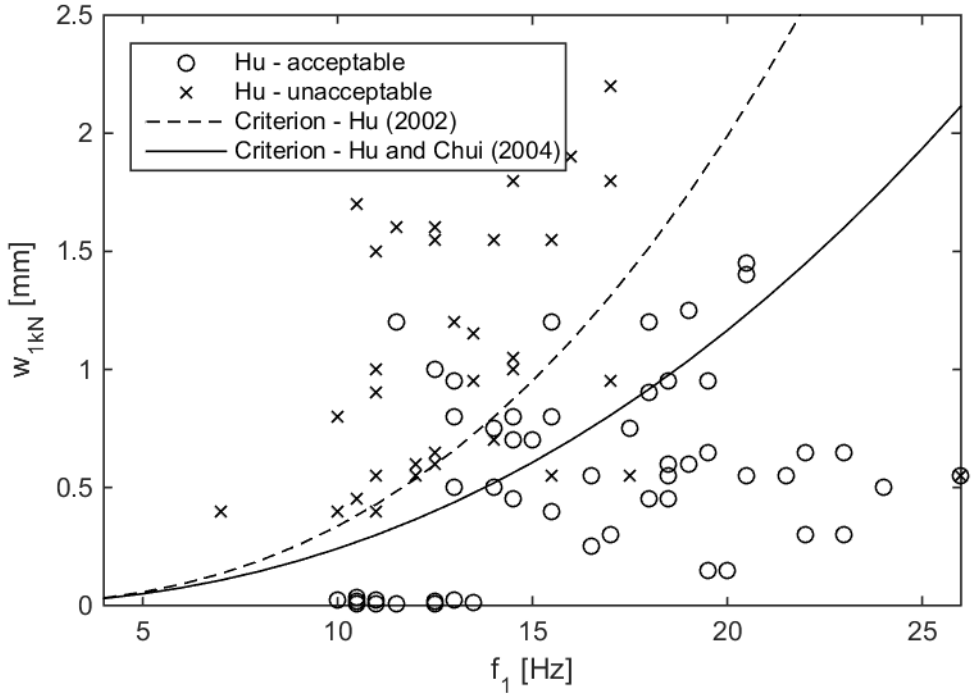

Figure 2.8 Diagram showing the criterion of Hu (2002) as well as Hu and Chui (2004). The rated floors are measured by Hu (2002).

In Finland, Toratti and Talja (2006) tested timber floors, of which many had a heavy screed, and developed criteria for acceptance for five different classes on the basis of first eigenfrequency, point load deflection, peak vertical displacement and peak vertical velocity. The authors divided the deflection into local deflection by the top plate, with measuring points at a distance 600 mm away from each other, and global deflection by the main joists. This is to account for the local springy effect that can be experienced with compliant floor toppings.

In Australia, Bernard (2008) tested a number of measures to reduce the dynamic problems of timber floors. All the floors he tested had a first eigenfrequency well above the frequency for human bodily oscillation (4-8 Hz). The measures he performed on his test objects to increase rigidity did not improve the subjective dynamical perception of the floors. He concluded that a higher rigidity did not mean an improvement in the subjective vibration response, as long as the first eigenfrequency is above the critical frequencies for bodily oscillation. In the higher frequency range other problems, like shaking or drumminess, occurred which led him to the conclusion that there is a need for criteria limiting these high-frequency problems. The experiments he performed which increased the damping and as a consequence lowered the structural rigidity did show better results when rated subjectively. The best rating in his study was achieved by a floor with rubber inserted into the middle of the cross-section of the floor joist, reducing the first eigenfrequency by 43% to 10.8 Hz, but increasing the modal damping ratio by 213% to 6.6%.

Hamm (et al. 2010) investigated many timber floors with both light and heavy screed and derived criteria for three different categories based on the demands; higher, lower and without demands. She used criteria on the first eigenfrequency and the deflection due to a 2 kN point load. Since the demands on deflection were relatively hard, none of the floors with light screed reached the limits of the higher demand category.

Recent Swedish works (Jarnerö et al. 2014) states, through a study on Swedish floors with a survey and measurements in-situ, that point load deflection has a good correlation to how the floor is perceived. A stricter requirement on point load deflection, than the present Swedish one, is suggested; 0.75 mm instead of 1.5 mm.

(Negreira et al. 2015) performed measurements and subjective tests at five different all-timber floors all acceptable according to Eurocode 5. Three of the five floors fail to reach acceptable in the subjective evaluations. The criteria of both Hu and Chui (2004) as well as Dolan (et al. 1999) manage to single out these floors as unacceptable.

2.5.4 Summary of criteria

1. Ohlsson, 1988

Deflection due to 1 kN point load at most flexible point	$w_{1kN} < 1.5$ mm
Maximum impulse velocity response due to a 1 Ns impulse, considering first eigenfrequency and damping ratio	h'_{max} restricted by Figure 2.7.
RMS value of vibration velocity	For dwellings: $v'_{RMS} < 0{,}015$ m/s For offices: $v'_{RMS} < 0{,}010$ m/s

2. Onysko, 1985

Deflection due to 1 kN point load at the mid-point of the floor	$w_{1kN} < min\begin{cases}\frac{8}{L^{1.3}}\\ 2\end{cases}$ mm

3. Smith and Chui, 1987

First eigenfrequency	$f_1 > 8$ Hz
Frequency-weighted RMS acceleration during first second	$a_{RMS} < 0.45$ m/s^2

4. Dolan, 1999

First eigenfrequency	For occupied floors: $f_1 > 14$ Hz For unoccupied floors: $f_1 > 15$ Hz

5. Hu, 2002

Ratio between first eigenfrequency and deflection, based on measurements	$15.3 \leq \frac{f_1}{w_{1kN}^{0.39}}$

6. Hu and Chui, 2004

Ratio between first eigenfrequency and deflection, for analytic design	$18.7 \leq \frac{f_1}{w_{1kN}^{0.44}}$

7. Toratti, 2006

First eigenfrequency	$f_1 > 10$ Hz
Local deflection due to a 1 kN point load	Class B: 0.25 mm Class C: 0.5 mm
Global deflection due to a 1 kN point load	Class B: 0.25 mm Class C: 0.5 mm

8. Hamm, 2010

First eigenfrequency	High demands $f_1 > 8$ Hz Low demands $f_1 > 6$ Hz
Deflection due to a 2 kN point load	High demands: 0,5 mm Low demands: 1,0 mm

2.5.5 **Design criteria – discussion**

Since there have been recent complaints on floors accepted by the criteria of Eurocode 5, other criteria need to be used. A ratio between the first eigenfrequency and the deflection was recommended by Hu and Chui (2004). It was verified by Negreira et al. (2015) in a Swedish context, although his study was small. In the study of Negreira the criterion of Dolan also worked well. This criterion is, however, a bit blunt, since it only addresses a lowest acceptable level of first eigenfrequency, making stiff but heavy timber-concrete composite floors less likely to pass.

In addition to this, the criterion of Hu and Chui works well in predicting the subjective experience in the study of Toratti & Talja (2006). The correlation between their results and the criterion of Hu and Chui can be seen in Figure 2.9. However, a weakness of the criterion is that no regard is taken to the damping, even though both Ohlsson (1988) and Bernard (2008) indicate that the damping is important for the subjective perception. The damping is, however, difficult to estimate.

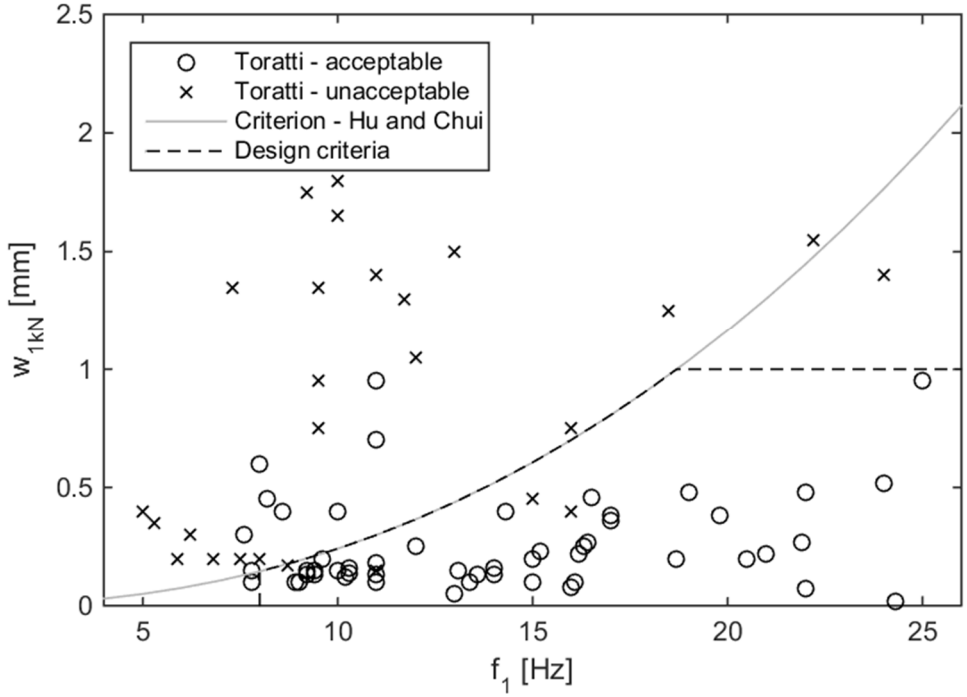

Figure 2.9 Diagram showing the criterion of Hu and Chui (2004) and the design criteria that is suggested in this project. The rated floors are measured by Toratti and Talja (2006).

The findings of Bernard (2008) and especially the subjective ratings in his article indicated that the problem of shake decreases as the feeling of springiness increases. This leads to the conclusion that a higher limit as well as a lower limit of the first eigenfrequency could be motivated. There is however, not enough research on the subject to put forth a limiting value.

Most of the researchers do find that the point load deflection is a good parameter to use for design of high-frequency floors. The limit value does, however, differ somewhat between the reports. The results presented in Figure 2.8 and especially Figure 2.9, show that not many floors with a 1 kN point load deflection above 1 mm were regarded acceptable. Thus, this could be a reasonable limit. The deflection should, according to Hu and Chui (2004), be calculated with the point load at mid-span directly above a joist. According to Ohlsson (1988), on the other hand, the point load should be placed at the most flexible point. This is naturally at mid-span between two joists, to take account of the local deformation of the top plate. One problem with the guidelines of Ohlsson is that the local deflection is hard to predict for floors with a light upper flange; the screed will add a considerable amount of stiffness to the upper flange that is difficult to estimate.

2.5.6 **Design criteria – conclusion**

In the evaluation of the floor concepts in this project, the criteria developed by Ohlsson and implemented in Eurocode 5 were used, since they are the basis for timber floor construction in Sweden.

From the discussion above some additional criteria were suggested: a lower limit to the first eigenfrequency,

$$f_1 > 8 \text{ Hz} \tag{2.15}$$

a ratio between first eigenfrequency and deflection

$$18.7 < \frac{f_1}{w_{1kN}^{0.44}} \tag{2.16}$$

and an upper limit to the deflection due to a 1 kN point load placed directly over a joist at mid-span

$$w_{1kN} < 1.0 \text{ mm} \tag{2.17}$$

The limit for the first eigenfrequency was developed by Ohlsson (1988) and implemented in Eurocode 5. The ratio between first eigenfrequency and the deflection was developed by Hu and Chui and the deflection limit of 1.0 mm was based on the measurements presented in Figure 2.8 and Figure 2.9.

To simplify the calculations of the deflection it is the recommendation from this project to place the 1 kN point load over a joist and to choose the materials and dimensions in the top layer out of experience so as to minimise the feeling of springiness between joists.

For this project the formula in UK National Annex to Eurocode 5 was used to calculate the load distribution, see Equation (2.18). This is an accepted easy-to-use formula in a European context. It does also predict the deflection quite well in the experiments conducted in this project, see Figure 3.4. The formula takes the transversal stiffness and shear deformations into account.

$$w_{1kN} = \frac{1000 k_{dist} L^3 k_{amp}}{48 (EI)_L} \tag{2.18}$$

Where k_{dist} gives the proportion of the 1 kN load supported by a single joist according to

$$k_{dist} = max\left\{k_{strut}[0.38 - 0.08 \ln\left[\frac{14(EI)_B}{s^4}\right]; 0.30\right\} \tag{2.19}$$

$k_{strut} = 1$ or, in the case of solid timber joist which have transverse stiffness provided by a single or multiple lines of blocking with a depth of at least 75% in addition to the stiffness provided by the decking or ceiling, $k_{strut} = 0.97$.

k_{amp} in Equation (2.18) is an amplification factor that takes into account the effect of shear deflection and should be taken as 1.05 for solid timber joists, 1.20 for glued thin-webbed joists and 1.30 for mechanically-jointed floor trusses.

It should, however, be noted that by choosing another way of calculating the load distribution when considering the 1 kN point load deflection, the results could be quite different. This could lead to rejecting or accepting a concept that in reality behaves differently. It would be beneficial for the European timber industry to achieve some coherence on the way the load distribution should be calculated and what limit should be used for the 1 kN point load deflection.

3 Analysis of the benchmark floor

In this project, a benchmark timber floor made by the timber house producer A-hus was studied. This type of timber floor is used in their multi-story timber houses.

The purpose of this sub-study was to test the analytical and numerical prediction methods against measurements from a full-scale experiment on two test specimens. Furthermore, this full-scale experiment was conducted for the simple reason of gaining experience in performing an experimental modal analysis (EMA). The test specimens were tested with and without a damping material at the boundary conditions in order to evaluate if this will increase the modal damping of the benchmark floor. Note that the benchmark floor is tested without any non-structural dead weight, e.g. gypsum boards. The full-scale experiment was performed in the production facilities of A-hus.

3.1 Description of the benchmark floor

The timber floor consists of elements with a width of approximately 2400 mm that are connected to create a floor. The structural system is open and consists of a top flange made of particleboard, beams made of LVL-timber and blockings of structural timber. The blockings are generally placed close to mid-span. A thorough description of the test specimens can be found in Appendix A. The purposes of the blockings are to distribute load amongst the beams and to add stiffness in the transversal direction.

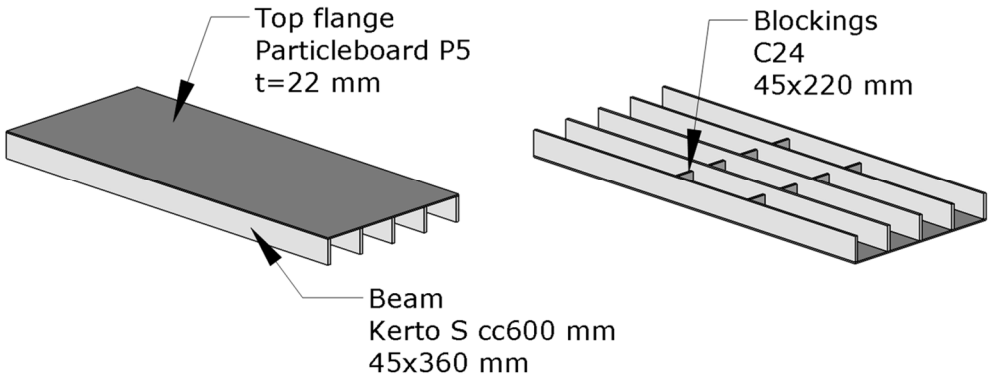

Figure 3.1 Principle sketch of the benchmark floor.

The blockings are fastened to the beams by manually skew nailing them, after this glue is manually applied to the beams and the blockings. The top plate is then put in place. The whole floor structure is rolled through an automatic nailing machine. The nails connect the joists to the top flange.

At the construction site the timber floor elements are connected to each other through screwing and gluing of the top plate of one element to the next element. The blockings of one element are, however, neither nailed nor glued to the next element. Thus, the floor cannot transfer moment transversally.

Particleboard P5 is mainly used for humid conditions, i.e. in bathrooms. Generally P4 is used for this type of timber floor, however the test specimens were produced with

P5 and this material is thus considered further on. The stiffness properties of P5 are approximately 12% higher than those of P4.

In order to achieve sufficient fire-resistance and sound attenuation of the structural system gypsum boards are added on top and bottom of the timber floor. The gypsum boards are assumed not to contribute with any stiffness to the structural system and are hence only considered as a non-structural dead weight. An increased dead weight will decrease the eigenfrequencies of the floor. However, as the test specimens are not equipped with this extra dead-weight all of the eigenfrequencies presented in Chapter 3.2.2 will exclude the gypsum board. Note that in Chapter 4.4 the analytically calculated first eigenfrequency of the benchmark floor includes this non-structural dead weight. When designing a floor any extra dead weight should always be included.

3.2 Analysis of the benchmark floor – Methods and results

The performance of the benchmark floor is analysed with analytic and numerical calculations, as well as measurements from experiments. Here follows a brief summary of the results from the different methods of analysis. A thorough description of the measurements as well as the numerical analysis is found in Appendix A respective Appendix B.

3.2.1 Analysis methods

The boundary conditions of the test-specimens were simply supported on two sides, with an effective span length of 5920 mm, see Figure 3.2.

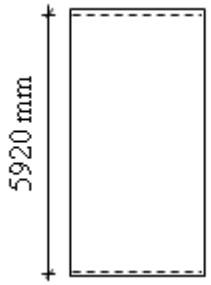

Figure 3.2 Boundary conditions of the test-specimens.

In order to extract pertinent parameters such as eigenfrequency and damping an experimental modal analysis (EMA) was carried out on the test-specimens. The main concept of an EMA is to measure an input and the resulting output to a system, the system being the test-specimen of interest. This allows the experiment conductor to draw important conclusions about the system, e.g. how the system will react to a certain input.

The EMA was conducted using an impact hammer, two accelerometers and a data acquisition system. An accelerometer is used to measure the acceleration in a specific point and an impact hammer is used to put an object into motion while measuring the input. The data acquisition system is used to transfer these measurements to a PC for data-logging.

The impact hammer was used to strike the test-specimen in an ordered manner while measuring input given to the test-specimen, the acceleration was simultaneously measured at two specific points.

The acquired input and output data is expressed in the time-dependent acceleration during the measurement duration. By performing a Fast-Fourier Transform (FFT) this data can be transformed from the time-dependent acceleration to the frequency-dependent acceleration. The frequency-dependent data can then be further analysed and modal parameters such as eigenfrequency and damping can be extracted for each vibration mode.
A static deflection measurement was also carried out in order to establish the 1 kN point load deflection for the test-specimens. This was done by loading the test-specimen with 0.85 kN at mid-span while measuring the deflection using a deflection measuring gauge. The acquired deflection was then extrapolated to 1 kN assuming linearity.

Furthermore, the test-specimens were modelled in Abaqus/CAE. The models were used to numerically extract eigenfrequency for each vibration mode as well as the 1 kN point load deflection.

Finally, the eigenfrequency and 1 kN point load deflection was calculated using the simple analytical methods available described in Chapter 1.5 and Chapter 2.5.6.

3.2.2 **Results from the modal analysis**

For comparison the order of eigenmodes are decided by the order obtained from the measurements:

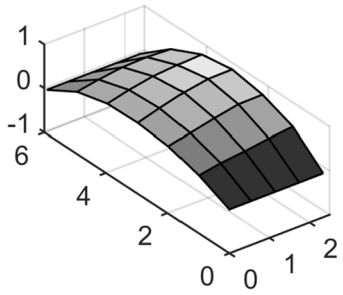

Mode 1: The first longitudinal bending mode.

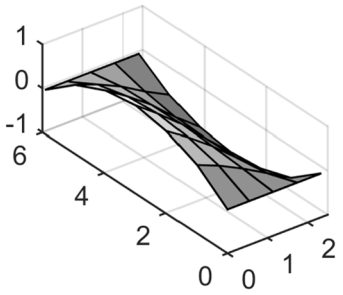

Mode 2: The first longitudinal bending mode with a transversal rotation.

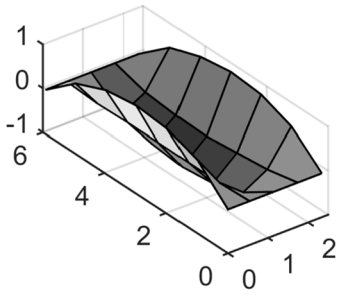

Mode 3: The first transversal bending mode.

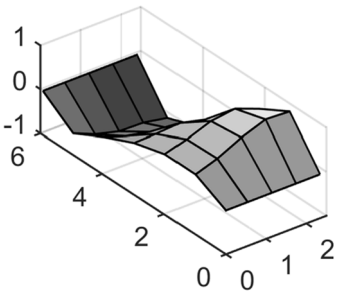

Mode 4: The second longitudinal bending mode.

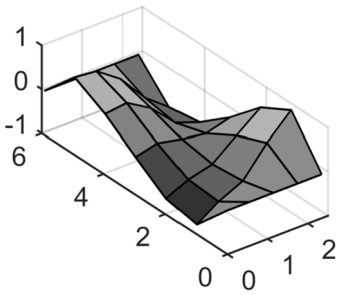

Mode 5: The second longitudinal bending mode with a transversal rotation.

Figure 3.3 Measured eigenmodes

Table 3.1 Measured and predicted eigenfrequencies.

Mode	Analytical	Numerical	Numerical (with springs between blockings and joists)	Measurement
1	19.7 Hz	17.1 Hz	17.1 Hz	16.2 Hz
2	-	18.5 Hz	18.5 Hz	18.3 Hz
3	-	57.9 Hz	32.4 Hz	33.0 Hz
4	78.6 Hz	50.3 Hz	49.5 Hz	41.1 Hz
5	-	62.7 Hz	61.3 Hz	47.1 Hz

Table 3.2 Measured modal parameters with and without sylomer® sr28 damping blocks at boundary conditions.

	Measurements		Measurements with sylomer® sr28	
Mode	Eigenfrequency	Damping ratio	Eigenfrequency	Damping ratio
1	16.2 Hz	0.79%	14.4	1.34%
2	18.3 Hz	0.78%	15.9	1.41%
3	33.0 Hz	1.06%	31.7	1.19%
4	41.1 Hz	3.51%	32.5	2.71%
5	47.1 Hz	1.23%	37.2	2.62%

3.2.3 **Results from static analysis**

The measured 1 kN point load deflection (extrapolated from 0.85 kN, see Appendix A) is compared to analytical and numerical predictions in Figure 3.4.

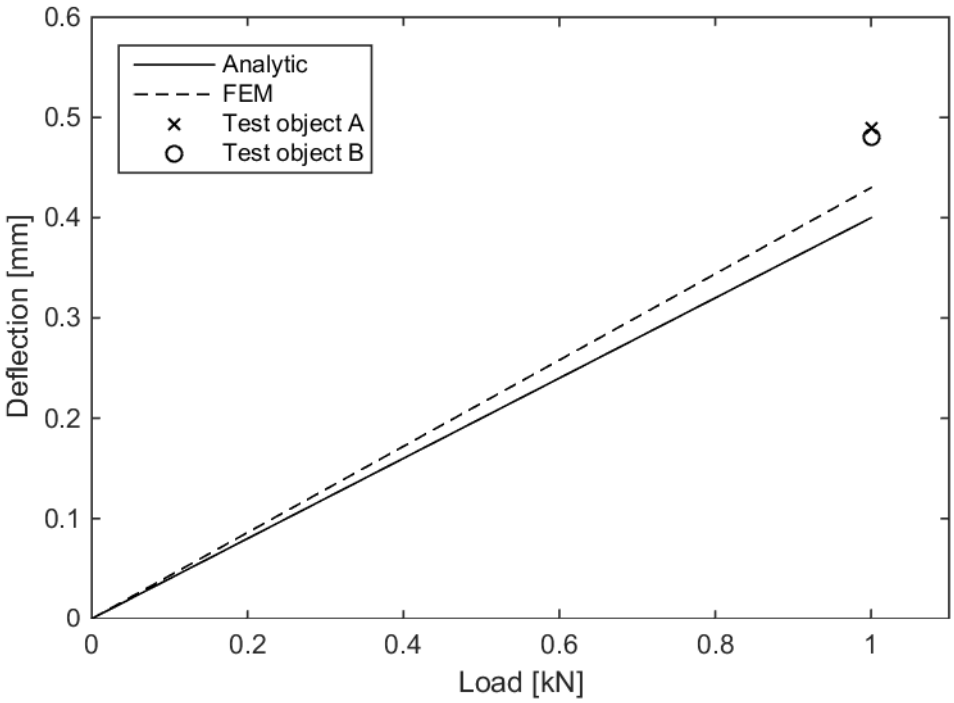

Figure 3.4 Measured deflections and the corresponding predicted deflections.

3.3 Analysis of the benchmark floor – Discussion

In Table 3.1 the eigenfrequencies obtained from each method of analysis are compared. In general the predicted eigenfrequencies are higher than those measured. This indicates that the material stiffness, stiffness of joints, or the material weight differs from what is assumed.

Primarily the longitudinal modes are considered (mode 1, 2, 4 and 5). Most probable is that the stiffness of the joints is overestimated. In both prediction methods a full interaction between the joists and the top plate is assumed. Variation of material quality could also be probable. However as the difference between prediction and measurement drastically increases for mode 4 (the second bending mode) this

indicates that the stiffness of the joints is overestimated – more deformation is introduced in the joint due to the mode shape and the stiffness of the joints affect the flexural rigidity of the timber floor to a greater extent. The beams are glued and nailed to the chipboard and a stiffer way of fastening them would be to use screws and glue (Bernard 2008).

The numerically predicted first eigenfrequency is 13 % lower than the analytically predicted, probably because shear deformations are neglected in Euler-Bernoulli theory. The difference is larger than first was expected since the benchmark floor is not thin-webbed. The shear rigidity of the Kerto beam is however relatively low, which explains the large difference.

Secondly, the transversal bending mode is considered (mode 3). The difference between the numerical prediction and the measurement is high. In the numerical analysis full interaction of all blockings is considered – this is not at all true. The blockings are in reality only skew-nailed and it is very difficult to obtain a good interaction. Moreover, shrinkage effects will further influence the interaction. The FE-model was improved, to better mirror the real behaviour of the test object by inserting springs connecting the blockings with the joists – this is presented in Table 3.1. Significant transversal stiffness would probably be hard to obtain if not continuous transversal elements were used instead of blockings.

The effect of adding a viscoelastic damping material at the boundary conditions of test specimen A is presented in Table 3.2. Sylomer® sr28 damping blocks (a visco-elastic material made of rubber in the shape of a rectangular block) increase damping but decrease the first eigenfrequency. The effects of these changes on the subjective perception are a bit ambiguous. The evaluation criteria chosen in Chapter 2.5.6 fail to recognise the positive effect of the sylomer® blocks since the damping has been omitted from the criteria. Thus, from the view of the performance criteria the sylomer® blocks are negative only, since they lower the first eigenfrequency. Since the damping is relatively much influenced and the first eigenfrequency does not go below 10 Hz, the sylomer® blocks would probably have a positive impact on the subjective perception of the floor (Bernard 2008). The damping coefficient σ_0 which is given much importance in the conclusions of Ohlsson (1988) is increased with the sylomer® blocks. Bernard (2008) came to similar conclusions (although he worked with sylomer® blocks within the cross-section rather than at the boundaries). Furthermore, the sylomer® blocks may have a positive impact when it comes to flanking sound. This is, however, beyond the scope of this project.

Figure 3.2 shows the predicted deflection due to a 1 kN point load compared to the measured deflection. The deflection can be predicted with approximately 12% difference and is underestimated by both the analytical and numerical calculations. When springs are inserted between the blockings and the beams the deflection is instead overestimated by 18%, see Table 3.3 in Appendix B.

4 Improvement of the benchmark floor

Other products similar to the benchmark floor were studied through literature and compared to the benchmark floor. The purpose of this sub-study was to establish how well the benchmark floor performs, in relation to the design criteria and other products, and to understand how to improve it. Competitive products were sought for on both the Swedish and European market.

Furthermore, different changes that could improve the benchmark floor were investigated. The suggested changes were established by observing how the cross-sections were organised in the other products in Chapter 4.1.

Finally, the possibility of introducing two-way action as a way to increase the first eigenfrequency of a structural system was investigated.

4.1 Study of other competitive products

Five adequate timber floor products were found. Not all of these are strictly designed as floor products but could nevertheless work very well for this purpose. The products are presented in this section with a principal sketch and some general information The specific material and cross-section dimensions are presented in Table 4.1. All of the products have a construction height similar to the benchmark floor in order to be able to grade the products mutually – approximately 382 mm.

As the actual producer is irrelevant for this purpose the names will be omitted. Also note that the sketches below only visualise the products in principle.

4.1.1 Product 1 (Swedish market)

The structural system of this timber floor is open and consists of a top flange made of CLT, webs of glulam and bottom flanges of glulam. No blockings are added – the CLT panel provides enough transversal flexural rigidity.

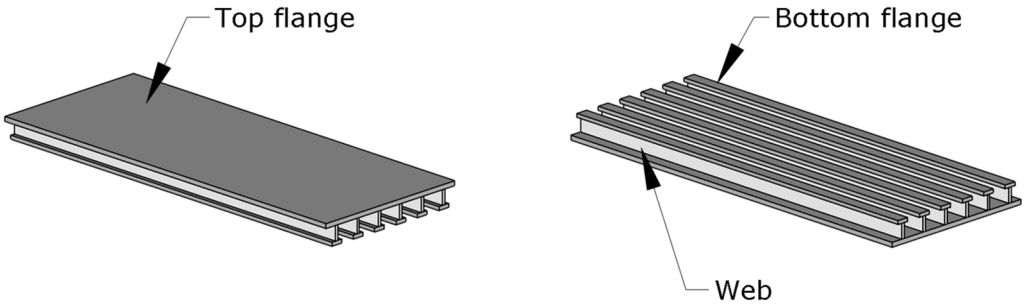

Figure 4.1 Principal sketch of product 1.

A self-supporting ceiling is used in order to improve the acoustic performance of the timber floor. It is thus assumed that extra weight from gypsum boards is only added on one side of the structural system resulting in a 25 kg/m^2 increased dead weight.

4.1.2 **Product 2 (Swedish market)**

The structural system of this timber floor is open and consists of a top flange made of LVL, webs of LVL, bottom flanges of LVL and blockings of LVL. The blockings are generally placed in the proximity of mid-span. The blockings are used to distribute load amongst the beams.

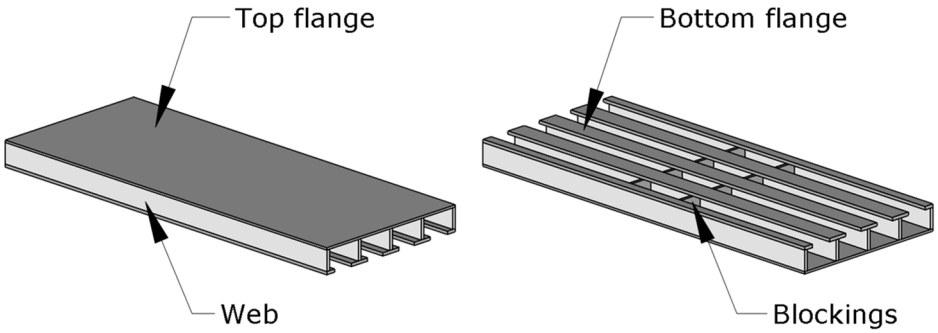

Figure 4.2 Principal sketch of product 2.

No further information is given; it is thus assumed that gypsum board for fire-protection is needed on top and on bottom of the timber floor resulting in a 50 kg/m^2 increased dead weight.

4.1.3 **Product 3 (Swedish market)**

The structural system of the this timber floor is a closed system and consists of a top flange made of LVL, Masonite beams as webs, a bottom flange of steel sheet and blockings of Masonite beams. The blockings are evenly spaced but no information is given about the spacing distance.

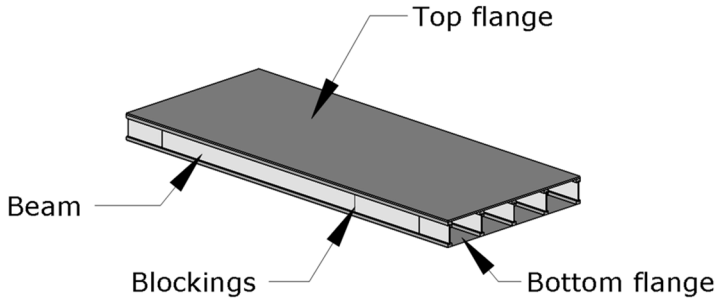

Figure 4.3 Principal sketch of product 3.

No further information is given; it is thus assumed that gypsum board for fire-protection is needed on top and bottom of the timber floor resulting in a 50 kg/m^2 increased dead weight.

4.1.4 **Product 4 (European market)**

The structural system of this product is a closed system and consists of a top flange, webs, a bottom flange and blockings, all made of structural timber. The blockings are evenly spaced – no information is given about the spacing distance.

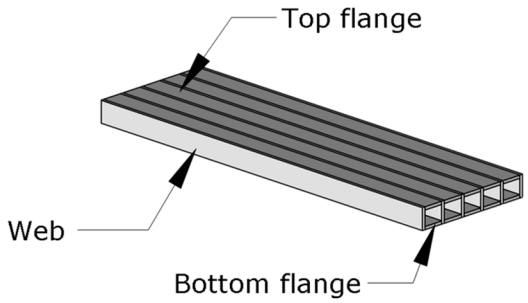

Figure 4.4 Principal sketch of product 4.

Standard elements are not fire-resistant and must thus be complemented with gypsum boards. However, elements with fire-resistant bottom are available and gypsum board would thus only be needed on top resulting in a 25 kg/m^2 increased dead weight.

4.1.5 **Product 5 (European market)**

The structural system of this product is a closed system and consists of a top flange made of structural timber, webs of OSB and a bottom flange of structural timber. As the webs are slanted they create a simple truss effect and no blockings are added.

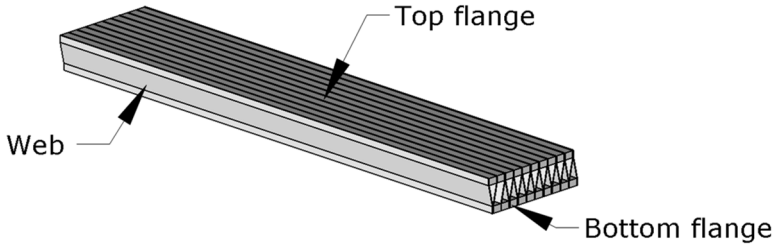

Figure 4.5 Principal sketch of product 5.

Standard elements are not fire-resistant and must thus be complemented with gypsum boards. However, elements with fire-resistant bottom are available and gypsum board would thus only be needed on top resulting in a 25 kg/m^2 increased dead weight.

4.1.6 **Properties of the different products**

Table 4.1 Properties of the various products studied.

Type	Top flange	Web/Beam	Bottom flange	Blockings
Benchmark	Particleboard P5 t=22 mm	Kerto S 45x360 mm^2	-	C24 45x220 mm^2
Product 1	CLT t=70 mm	Glulam LK20 45x220 mm^2 cc400	Glulam L40c 56x180 mm^2	-
Product 2	Kerto Q t=33 mm	Kerto S 51x300 mm^2 cc600	Kerto S 45x300 mm^2	Kerto S 51x300 mm^2
Product 3	Plywood P30 t=24 mm	Masonite beam h=350 mm cc600	Steel sheet t=0.7 mm	Masonite beam h=350 mm
Product 4	C24 243x33 mm^2	C24 33x217 mm^2 cc243	C24 243x33 mm^2	-
Product 5	C24 102x57 mm^2	OSB/3 8x266 mm^2 cc110	C24 102x57 mm^2	-

Table 4.2 Structural properties of the various products studied.

Product	$(EI)_L$ [MNm^2/m]	$(EI)_L/m$ [MNm^4/kg/m]	Cross-section area [m^2/m]
Benchmark	5.33	0.069	0.049
Product 1	14.6	0.201	0.120
Product 2	21.6	0.236	0.081
Product 3	10.6	0.138	0.045
Product 4	12.0	0.135	0.092
Product 5	28.8	0.286	0.116

4.2 Study of improvements to the benchmark floor

By changing some parameters or adding new parts to the benchmark timber floor the performance of it could be improved. The process of doing so will also help improve the designer's understanding for what type of parameters are important for the flexural rigidity of the timber floor.

The following changes are considered:

1. Using a self-supporting ceiling: by introducing a self-supporting ceiling the added weight of gypsum boards can be reduced by 25 kg. Reducing the added weight on the structural system will increase the first eigenfrequency.

2. Change of material of the top flange: it can be seen that no other producers use particleboard as top flange. Most other timber products have higher stiffness-to-

weight ratio than particleboard and could therefore increase flexural rigidity of the benchmark floor. The following material changes are considered; Plywood P30, OSB/4 or Kerto Q all with a cross-section thickness of 22 mm.

In order to compare with the benchmark floor the thickness of the top flange is not changed. However, the materials considered might not be available with a thickness of 22 mm.

3. Addition of a bottom flange: All other floor products presented have a bottom flange. Adding a bottom flange could drastically improve the flexural rigidity of the benchmark floor. The following bottom flange is considered; Kerto S with the cross-section area 45x180 mm^2.

4. Change of material of the top flange and addition of a bottom flange: in order to keep the neutral layer close to the centre of the cross-section the added stiffness of a bottom flange should be balanced with a stiff top flange. By also changing the top flange material when adding a bottom flange the flexural rigidity could be further increased. The following combination is considered; Plywood P30 top flange with a thickness of 22 mm and a Kerto S bottom flange with the cross-section area 45x180 mm^2.

Table 4.3 Structural properties of the considered changes to the benchmark floor.

Type	$(EI)_L$ [MNm^2/m]	$(EI)_L/m$ [MNm^4/kg/m]	Cross-section area [m^2/m]
Benchmark	5.33	0.069	0.049
Self-supporting ceiling	5.33	0.101	0.049
Change of top flange, P30	8.16	0.110	0.049
Change of top flange, OSB4	6.78	0.089	0.049
Change of top flange, Kerto Q	9.24	0.123	0.049
Addition of bottom flange	11.6	0.137	0.0625
Change of top flange and addition of bottom flange	17.6	0.218	0.0625

4.3 Study of a simple two-way action example

Three pure theoretical homogenous plates simply supported on either two or four sides are considered, see Figure 4.6, with a span length L=5920 mm and a span width B that varies from L to 2L. The properties of the various plates considered are presented in Table 4.4.

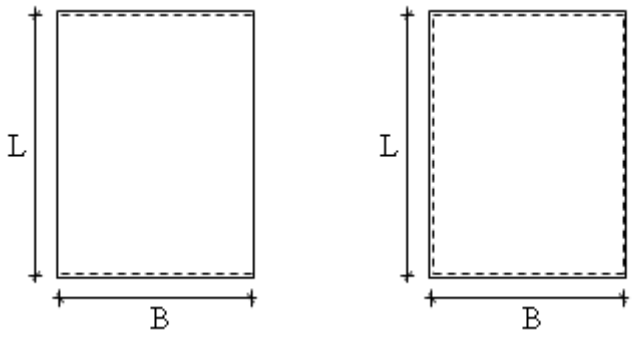

Figure 4.6 *Boundary conditions considered. From the left; two-sided simply-supported (one-way action) and four-sided simply-supported (two-way action).*

Table 4.4 *Properties of the various plates.*

Plate	Type of action	EI [MNm^2/m]	m [kg/m^2]	Cross-section area [m^2/m]
A	One-way	11	81	A
B	One-way	22	81	2A
C	Two-way	11	81	2A

As timber products are orthotropic at least two layers of the material is needed to achieve stiffness in two directions. The consequence of this is that plate C basically will need a cross-section twice that of plate A. The most interesting comparison will thus be the effect of two-way action (plate C) compared to the effect of one-way action with all layers in one direction (plate B) and thus a much higher flexural rigidity in that direction.

4.4 Improvement of the benchmark floor – results

The span length for all sub-studies presented here was set to 5.92 m as in Chapter 3.

4.4.1 Performance of competitive products

In Figure 4.7 the first eigenfrequency is plotted against the 1 kN point load deflection of the products described above, according to the design criteria suggested in this project. The parameters are assessed analytically and the results are compared to the benchmark floor.

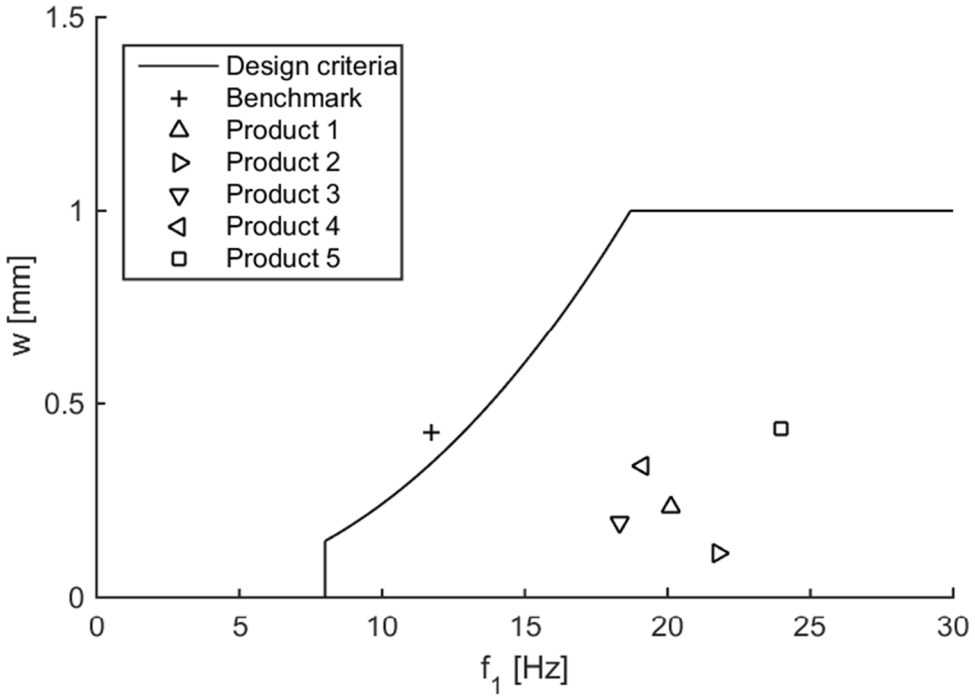

Figure 4.7 Performance of timber floor products available on the Swedish or European market.

4.4.2 **Performance of improvements to the benchmark floor**

In Figure 4.8 the first eigenfrequency is plotted against the 1 kN point load deflection of the suggested improvements to the benchmark floor, according to the design criteria suggested in this project. The parameters are assessed analytically and the results are compared to the benchmark floor.

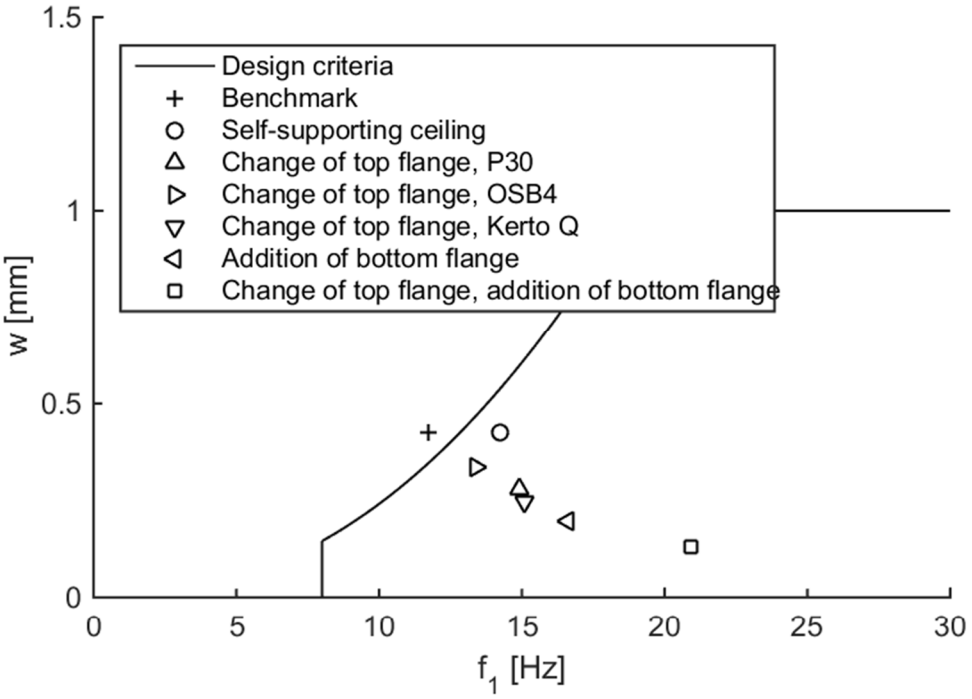

Figure 4.8 Performance of the considered changes to the benchmark floor.

4.4.3 **Effect of two-way action**

In Figure 4.9 the results of the parametric study on the effect of introducing two-way action to a homogenous plate is presented. The first eigenfrequency is plotted against the span width to span length ratio B/L. The boundary conditions can be seen in Figure 4.6.

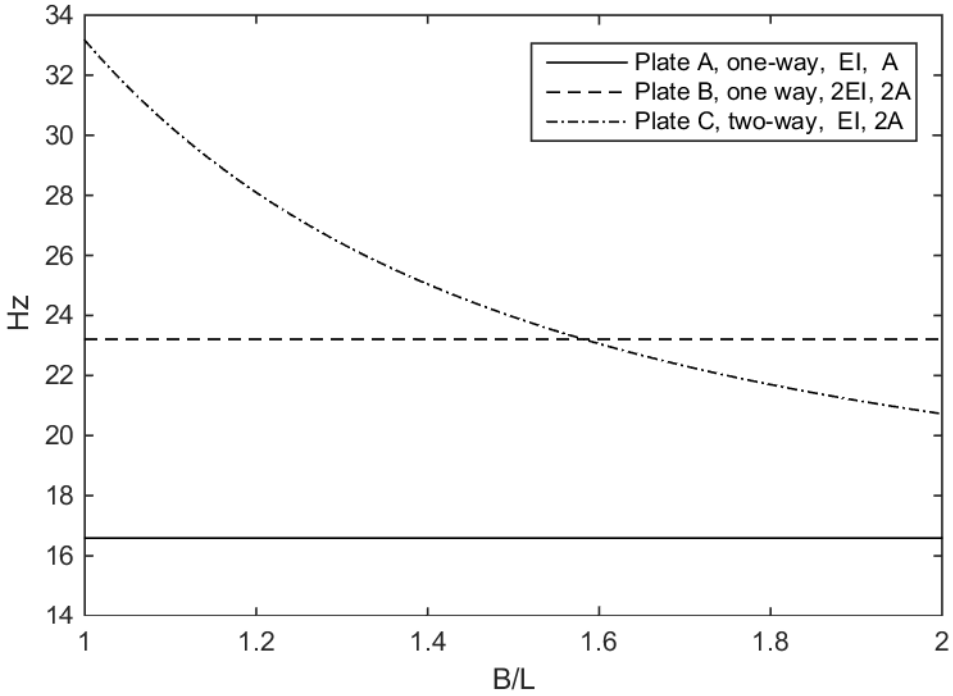

Figure 4.9 Effect of two-way action for a homogenous plate.

4.5 Improvements of the benchmark floor – Discussion

The benchmark floor fulfils the service limit state requirements regarding vibration set by Eurocode 5. However, as proposed by the authors of this report other criteria are used. As seen in Figure 4.7, the benchmark floor does not fulfil these criteria. By comparison to the other products presented in this chapter it is obvious that the structural system of the benchmark floor is rather simple. All other manufacturers try to organise the cross-section of their products so that the material is used in a more effective manner – high quality material is put far away from the neutral layer. It can be observed that product 3, 4 and 5 uses a closed system, and their cross-sections are in principle organised as shown in Figure 4.10. Furthermore, it can be observed that product 1 and 2 uses an open system, and their cross-sections are in principle organised as shown in Figure 4.11.

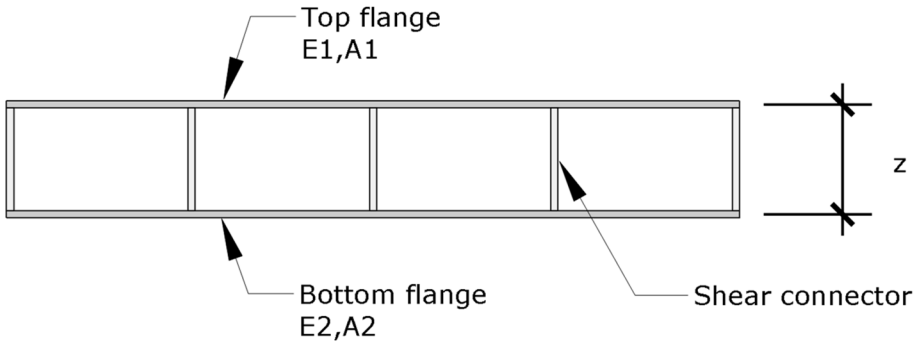

Figure 4.10 Example of a closed cross-section.

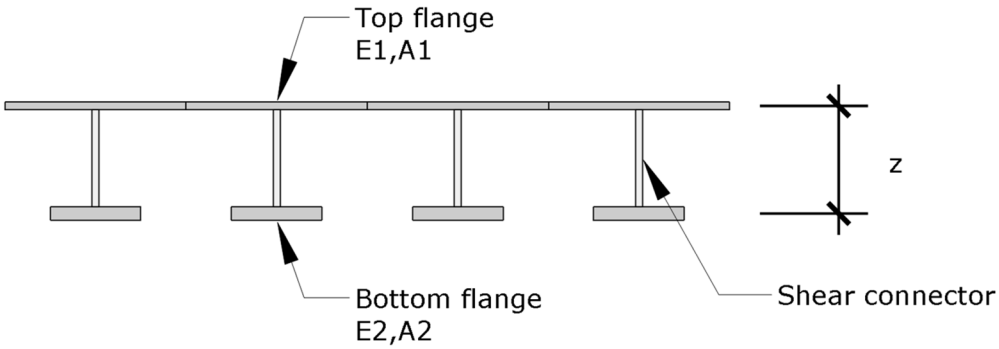

Figure 4.11 Example of an open cross-section.

Both product 1 and 5 uses a lower quality material for the web, utilising the fact that the problem of vibration is highly governed by the flexural rigidity and not utilisation of the material strength. It is wise to put high quality material far away from the neutral layer, i.e. at the flanges, and lower quality material could be used close to the neutral layer, i.e. as web. However, the web material should not exhibit large shear deformations. Furthermore, it is important to keep balance between the two flanges, i.e. $E1A1 \approx E2A2$, so that the neutral layer is close to the centre of the cross-section.

In Figure 4.8 it can be seen that by changing the material of the top flange to any of the proposed materials the benchmark floor fulfils the design criteria suggested in this project. It can also be seen that the most effective way to improve the performance of

the benchmark floor is to add a bottom flange while also changing the top flange. This is much more effective than just adding a bottom flange.

Figure 4.9 shows that as the span length to span width ratio is close to 1 (quadratic floors) it could be very beneficial with two-way action regarding the first eigenfrequency. This makes it interesting to consider concepts that can successfully carry load in two directions. It might be difficult, though, to achieve a two-way bearing floor in practice as the structural system should have a similar cross-section present in the longitudinal and transversal direction.

First of all timber has different stiffness in different directions, it is thus difficult to utilise the material in an effective manner when considering two-way action. Second it might be very difficult to obtain equal flexural rigidity in both directions as it is only possible to have joint-free webs in one direction. Nevertheless, there are some geometric forms that allow for transfer of shear forces in both span directions, e.g. trapezoidal webs, crossed truss webs or crossed panel webs as shown in Figure 4.12. Note that the examples below only show principal sketches of the part of the structural system that transfers shear.

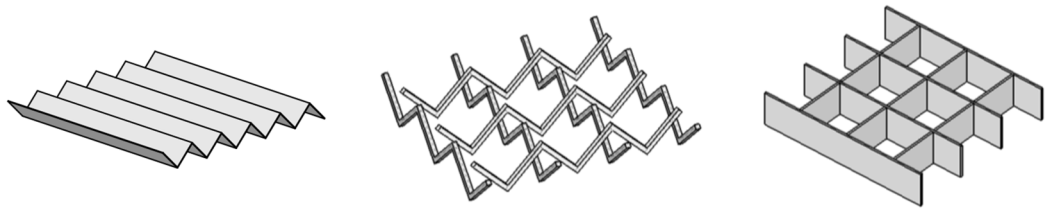

Figure 4.12 Examples of geometric forms that could allow for transfer of shear forces in two directions. From the left; trapezoidal web, space truss, crossed panel web.

The trapezoidal panel web works as a regular web in one direction and as a truss in the other direction. Crossed truss webs allows for intersection of the trusses if designed properly. Crossed panel webs are not possible to produce in timber without joints, and as discussed in Chapter 3.3 it can be very difficult to obtain good interaction in these joints.

5 New concepts

Through the learning process in this project, ideas are formed that sometimes are rejected and sometimes worth developing. In this chapter some principles of new concepts are formulated, based on the understanding gained through the previous parts in this project.

The purpose of this sub-study was to find promising concept for a timber floor. This was done by generating new concepts of timber floors that can compete with the other products available, see Chapter 4.1. The concepts generated were tested using the design criteria proposed in this project.

Furthermore, some concepts using a two-way action structural system was sought for. Specifically in order to further investigate the potential of such structural systems. These concepts were numerically evaluated within the width to span length ratio B/L=1.0-1.5.

To be able to grade the concepts mutually the construction height was set to be similar for all of the concepts – approximately 382 mm.

5.1 Generating concepts

As a way to imagine new concepts an iterative model building process was carried out. Building models is a great way to play with form and rigidity; it is possible to physically twist and bend the models and this allows a fundamental understanding of how to organise the material. Moreover the models are a superior tool for dialog and an initially bad concept can be further developed through discussion. The process of building models will in a sketchy fashion also provide some understanding of manufacturing challenges, as similar challenges are present when assembling the parts of a physical model. The models were built in a scale of 1:20 in cardboard.

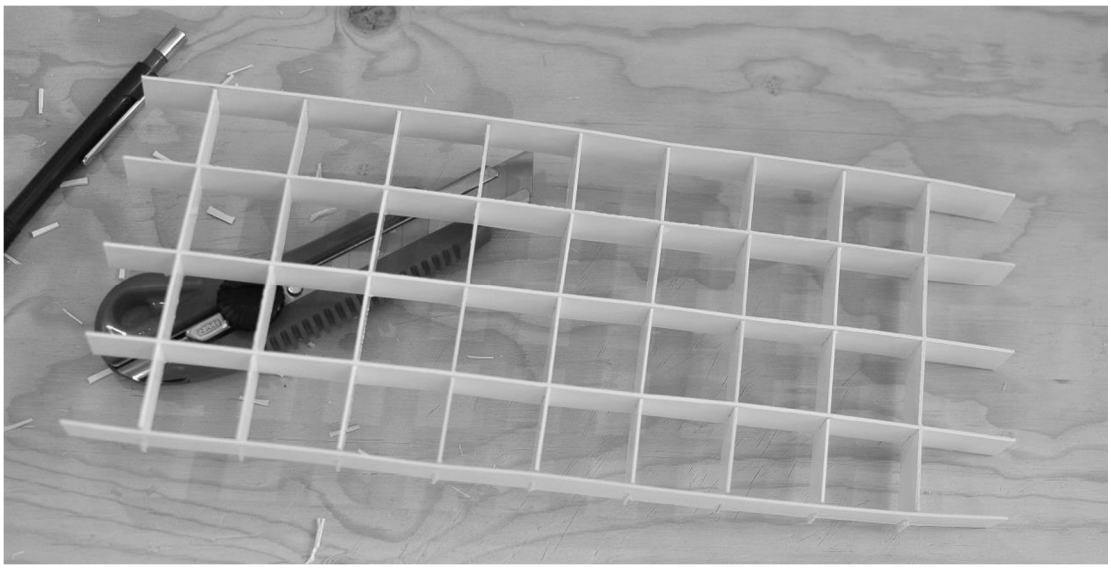

Figure 5.1 Building a model with cardboard.

5.1.1 **Trapezoid**

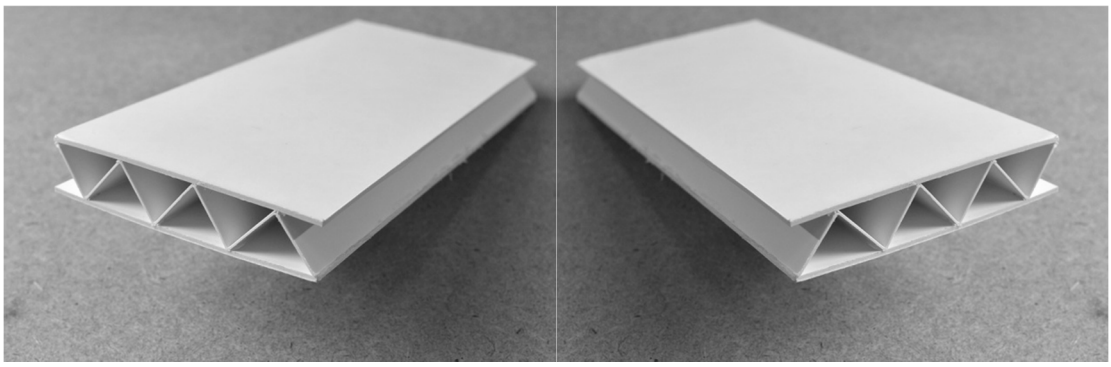

Figure 5.2 Model of the trapezoidal web concept.

This proposed structural system is closed and this would be a simple way to achieve good flexural rigidity in both longitudinal and transversal direction. The structural system will have different stiffness in different directions. The model is very rigid in bending in both longitudinal and transversal direction. It is also very rigid in torsion.

Table 5.1 Alternative material combinations for the trapezoid concept.

	Type of action	Compression flange	Web	Tension flange
1	Two-way	Plywood P30 t=40 mm	Corrugated steel h=302 mm t=1.5 mm	Plywood P30 t=40 mm
2	One-way	Kerto Q t=33 mm	Corrugated steel h=325 mm t=1.5 mm	Kerto S t=24 mm
3	One-way	Kerto Q t=33 mm	ECOR/Wellboard h=325 mm t=5 mm	Kerto S t=24 mm

ECOR and Wellboard are both cellulose fibre based board material without adhesives, they have similar stiffness as OSB but are to a greater extent formable and could be used to create corrugated shapes. However, today they are mainly used for smaller application.

Note that when using steel sheets it is important to understand how this might affect moisture transport in the building.

5.1.2 **Grid**

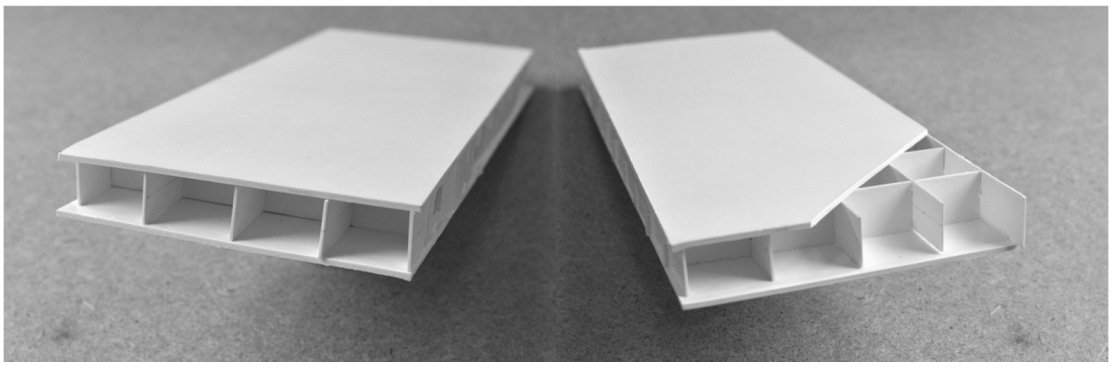

Figure 5.3 Model of the crossed panel web concept.

The proposed structural system is closed. The grid is built up by webs in the longitudinal direction that are complemented with blockings in the transversal direction – a crossed panel web. It is theoretically possible to create a homogenous plate - it might not be practical, however, as the interaction of the blockings might be very poor. The model is very rigid in bending in both longitudinal and transversal direction. The model is also very rigid in torsion.

Table 5.2 Alternative material combinations for the grid concept.

	Type of action	Compression flange	Web	Tension flange
1	Two-way	Plywood P30 t=40 mm	OSB3 45x302 mm^2	Plywood P30 t=40 mm
2	One-way	Kerto Q t=33 mm	OSB3 45x325 mm^2	24 mm Kerto S

5.1.3 **Big-flange**

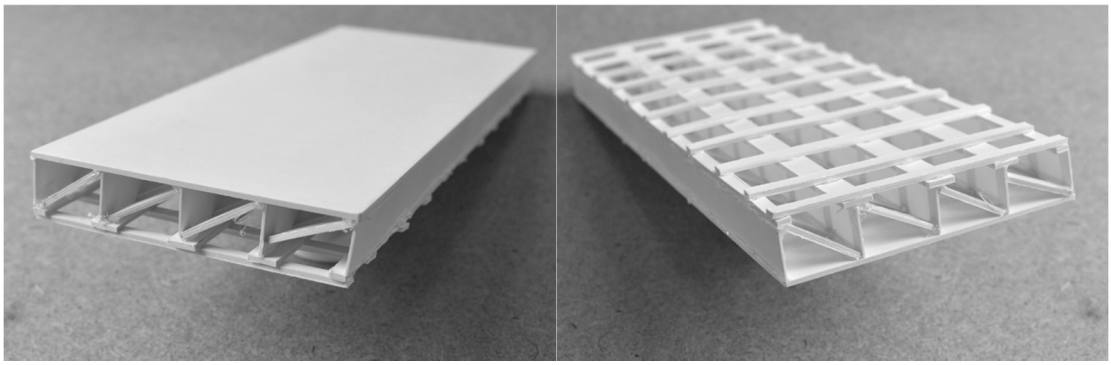

Figure 5.4 Model of the big flange concept.

The proposed structural system is open. A transversal flexural rigidity is created by introducing a truss between the webs. The structural system will have different flexural rigidity in the two directions. The system could very well be used for two-way action; plenty of truss pieces would, however, be necessary. This might not be practical during production. In this study the structural system is mainly considered for one-way action.

The model is very rigid in bending in both longitudinal and transversal direction. It is not at all rigid in torsion.

Table 5.3 Material combination for the big-flange concept.

	Type of action	Compression flange	Web	Tension flange
1	One-way	Kerto Q t=33 mm	OSB3 45x325mm^2	Kerto S 51x300 mm^2

5.1.4 **Fat-beam**

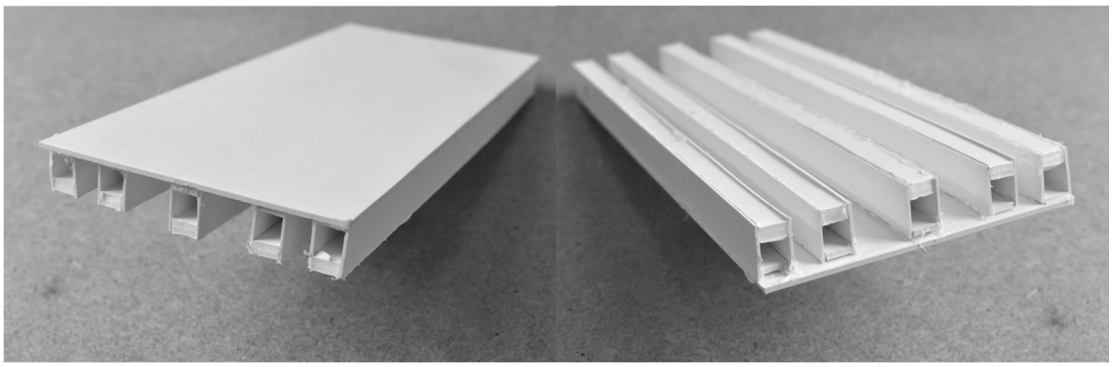

Figure 5.5 Model of the fat-beam concept.

The proposed structural system is open. A transversal flexural rigidity could be introduced by adding a strongback or a truss. The structural system is mainly considered for one-way action.

The model is very rigid in bending in longitudinal direction. It is not rigid in transversal direction or in torsion.

Table 5.4 Alternative material combinations of the fat-beam concept.

	Type of action	Compression flange	Web	Tension flange
1	One-way	Kerto Q t=33 mm C14 45x220 mm^2	OSB3 349x9 mm^2 (2 pcs)	Glulam 90x220 mm^2
2	One-way	Kerto Q t=33 mm C14 45x220 mm^2	OSB3 349x9 mm^2 (2 pcs)	Kerto S 75x220 mm^2

5.1.5 Properties of the different concepts

The cross-section properties of the proposed concepts are gathered in Table 5.5.

Table 5.5 Cross-section properties of the proposed concepts.

	$(EI)_L$ [MNm^2/m]	$(EI)_L/m$ [MNm^4/kg/m]	Cross-section area [m^2/m]
Benchmark	5.33	0.069	0.049
Trapezoid 1	23.8	0.252	0.082
Trapezoid 2	21.2	0.269	0.059
Trapezoid 3	21.3	0.259	0.075
Grid 1	18.2	0.184	0.125
Grid 2	22.3	0.241	0.081
Big flange	21.9	0.237	0.081
Fat-beam 1	22.4	0.257	0.094
Fat-beam 2	25.1	0.280	0.089

5.2 New concepts – Results

The concepts with respective materials were evaluated with regard to the design criteria suggested in this project. Calculations were performed analytically using Euler-Bernoulli theory with the assumption of full interaction. The results give an indication of the performance, but are overestimated. The performance of the two-way action concepts are predicted numerically using FEM. The results are divided into two separate graphs in order to further stress that Euler-Bernoulli omits shear deformation and thus overestimates the first eigenfrequency.

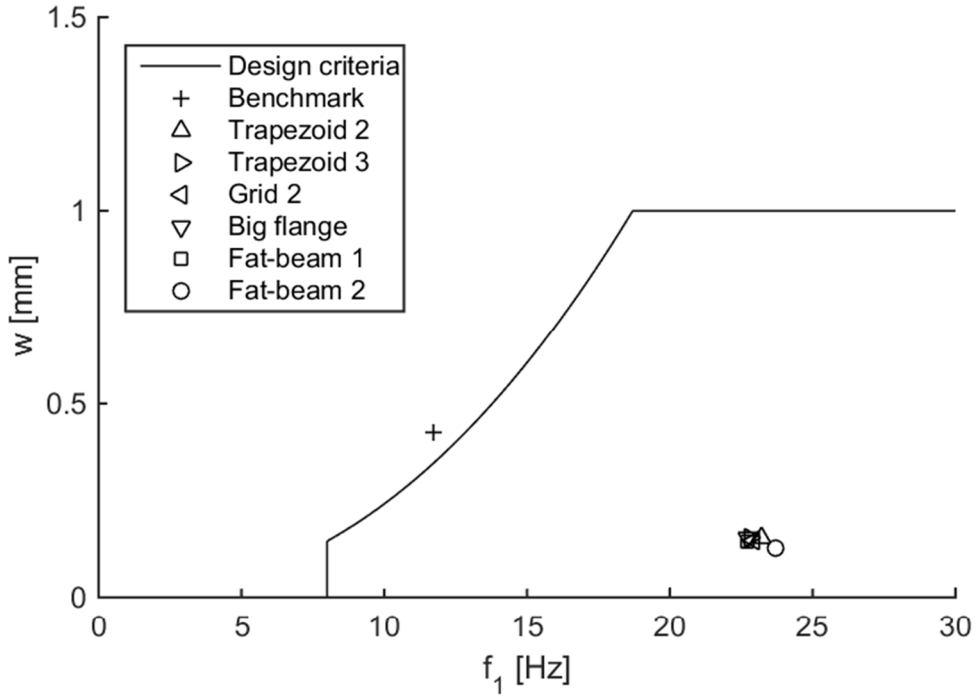

Figure 5.6 Performance of the new concepts with one-way action.

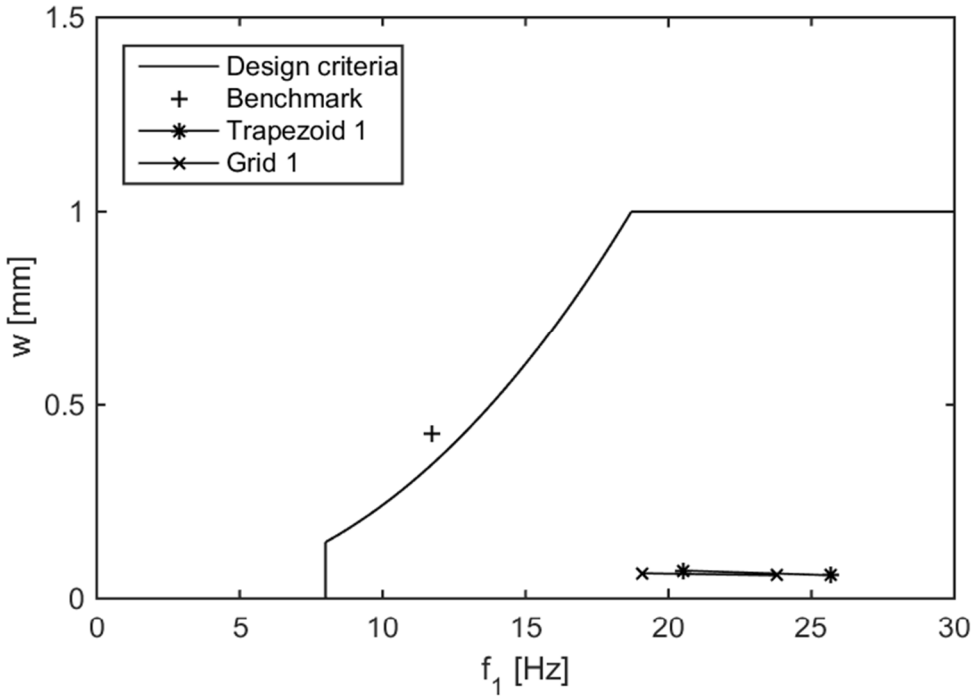

Figure 5.7 Performance of the new concepts with two-way action. The first mark from the left is B/L=1.5 and the second mark is B/L=1.0.

5.3 New concepts – Discussion

Figure 5.6 shows the performance of all the one-way action alternatives in relation to the design criteria suggested. As all concepts were given the same compression flange, 33 mm Kerto Q, or equivalent plywood, they were thus also given the same E_1A_1. In order to balance the cross-section and keep the neutral layer in the centre of the cross-section all concepts were given a similar E_2A_2 – thus they perform equally. All the concepts use significantly more material than the benchmark floor. The materials are also relatively stiff. Thus, it is not surprising that the new concepts perform much better than the benchmark floor when evaluated theoretically.

Figure 5.7 shows the performance of the trapezoid 1 and grid 1 concepts evaluated with two-way action in the B/L range 1.0-1.5. Even though full interaction in all joints is assumed the improved effect of two-way action when B/L=1.0 is not substantial. However, the comparison between the numerical and analytical evaluations in Figure 5.6 is not very fair. The numerical evaluation includes the effect of shear which is omitted in when using Euler-Bernoulli beam theory. For concepts with thin webs the effect of shear can contribute to a considerable reduction of the first eigenfrequency.

The main drawback for timber compared to steel or concrete when it comes to two-way action is that no timber material is stiff in two directions in the same plane. Plywood, for example, does not utilise its plies in the transversal direction when loaded in the longitudinal direction. Manufacturing and assembling a two-way system might also be much more complex than a one-way system.

However, the possibility of casting concrete on the top plate might make a two-way floor worth developing. Concrete, with its isotropic properties in compression, would add stiffness in two directions if situated in the compression zone. Historically it has been too complicated to create a stiff connection in-between the materials; an old Tuscan proverb says: "No art, no skill are so good to match cement to wood". This is, however, not true anymore since techniques have been developed to achieve full composite action of a concrete layer in compression cast upon timber members in tension (Ceccotti 2002). If this is done the stiffness is dramatically increased (Persaud & Symons 2006).

Concrete-timber floors are used in several countries. In Finland, it is quite common with concrete on top of a timber floor for acoustic reasons and not that common with composite action, although it exists[1]. The concrete is cast either in a factory or in situ. For the in situ casting a plastic is used between the timber and the concrete to limit the amount of moisture transfer. Nail plates are punched through the plastic to ensure the composite action.

The two-way action structural systems are considered too complicated to further develop in this project but if such a system could be easily manufactured, especially one with a trapezoidal web, it would be an excellent solution for a timber floor with concrete on top.

The one-way fat-beam concept offers a simple solution to achieve a high flexural rigidity using a good mixture of low quality and high quality material, see Figure 5.8. The structural system is open and as the webs will carry minimal stresses, holes can be introduced to allow for transversal installations or strongbacks. The double web makes it easy to use a large bottom flange while the cross-section remains robust and insensitive to impacts during the building time. The large surfaces where connections are to be made will make the concept easier to prefabricate. Large areas that can be glued give less slip in the joints. Especially, the broad stud at the upper flange makes the vital connections between beam and upper plate as well as between whole pre-fabricated floor elements easier. If the space at the building site does not allow for installation of whole floor elements with 2.4 metres width, it is possible to prefabricate the beams only and make the connection between the upper flange and the top plate on site.

A possible problem with the fat-beam concept could be distortions of the stud at the upper flange. To achieve the rigid connection it is important that cupped, twisted or crooked specimen are omitted from the manufacturing process after drying to 12% moisture content.

[1] Mail correspondence 2015-05-04 with senior advisor Tomi Toratti at Confederation of Finnish Construction Industries.

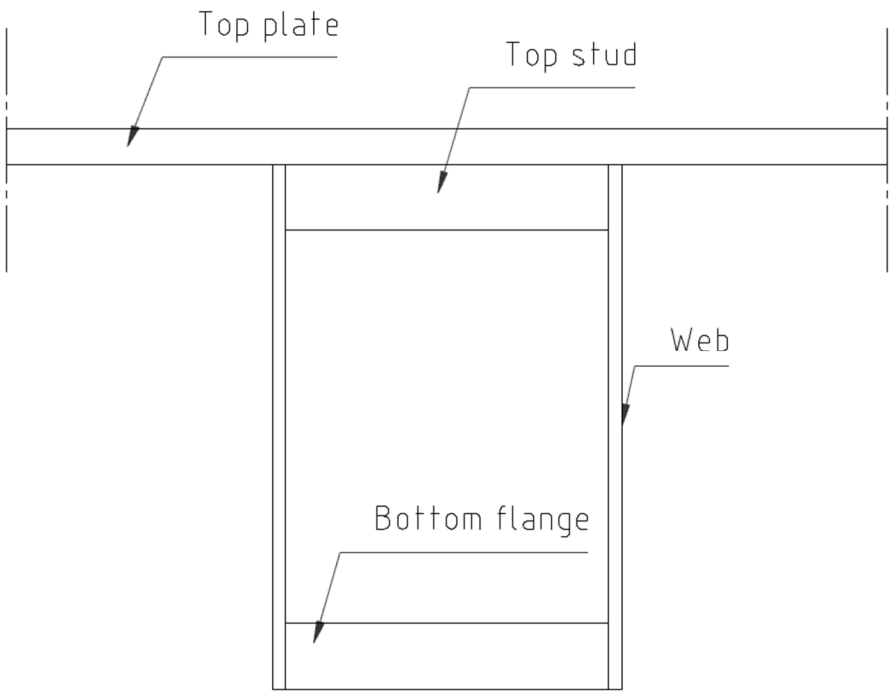

Figure 5.8 A principal sketch of the cross-section of the fat-beam.

6 The fat-beam concept

From the discussion in the previous chapter it is concluded that the fat-beam concept is promising. The purpose of this chapter is to further evaluate this concept regarding the aspects span length, openings in the web and interaction with a primary beam. A comparison between the analytical and numerical results will also be conducted since thin-webbed beams may have large shear deformations affecting the longitudinal eigenfrequencies. For a thorough description of the modelling procedure and results see Appendix B.

6.1 Evaluation of the fat-beam concept

As mentioned in Chapter 1, the possibility of spanning greater lengths is important for the increased use of timber floors. It is also beneficial to being able to make openings in the web for insertion of continuous transversal stiffeners and technical installations. To be able to use primary beams as supports, instead of walls, is important if timber floors should gain a greater market in the commercial building sector. Flexibility of the floor plan is often a great concern in such projects.

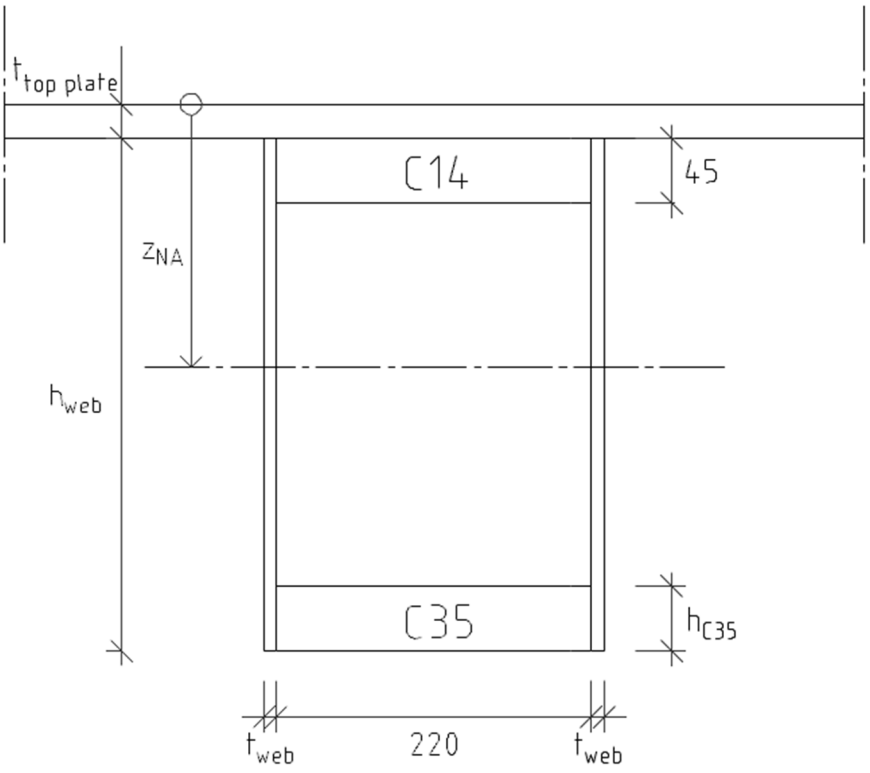

Figure 6.1 Cross-section of the fat-beam

In Table 6.1 the properties of the various fat-beam cross-sections can be seen. The reason for choosing plywood instead of Kerto Q in the top plate is that the local deflection, between the beams, will decrease.

Table 6.1 Cross-section properties of the various fat-beam versions studied.

	Total construction height	Compression flange	Web	Tension flange
A	300 mm	Plywood (P30) $t_{top\ plate}$ = 24 mm	OSB/3 h_{web} = 276 mm t_{web} = 9 mm	Structural timber (C35) h_{C35} = 45 mm
B	350 mm	Plywood (P30) $t_{top\ plate}$ = 24 mm	OSB/3 h_{web} = 326 mm t_{web} = 9 mm	Structural timber (C35) h_{C35} = 70 mm
C	382 mm	LVL (Kerto Q) $t_{top\ plate}$ = 33 mm	OSB/3 h_{web} = 349 mm t_{web} = 9 mm	Structural timber (C35) h_{C35} = 70 mm
D	450 mm	Plywood (P30) $t_{top\ plate}$ = 48 mm	OSB/3 h_{web} = 402 mm t_{web} = 9 mm	Structural timber (C35) h_{C35} = 90 mm
E	382 mm	Plywood (P30) $t_{top\ plate}$ = 24 mm	OSB/3 h_{web} = 349 mm t_{web} = 9 mm	Structural timber (C35) h_{C35} = 45 mm
F	382 mm	Plywood (P30) $t_{top\ plate}$ = 24 mm	OSB/3 h_{web} = 349 mm t_{web} = 15 mm	Structural timber (C35) h_{C35} = 45 mm
G	382 mm	Plywood (P30) $t_{top\ plate}$ = 24 mm	OSB/3+Steel h_{web} = 349 mm $\mathbf{t_{web}}$ = 9+2 mm	Structural timber (C35) h_{C35} = 45 mm
H	750 mm	Plywood (P30) $t_{top\ plate}$ = 48 mm	OSB/3 h_{web} = 702 mm t_{web} = 12 mm	Structural timber (C35) h_{C35} = 90 mm

Table 6.2 Geometry of the modelled fat-beam concepts

	Span x width	Boundary conditions	Number of strongbacks	Size of strongback
E1/F/G	5.92 x 2.4 m^2	Two simply supported, two free	1	220 x 45 mm^2
E2	5.92 x 2.4 m^2	Two simply supported, two free	3	220 x 45 mm^2
E3	5.92 x 7.2 m^2	Simply supported along all four edges	3	220 x 45 mm^2
H	9.6 x 16.2 m^2	Simply supported along all four edges	5	500 x 70 mm^2

6.1.1 **Span length**

The possible span length is dependent on the construction height and the distance between the joists. For this study a spacing between the joists of 600 mm was assumed while the construction height and span was altered. A non-structural mass of 50 kg was also added. One strongback, at mid-span, was modelled. The versions studied were A, B, C and D.

6.1.2 Openings in the web

The material strength in ULS is almost never a limiting parameter for timber floors, in most cases the stiffness and dynamic properties in SLS will be deciding. This means that timber beams in general, have a low utilization ratio of material stresses, making holes in the web possible quite near the supports.

The shear stresses around a hole in a timber beam are not easily calculated with accuracy. The Eurocode does not include equations concerning this and the recommendations in the German standard DIN 1052 were withdrawn in 2007 since they were thought to lead to unsafe design (Danielsson, 2008). Anyhow, the average shear stress can be calculated by Equation (6.1), which was done for the fat-beam concept. Only the area of the flanges was considered since a hole would preferably be as large as the distance between these. A similar check was made for the bending stress with the use of Equation (6.2). The utilization ratio of the average shear stress was then added to that of the bending moment. If their sum is less than 1.0, the flanges can carry both the bending moment and the shear force.

$$\tau(x) = \frac{V(x)}{A} \tag{6.1}$$

where $V(x)$ is the shear force and A is the area of the cross-section

$$\sigma(x) = \frac{M(x)}{I} z_{NA} \tag{6.2}$$

where $M(x)$ is the bending moment, I is the moment of inertia and z_{NA} is the distance to the neutral axis.

One span length for each of the concepts A, B, C and D is chosen for the control; the longest acceptable span according to Figure 6.2. The load considered is that of residential load in ULS, 2 kN/m^2, times the γ-factor 1.5. The dead weight is multiplied by the γ-factor 1.35.

Another issue with openings in the webs is that they influence the eigenfrequencies. To investigate to what extent these holes affect the first eigenfrequency the fat-beam concept was modelled with one and three holes respectively (versions E1 and E2).

6.1.3 Transversal stiffness

To calculate the impact of the strongbacks on the first eigenfrequency, the fat-beam concept E was modelled as one element (2.4 x 5.92 m^2) supported on two sides and a whole floor (7.2 x 5.92 m^2) supported on four sides (versions E2 and E3). The strongbacks increase the first eigenfrequency only when the floor is supported on four sides.

6.1.4 Comparison between analytical and numerical results

As the webs of the fat-beam concept are thin compared to other timber floors it might show larger differences between analytical and numerical calculations than comparable products, due to shear deformations. Therefore a parametric study on the

stiffness of the web was conducted. The first eigenfrequency of three models with different webs were compared; E1, F and G in Table 6.1.

6.1.5 Case study – Landvetter airport

One of the strengths of timber is its low weight. This property can be particularly important in retrofitting projects where the space for lifting equipment is limited. Version H is the one that is considered.

6.1.5.1 Properties of the building

The hall of Landvetter airport for domestic flights spans the height of two storeys and a new level should be retrofitted in-between these. It is a complex building situation since as much as possible of the surrounding activitites should continue during the building time, making it difficult to use large and heavy pre-fabricated elements.

The customer stresses that how the floor feels is of paramount importance. It is important that people do not experience a difference when walking on the new floor compared to the adjacent concrete floors.

The floor needs to be supported on a primary beam with a length equal to the floor width. The first eigenfrequency of this beam will affect the first eigenfrequency of the whole system. A lower bound solution for the frequency of the whole system is obtained using Equation (1.2). The deflection as a result of a 1 kN point load is calculated for the whole system considering deflection of the floor structure and the primary beams.

6.1.5.2 Suggested solution

The suggested properties for the floor are according to version H in Table 6.1 and Table 6.2. The maximum construction height is 1 metre. A welded steel beam 1000 mm high with 30 mm flanges is suggested as primary beam to span the whole floor width. Another alternative would be to put a column at mid-span. Then there would be two steel beams each spanning 8.0 metres. An FE-model was created for the timber floor while the results for the beams were calculated analytically only.

Table 6.3 Properties of the structural elements of the case study.

	EI	Self-weight	Added dead weight
Floor structure	104 MNm^2/m	56 kg/m^2	50 kg/m^2
Steel beam	1,0 GNm^2	214 kg/m	510[1] kg/m

6.2 Performance of the fat-beam concept – Results and discussion

The results from the dynamic and static controls of the fat-beam concept are presented below together with the results from the case study.

[1]Total weight from the floor self-weight and added dead weight on each beam.

6.2.1 **Span length**

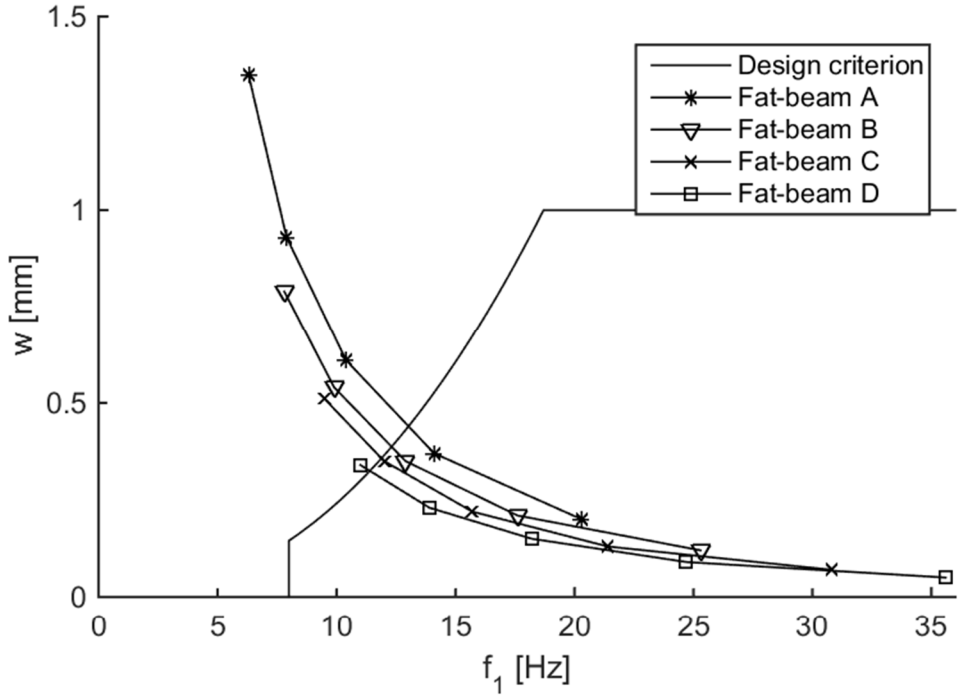

Figure 6.2 *First eigenfrequency and deflection for versions of the fat-beam concept. The marks represent the span lengths; beginning with five metres for the rightmost mark of each line and increasing by one metre each mark, giving the leftmost mark of each line a span length of nine metres.*

The fat-beam concept performs well for the suggested span lengths, if the construction height is adjusted accordingly. Figure 6.2 indicates that a reasonable lowest limit of span-to-depth ratio is 1/20.

6.2.2 **Openings in the web**

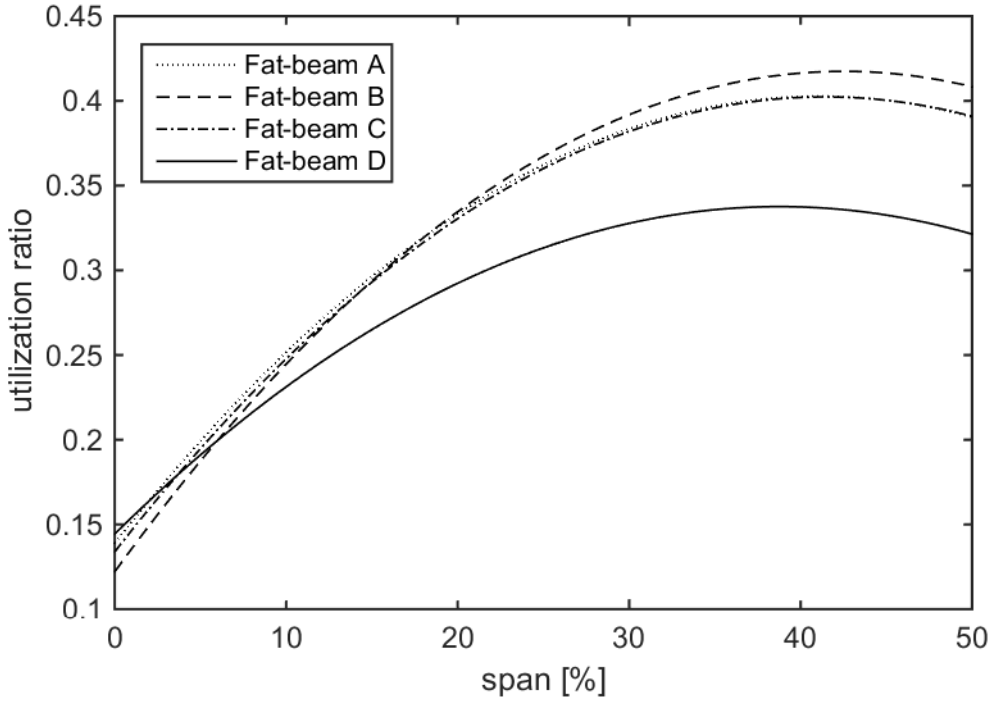

Figure 6.3 *Utilization ratios for longest acceptable span width according to Figure 6.2.*

The strength under static load (ULS) is not utilized to a great extent for any version that is regarded acceptable by the dynamic criteria, see Figure 6.3. This indicates that a limited amount of holes can be made in the web. The holes will not affect the first eigenfrequency to a great extent, as can be seen in Table 6.4.

Table 6.4 *The results from the calculations on the first eigenfrequency with one opening (E1) and three openings (E2) in the web.*

		E1	E2
First eigenfrequency	Numerical	15.4 Hz	15.3 Hz
	Analytical	20.0 Hz	20.0 Hz

6.2.3 **Transversal stiffness**

Table 6.5 *Comparison between a two-side supported floor element (E2) and a four-side supported floor (E3), each with three strongbacks.*

		E2	E3
First eigenfrequency	Numerical	15.3 Hz	17.0 Hz
	Analytical	20.0 Hz	20.0 Hz
1 kN point load deflection	Numerical	0.28 mm	0.19 mm
	Analytical	0.15 mm	0.15 mm

If supported on four sides, the first eigenfrequency is clearly affected by the introduction of transversal stiffness through the use of strongbacks, even though the

transversal stiffness is much less than the longitudinal. The deflection is also positively affected making it worth some effort to achieve two-way action in practice.

6.2.4 Comparison between numerical and analytical results

Table 6.6 Numerical and analytical results of first eigenfrequency with changes in the properties of the web.

		E1	F	G
First eigenfrequency	Numerical	15.4 Hz	16.4 Hz	19.5 Hz
	Analytical	20.0 Hz	19.8 Hz	19.6 Hz

Shear deformations have a large impact on the first eigenfrequency, as can be seen in Table 6.6. If OSB-webs of 9 mm or 15 mm thickness are used the numerical first eigenfrequency is 23% lower (E1) respectively 17% lower (F) than the analytical. If steel would be glued to the joists, the difference between the numerical and the analytical methods would decrease to almost nothing (G).

6.2.5 Case study

For the case study, version H of the fat-beam concept was studied.

Table 6.7 Results from the analyses of the floor.

Timber structure	f_1	Deflection, point load
Floor, FE-model	17 Hz	0.09 mm
Floor, analytic	17 Hz	0.10 mm

Table 6.8 Results from the analyses of the primary beam.

Loaded beam	f_1	Deflection, point load
Steel beam 16,2 m	7.2 Hz	0.04 mm
Steel beam 8,0 m	29 Hz	0.01 mm

Table 6.9 Results from the analyses of the system.

Whole system	f_1	Deflection, point load
Steel beam 16,2 m	6.7 Hz	0.14 mm
Steel beam 8,0 m	15 Hz	0.11 mm

The calculations from the case study show that light floor structures, like timber floors, should preferably be supported on continuous rigid supports, like walls, or on beams with a very high first eigenfrequency. When the beam with an eight metre span was used, the system is acceptable according to the performance criteria.

If supported on long beams it is very likely that the first eigenfrequency for the system will be lower than 8 Hz. The situation is quite similar to a case of a timber floor supported by steel beams studied by Salmela et al. (2006) where the users experienced annoying vibrations from people walking on the same floor. A first eigenfrequency of the system of 5 Hz was measured. This was a much smaller system

compared to the floor studied here, making the impact of a walking person relatively large. A low first eigenfrequency does not have to result in an unsatisfying dynamic performance, but the structure is no longer classified as a high-frequency floor. A deeper study, involving a more realistic load situation and more dynamic parameters needs to be performed. This is, however, not in the scope of this project.

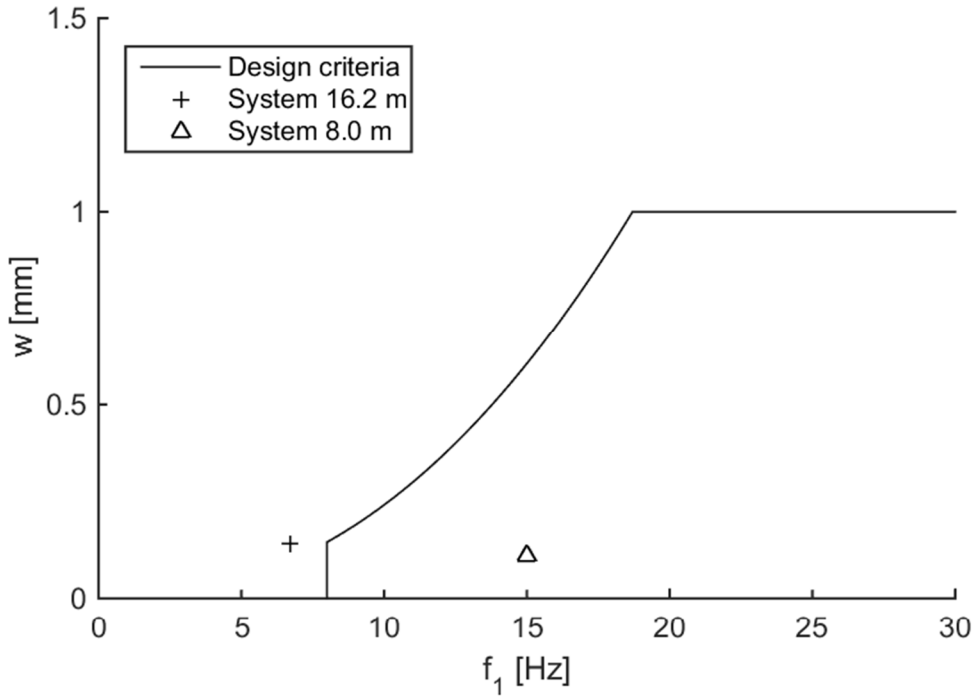

Figure 6.4 *Performance of the case study floor systems from Table 6.9 compared to the chosen criteria.*

7 Conclusions

In this chapter the most important conclusions from the sub-studies have been summarised.

7.1 Design criteria

The design criteria for evaluation of the dynamic response, in addition to the guidelines of Eurocode 5, were chosen as

$$f_1 > 8 \text{ Hz} \tag{7.1}$$

$$18.7 \leq \frac{f_1}{w_{1kN}^{0.44}} \tag{7.2}$$

$$w_{1kN} \leq 1.0 \text{ mm} \tag{7.3}$$

The 1 kN point load deflection was calculated according to the UK National Annex to Eurocode 5, see Equation (2.18). It would be beneficial for the European timber industry to achieve some coherence on the way the load distribution should be calculated and what limit should be used for the 1 kN point load deflection.

When evaluating a composite beam with a web made of wood-based products, the analytically calculated first eigenfrequency will be overestimated since the Euler-Bernoulli beam theory neglects the shear deformations. This is important to bear in mind during the design.

7.2 Benchmark floor

The results from the experiment show a small overestimation of the first eigenfrequency (first longitudinal mode) from the prediction methods to reality, and a larger overestimation of the second longitudinal mode. This was probably due to slip in the connection between the top flange and the joist. The connection would have been stiffer if screws had been used instead of nails (Bernard 2008). Still, if the connection lowers the stiffness in such a simple construction as this, it is probably not easy to make a more complicated composite beam considering full composite action.

The overestimation of the transversal modes in the numerical model is very large. This shows that the blockings do not contribute to the transversal stiffness to a great extent during dynamic loading. They do, however, distribute the load between the beams when statically loaded. Significant transversal stiffness would probably be difficult to obtain if not continuous blockings were used.

The use of sylomer® blocks sr28 at the supports does increase the damping but lowers the first eigenfrequency. The effect of this is ambiguous and more research is needed.

An easy way to improve the benchmark floor would be to change the material of the top flange to a stiffer one, for example plywood P30.

7.3 New concepts

A structural system with flexural rigidity in two directions (i.e. two-way action) could be an effective way to increase the first eigenfrequency, in particular if the floor has an equal width and span length. In order to achieve similar flexural rigidity in both directions it would be beneficial to use a material that is stiff in both directions. A way to achieve a better concept than the one proposed in this project might be to introduce a timber-concrete composite floor. However, more development is needed on the subject in order to introduce a two-way action system that is practical to produce and assemble.

The fat-beam concept presented in Chapter 5.1.4 and Chapter 6 is considered as a very promising concept for further development;

1. It enables the use of low-quality material where it is possible and high-quality material where it is crucial, due to a good arrangement of the cross-section.

2. It utilises an open structural system, making the insertion of technical installations possible on site.

3. Holes can be cut in the web making the insertion of continuous strongbacks and technical installations possible.

4. The contact areas between the different parts in the cross-section are large making it possible to achieve good interaction.

The analytical evaluation of the fat-beam concept shows that a suitable minimum span-to-depth ratio would be 1/20. However, the numerical calculations are more reliable since they take shear deformations into account. To decrease the impact of the shear deformations of the web it is suggested to use a thin steel sheet glued to the OSB web. If this is done, simple analytical calculations show good results in predicting the first eigenfrequency.

8 Suggestions for further research

This project has been limited to high-frequency floor structures, since most of the timber floors can be classified as such. However, if concrete is to be used on the top plate, preferably in full composite action with the rest of the structure, the self-weight could be increased several times. The structure might then fall outside the high-frequency limit of 8 Hz and the evaluation. More research on the acceptability of such timber-concrete composite floors is needed.

Would it be possible to create a practical two-way action system using timber as a main material? Another suggestion for further research is to develop such a system that could be used for quadratic floors with long spans and that is practical to produce and assemble.

Most design criteria available today omits the damping of the floor as it is very difficult to estimate. However, Bernard (2008) obtained a very good subjective rating on an excessively damped floor $\zeta_1 = 6.6\%$ with a low first eigenfrequency $f_1 = 10.3$ Hz. Table 3.2 shows how the modal damping is increased for the first mode of the benchmark floor while the first eigenfrequency is decreased when using sylomer® dampers at the supports. The possible positive effect of this increased modal damping is not recognised by the design criteria suggested for this project. A subjective rating of excessively damped light-weight floors would be interesting for a further understanding of the impact of the relation between eigenfrequency and damping on the perception of vibration in light-weight floors.

Ohlsson (1988) points out the importance of measuring the 1 kN point load deflection at the most flexible point of the floor, considering both local and global deflection. The local compliance might contribute to the perception of vibration but the experience of the authors is that it is customary in Sweden to consider only the global deflection when designing a timber floor. More research is needed on how the local deflection affects the overall performance of the floor.

9 References

Al-Foqaha'a, A.A., 1997. *Design Criterion for Wood Floor Vibrations via Finite Element and Reliability Analyses*. Ann Arbor: UMI. (Doctoral Dissertation at the Department of Civil and Environmental Engineering, Washington State University, UMI Number 9907074).

Bernard, E.S., 2008. Dynamic Serviceability in Lightweight Engineered Timber Floors. *Journal of Structural Engineering*, vol. 134, pp. 258–268.

Ceccotti, A., 2002. Composite concrete-timber structures. *Progress in Structural Engineering and Materials*, vol. 4, no. 3, pp. 264–275.

Chui, Y.H., 2002. Application of ribbed-plate theory to predict vibrational serviceability of timber floor systems. In *Proceedings of the 7th World Conference on Timber Engineering*.

Chui, Y.H., 1987. *Vibrational performance of wooden floors in domestic dwellings*. Ann Arbor: UMI. (Doctoral dissertation at Department of Applied Sciences, Brighton Polytechnic, U018989).

Craig Jr, R.R. & Kurdila, A.J., 2006. *Fundamentals of Structural Dynamics.* 2nd ed., Hoboken: John Wiley & Sons.

Danielsson, H., 2008. *The strength of glulam beams with holes*. (Licentiate Thesis at the Department of Construction Sciences, Structural Mechanics, LTH, Lund University, 1513943).

Dolan, J.D. et al., 1999. Preventing Annoying Wood Floor Vibrations. *Journal of Structural Engineering*, vol. 125, pp. 19–24.

Ewins, D.J., 2000. *Modal testing.* 2nd ed., Philadelphia: Research Studies Press Ltd.

Hamm, P., Richter, A. & Winter, S., 2010. Floor vibrations – new results. In *Proceedings of the 10th World Conference on Timber Engineering*. Riva del Garda, Italy.

Hu, L.J., 2002. Development of a performance criterion for controlling vibrations in wood-based floors. In *Proceedings of the 7th World Conference on Timber Engineering*. Shah Alam, Malaysia.

Hu, L.J. & Chui, Y.H., 2004. Development of a Design Method to Control Vibrations Induced by Normal Walking Action in Wood-Based Floors. In *Proceedings of the 8th World Conference on Timber Engineering*. Lahti, Finland.

Hu, L.J., Chui, Y.H. & Onysko, D.M., 2001. Vibration serviceability of timber floors in residential construction. *Progress in Structural Engineering and Materials*, vol. 3, pp. 228–237.

Jacobsen, L.S. & Ayre, R.S., 1958. *Engineering Vibrations with Applications to Structures and Machinery*, New York: McGraw Hill Book Company.

Jarnerö, K. et al., 2014. Vibration performance of lightweight floors in multi-family houses - Resident survey and field measurements. *Submitted to Applied Acoustics*.

Jarnerö, K., Brandt, A. & Olsson, A., 2010. In situ testing of timber floor vibration properties. In *Proceedings of the 11th World Conference on Timber Engineering*. Riva del Garda, Italy.

Lenzen, K.H., 1966. Vibration of Steel Joist-Concrete Slab Floors. *ENGINEERING JOURNAL-AMERICAN INSTITUTE OF STEEL CONSTRUCTION INC*, vol. 3, pp. 133–136.

Negreira, J. et al., 2015. Psycho-vibratory evaluation of timber floors – Towards the determination of design indicators of vibration acceptability and vibration annoyance. *Journal of Sound and Vibration*, vol. 340, pp. 383–408.

Ohlsson, S., 1982. *Floor vibrations and human discomfort*. Gothenburg: Chalmers Univeristy of Technology. (Doctoral Dissertation at the Department of Structural Engineering, Chalmers University of Technology, ISBN 91-7032-077-2).

Ohlsson, S., 1988. *Springiness and human-induced floor vibrations - a design guide*, Gothenburg: Swedish Council for Building Research.

Onysko, D.M., 1985. *Serviceability Criteria for Residential Floors Based on a Field Study of Consumer Response*, Ottawa: Canada´s Wood Products Research Institute.

Persaud, R. & Symons, D., 2006. Design and testing of a composite timber and concrete floor system. *Structural Engineer*, vol. 84, no. 4, pp. 22–30.

Salmela K., Källsner B. & Petersson.H., 2004. Vibrations of wooden floor elements on supporting steel framework, In *8th World Conference on Timber Engineering, Lahti, Finland*.

Smith, I., 2003. Vibrations of Timber Floors: Serviceability Aspects. In *Timber Engineering*. eds. H. Thelandersson & H. J. Larsen, pp. 241-266. Chichester: John Wiley & Sons.

Toratti, T. & Talja, A., 2006. Classification of Human Induced Floor Vibrations. *Building Acoustics*, vol. 13, no. 3, pp. 211–221.

Zhang, B. et al., 2013. Comparison of vibrational comfort assessment criteria for design of timber floors among the European countries. *Engineering Structures*, vol. 52, pp. 592–607.

Appendix A – full scale experiment

This appendix contains a dynamic test and a static test of two timber floor elements created by the timber house producer A-hus. The site of the test is in the production plant complex of A-hus in Anneberg, Sweden.

The main purpose of the test is to measure the eigenfrequency and damping ratio of the first five eigenmodes and the 1 kN point load deflection when the test specimen is simply supported on two sides.

The dynamic test is an experimental modal analysis and is in principle carried out by setting the test specimen in motion by striking them with an impact hammer while measuring the acceleration with an accelerometer. In order to introduce the reader to the concept a text on the very fundamentals of experimental modal analysis is added to this appendix.

The static test is in principle carried out by adding a load to the test specimens and measuring the resulting deflection.

1 Test site and test specimens

1.1 Test site

The testing site available is a building that is part of the A-hus production plant complex. The building is used for cutting material and supplies other parts of the production plant complex with pre-cut material. In this building there is a large unused area that is available for this test. However, there is ongoing manufacturing and truck traffic close to the testing site. It is important to note that this can disturb the measurements. It is in particular crucial when a truck passes as this might cause distinctive vibrations in the floor.

The floor of the building is made of concrete and the building is fully weather protected. The test site is equipped with an over-head crane that can be used to move and lift the test specimen.

Figur0.1 Testing site with the two test specimens and the steel I-beams used for the boundary conditions.

1.2 Test specimens

Two identical test specimens were produced uniquely for the purpose of this experiment. The specimens are called A and B. The specimens have the following geometry;

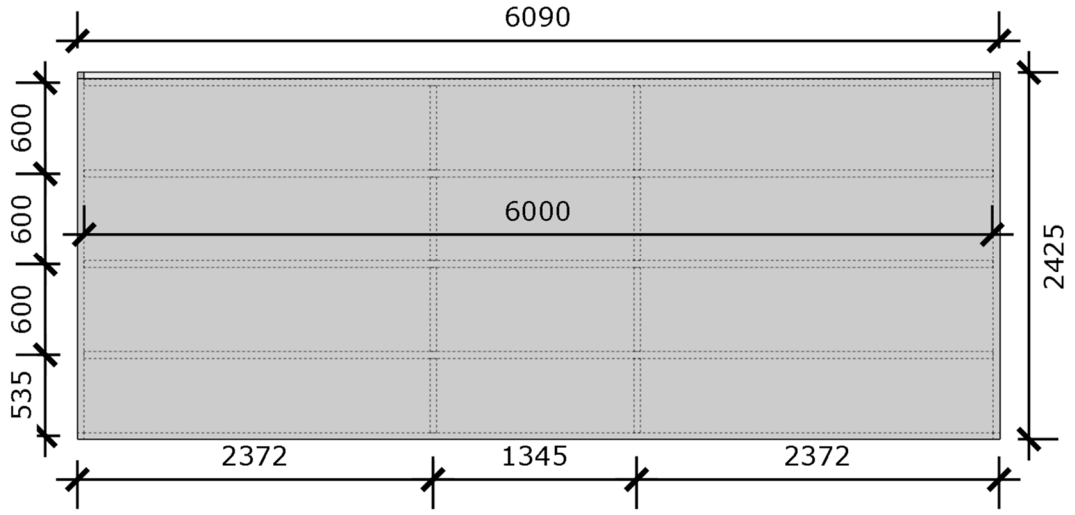

Figure 0.1 Plan sketch of the test specimen A and B.

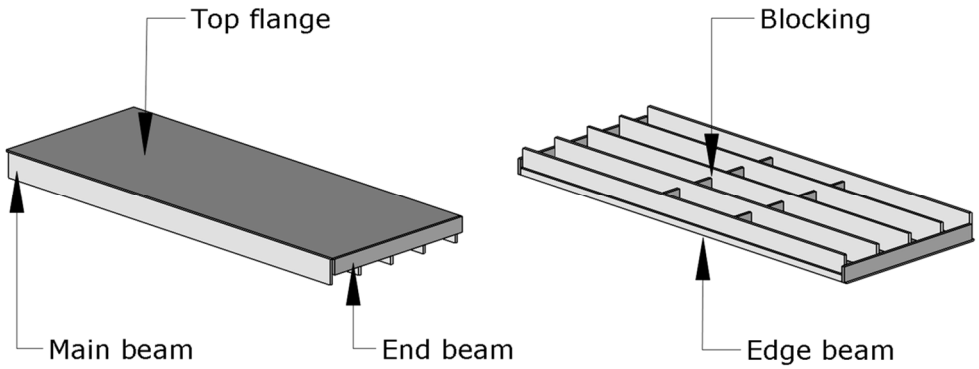

Figure 0.2 Perspective sketch of test specimen A and B.

The effective span of the test specimens is 5920 mm. The materials used for the test specimen are the following;

Table 0.1 Material and dimensions of the parts used for each specimen.

Part	Material	Dimension	Pieces
Top flange	Particleboard P5	22x2394x6090	1
Main beam	Kerto S	45x360x6000	5
Blocking	C24	45x220x555	6
Blocking	C24	45x220x490	2
Edge beam	C24	45x95x6000	1
End beam	C24	45x220x2380	2

2 Dynamic test

The purpose of the experiment is to extract eigenfrequencies and damping ratios from the first five eigenmodes of the test specimen. Furthermore, the mode-shapes of each eigenmode are extracted in order to visually control each eigenmode.

The measurement method used to extract these modal parameters is called *Experimental Modal Analysis*. For a thorough guidance through the theory, practice and application of experimental modal analysis the reader is directed to Ewins (2000).

2.1 Introduction to experimental modal analysis

The fundamental basis for experimental modal analysis is the relation between input and response of the system analysed

$$Input \cdot System properties = Response \tag{2.1}$$

Or with the appropriate notation

$$X_j \cdot C_{ij} = Y_i \tag{2.2}$$

Thus if you measure the input and the response you can find something about your system

$$C_{ij} = \frac{Y_i}{X_j} \tag{2.3}$$

When analysing dynamics of a structure the input and response are dependent on time. In this specific experiment the transient time dependent force $F(t)$ is theinputX_j, and the time dependent acceleration $a(t)$is the response Y_i.

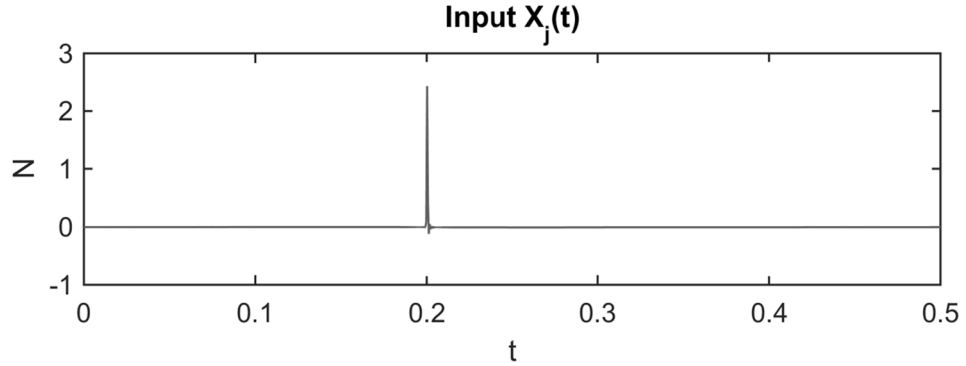

Figure 2.1 Example of a measured input acting on a system.

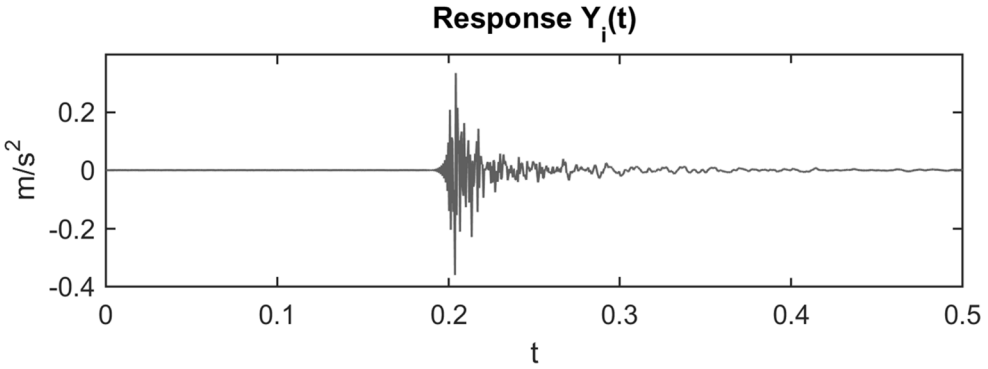

Figure 2.2 Example of a measured response of a system given the input in Figure 2.1.

The system is assumed to be linear meaning that a force at a certain frequency will only contribute to a resulting vibration at this exact frequency. This allows for transformation from the time-domain to the frequency domain. This transformation is called Fourier Transform and the specific technique used in computation is called Fast Fourier Transform – FFT.

$$X_j(t) \overset{FFT}{\longrightarrow} X_j(\omega) \tag{2.4}$$

$$Y_i(t) \overset{FFT}{\longrightarrow} Y_i(\omega) \tag{2.5}$$

The system can now be described by a load-independent transfer function. This transfer function is called a frequency response function, FRF.

$$FRF_{ij}(\omega) = \frac{Y_i(\omega)}{X_j(\omega)} \tag{2.6}$$

Or

$$C_{ij}(\omega) = \frac{Y_i(\omega)}{X_j(\omega)} \tag{2.7}$$

As damping is present the FRF will be complex and can visualised with a bode diagram as in

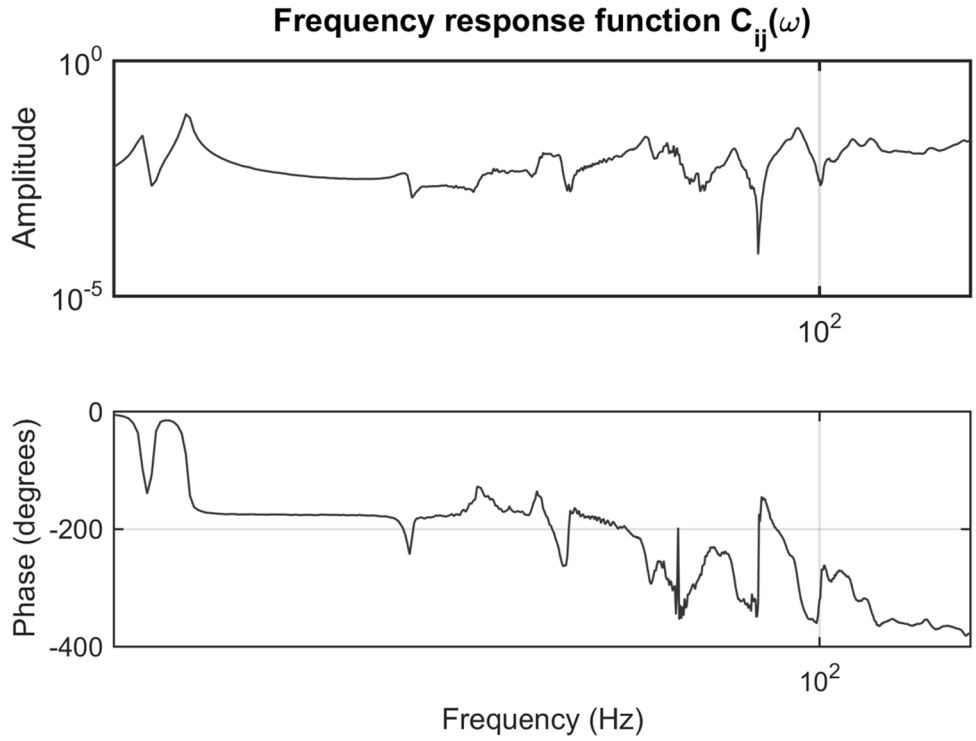

Figure 2.3 Example of a measured bode diagram of $C_{ij}(\omega)$.

A system with n degrees of freedom will have $n \cdot n$frequency response functions. Each FRF, $C_{ij}(\omega)$ holds information about the system and in particular the relation between the input at DOF j and the response at DOF i.

$$\begin{bmatrix} X_1 \\ X_2 \\ \vdots \\ X_n \end{bmatrix} \cdot \begin{bmatrix} C_{11} & C_{12} & \cdots & C_{1n} \\ C_{21} & C_{22} & & C_{2n} \\ \vdots & & \ddots & \\ C_{n1} & & & C_{nn} \end{bmatrix} = \begin{bmatrix} Y_1 \\ Y_2 \\ \vdots \\ Y_n \end{bmatrix} \tag{2.8}$$

Or

$$\tilde{X}(\omega) \cdot \tilde{C}(\omega) = \tilde{Y}(\omega) \tag{2.9}$$

In order to gain full information about the system a full FRF matrix must be obtained. This means that the response must be measured at each DOF while the system is excited by the input at each DOF. However, by assuming reciprocity it is sufficient to obtain one row or one column of the FRF matrix.

It is thus sufficient to measure the response at every DOF while the system is excited at **one** DOF – single input multiple output analysis. It would also be sufficient to excite the system at every DOF while the response is measured at **one** DOF – multiple input single output analysis.

Each FRF contains information about the eigenfrequency, damping ratio and mode amplitude of the system at each eigenmode. It is possible to extract the eigenfrequency and damping ratio from one single FRF. However, in order to establish mode shapes a FRF **matrix** with sufficient data is required.

The extraction of data from a FRF is performed by curve-fitting theoretical models to the measured FRF data - this can be done by numerical or graphical methods. There exist plenty of theoretical models to describe a structural dynamic system that hold the modal parameters of interest.

In this specific experiment a theoretical model called the state-space model is used for curve-fitting the measured FRF data. This is done by utilising the *System Identification Toolbox* for MATLAB.

2.2 Method

This chapter describes how the two test specimens are assessed with regard to the modal parameters of interest. The experiment is sub-divided into three parts:

- Experiment 1: Modal parameter extraction of test specimen A and B on simply supported boundary conditions with the effective span 5920 mm.
- Experiment 2: Modal parameter extraction of test specimen A on simply supporting boundary conditions resting on a damping material (viscoelastic material) with the effective span of 5920 mm.
- Experiment 3: Modal parameter extraction of local panel modes of test specimen A on continuous supports with the effective span of 0 mm.

2.2.1 Measurement equipment

In order to perform the experiment the following measurement equipment was used:

Table 2.1 List of measurement equipment

	Type	Product	Quantity
1	Accelerometer	PCB 333B32	2
2	Impact hammer	PCB 086C03	1
3	Data acquisition system 4CH module	NI 9234	1
4	Coaxial cable	10-32 to BNC plug	2
5	Coaxial cable	BNC to BNC plug	1
6	Beeswax	-	-

Figure 2.4 Measurement equipment.

A PC was used to log the data acquired from the measurements. The PC was equipped with the software TAMARA 0.218 that allowed for real-time FFT of the data andreal-time averaging of each strike.

2.2.2 **Set-up of equipment**

A table was erected at the side of the test specimen were the data acquisition system and the PC for data logging was put. The PC allowed for real-time observation of the measurements so that double strikes or other mistakes could be observed.

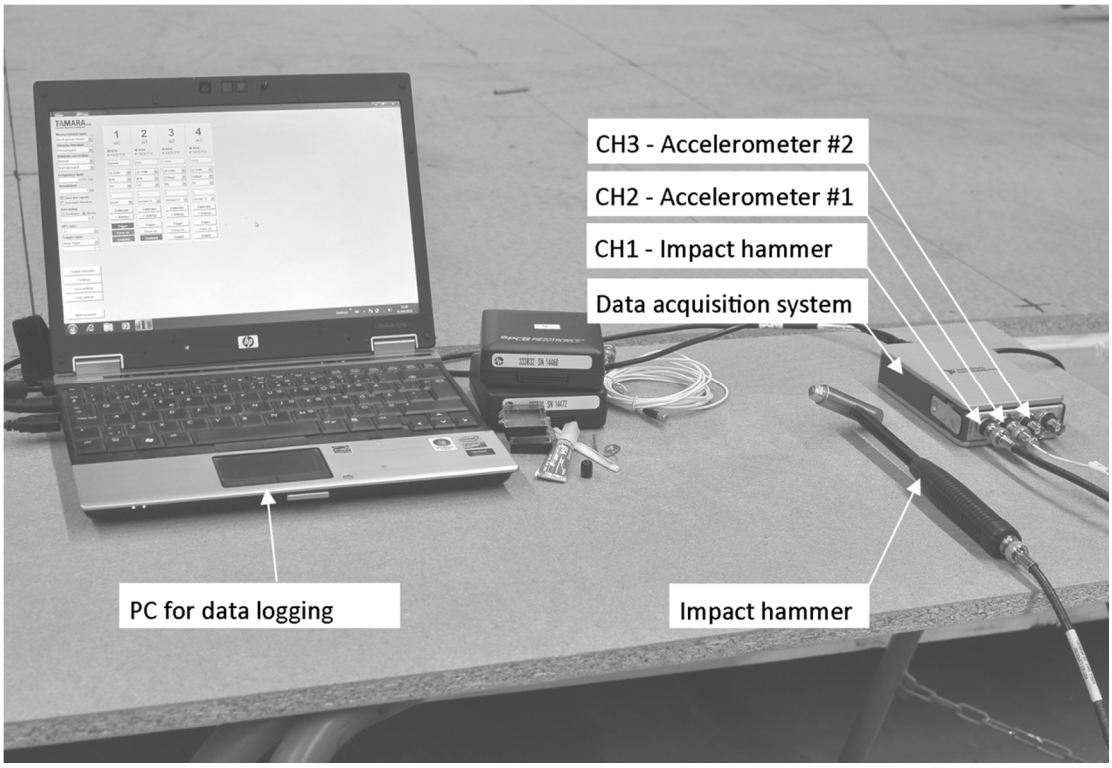

Figure 2.5 Set-up of equipment during experiment.

2.2.3 **Experiment 1 and 2**

Experiment 1 and 2 are presented together as the measurement method used is identical.

2.2.3.1 Measurement points (global bending modes)

In order to capture the first bending modes in both longitudinal and transversal direction 25 measurement points were placed on each test specimen in a grid in the following manner:

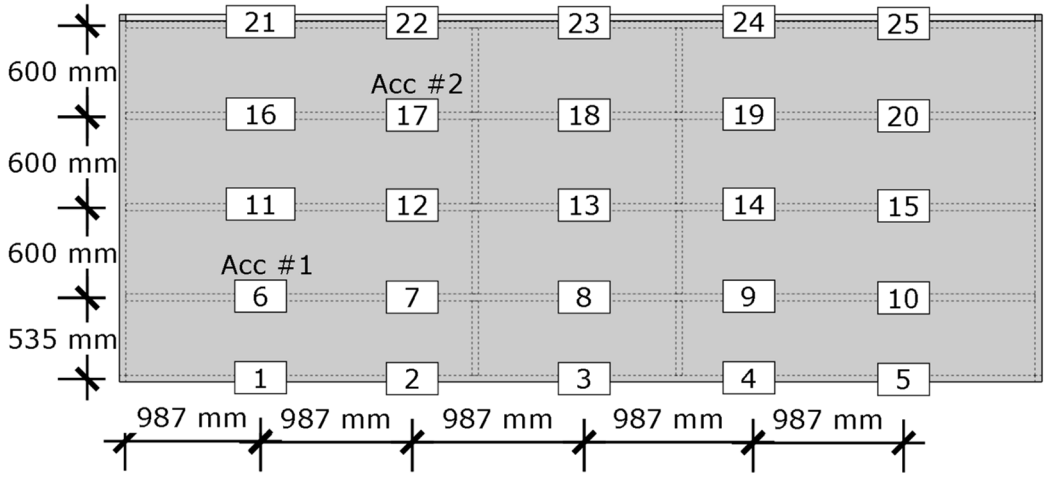

Figure 2.6 Positioning of measurement points.

The accelerometers were positioned at point 6 and 17 on the measurement point grid. To achieve interaction between the accelerometers and the particleboard on the test specimens, bee-wax was used to glue the accelerometers to the surface of the particleboard.

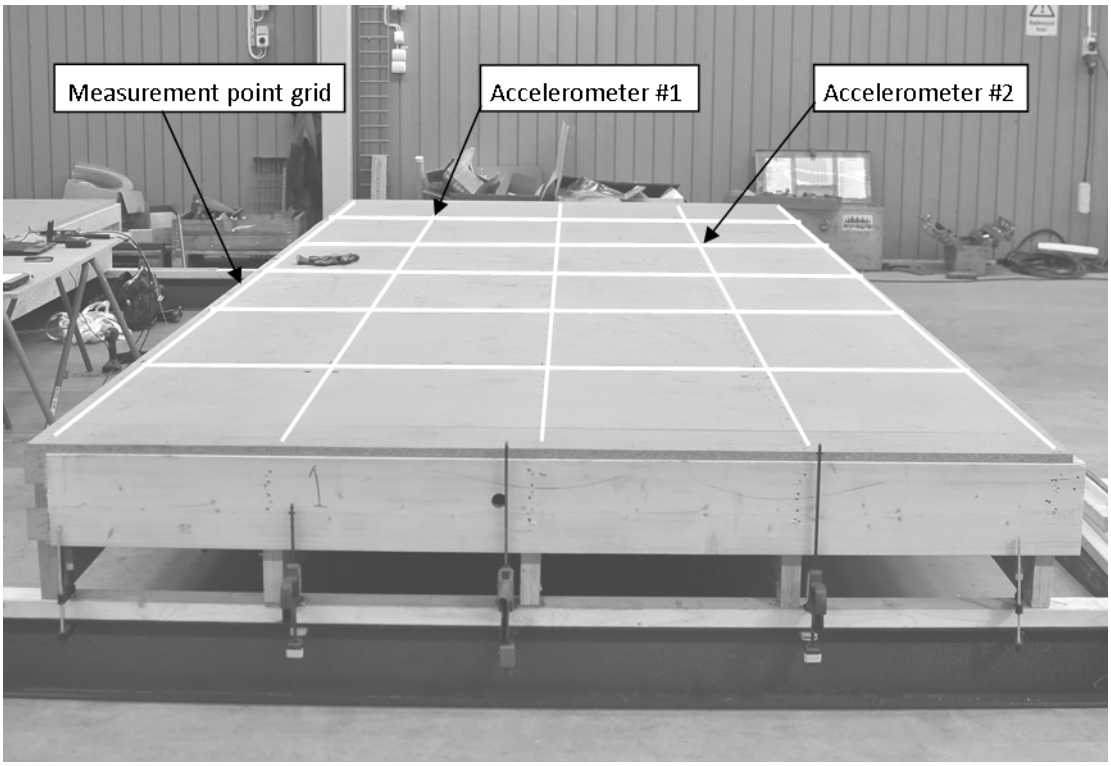

Figure 2.7 Test specimen A with the measurement grid visualised as well as positions for accelerometers.

2.2.3.2 Boundary conditions for experiment 1

The boundary conditions that were attempted to mimic was simply supported on both ends. The test specimens were screwed to a 45x70 timber stud which was fastened to a heavy steel I-beam with clamps in the following manner:

Figure 2.8 Simply supported boundary conditions for experiment 1.

The estimated effective span was with the boundary conditions considered to be 5920 mm.

As the I-beam is simply resting on a concrete slab it can be considered as resting on a spring-support. At low frequencies the whole system will vibrate and contribute with considerable noise to the measurements. However, most of these disturbing vibrations were observed below 10 Hz. As the first fundamental eigenfrequency of the test specimens is predicted above 15 Hz this set-up was considered to be sufficiently accurate.

2.2.3.3 Boundary conditions for experiment 2

The purpose of experiment 2 was to study the effect on the modal parameters of the test specimen when adding a damping material at the supports. The damping material is Sylomer® SR28 from the producer Getzner.

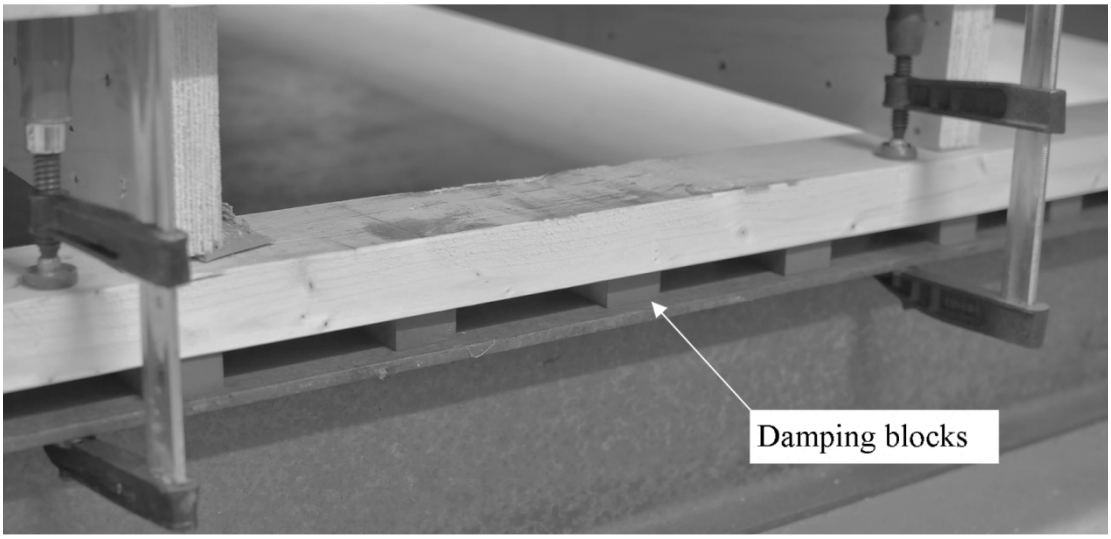

Figure 2.9 Simply supported boundary conditions with Sylomer® damping blocks for experiment 2.

2.2.3.4 Measurements

The impact hammer is used to excite every point on the measurement grid from 1-25. For each impact the response is measured with the accelerometers at point 6 and 17. Each measurement point is excited with the hammer 7 times so that the data can be averaged - this is simply done to get more reliable results.

The measurements are observed in real-time on the PC with the software TAMARA 0.218 so that double strikes and other measurement faults can be discovered and avoided. This is basically done by two means:

- The time-domain data for the impulse is observed after each strike, if more than one impulse peaks are present this is an indication that a double strike was performed. If a double strike is noticed the data can be erased before continuing.
- The frequency-domain data for the FRF is observed after each strike and the general quality of the FRF is controlled. Moreover the coherence between each of the 7 strike for each measurement point is checked. If any disturbance is present, such as trucks driving by on the concrete slab this will create noise in the

measurement that is not related to the strike – this will be noticeable as bad coherence. If the quality of the measurement for each strike is considered as insufficient the data can be erased before continuing.

When exciting at point 6 and 17 where accelerometers are placed it is very difficult to excite one of the accelerometers enough while not exciting the other too much. A work-around is used to avoid this problem by simply measuring the response of each accelerometer individually. It is thus needed to make two measurements at each of these points – one for each accelerometer. The data is then merged.

The data obtained for all 25 measurement points is processed with a MATLAB script created by the authors of this report. Furthermore, by using the IDENT function in the System Identification Toolbox the data is curve-fit and all necessary modal parameters are extracted.

2.2.4 **Experiment 3**

This experiment is a complement to experiment 1 and 2, and envisages to distinguish the global bending modes from any local panel modes. When exciting the simply supported structure global bending modes will be present as well as local panel modes, as the mode-shapes can be difficult distinguish by graphical means it is helpful to be able to exclude the eigenmodes that are local by other means. This can be done by assessing the eigenfrequencies for those local panel modes that can be expected.

2.2.4.1 Measurement points (local panel modes)

In order to capture local panel modes of the test specimen 6 panels were assessed. Due to symmetry it is sufficient to assess 6 out of 12 panel modes.

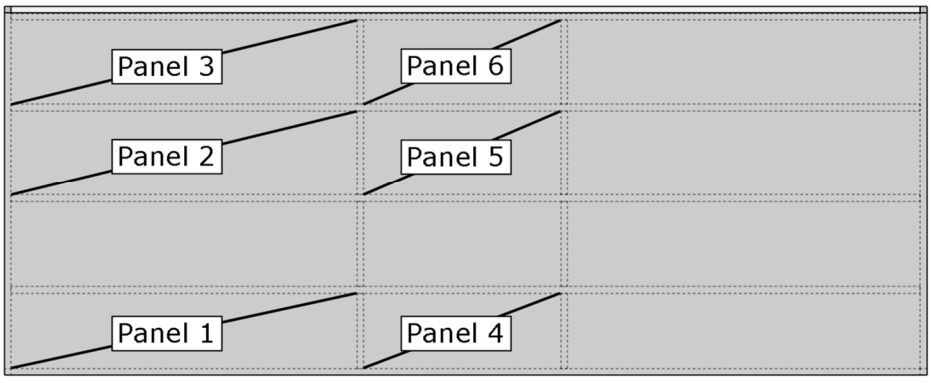

Figure 2.10 Position of panel modes tested.

As only the eigenfrequencies of the panel modes are of interest it is sufficient to obtain one FRF for each panel. For each panel the accelerometer is put in the absolute centre and the impact point is chosen as the quarter point on the diagonal of the panel.

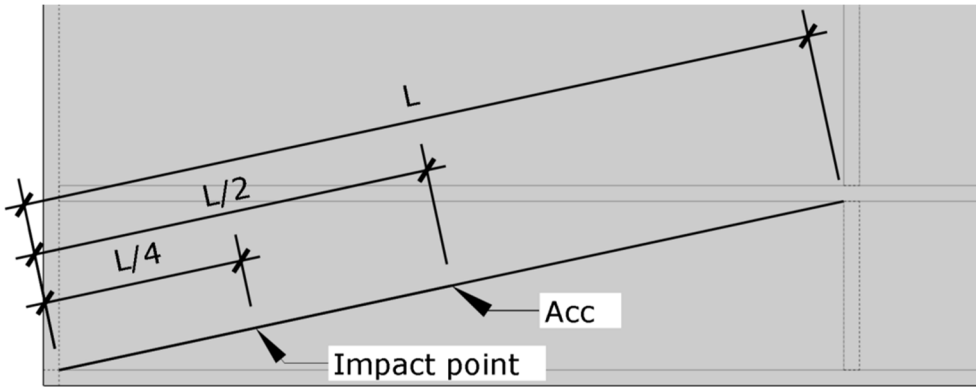

Figure 2.11 Set-up of accelerometer and impact point for panel 1.

Each panel is assessed individually and the accelerometer is moved to the next panel.

2.2.4.2 Boundary conditions

In order to make sure it is not possible to excite any global bending modes the test specimen is put directly on the floor. This will simulate continuous support on a flexible ground, and make it very unlikely to excite any global bending modes.

Figure 2.12 Continuous support boundary condition for experiment 3.

2.2.4.3 Measurements

The impact hammer is used the impact point on each panel 1-6. For each impact the acceleration is measured in the centre of respective panel. Each impact point is excited with the hammer 5 times so that the data can be averaged - this is simply done to get more reliable results.

The measurements are observed in real-time on the PC with the software TAMARA 0.218 so that double strikes and other measurement faults can be discovered and avoided – as explained in 2.2.3.4.

The data obtained from all 6 panels is processed with a MATLAB script created by the authors of this report. Furthermore, by using the IDENT function in the System Identification Toolbox the data is curve-fit and all necessary modal parameters are extracted.

As only one FRF is obtained for each panel no mode-shapes can be distinguished, however, the eigenfrequencies and respective damping ratios can be extracted.

2.3 Results

The extracted modal parameters for experiment 1 and experiment 2 are presented in Table 2.2, and for test 3 inTable 2.3. The mode-shapes for experiment 1 and experiment 2 are presented in chapter 3.3.2-2.3.4. The presentation of result has been limited to the first five modes as these are close to the range 0-40 Hz.

2.3.1 Modal parameters

Table 2.2 Modal parameters from experiment 1 and 2.

	Experiment 1				Experiment 2	
	Specimen A		Specimen B		Specimen A	
Mode	f [Hz]	ζ [%]	f [Hz]	ζ [%]	f [Hz]	ζ [%]
1	16.17	0.79	16.32	0.84	14.42	1.34
2	18.26	0.78	17.60	0.82	15.86	1.41
3	33.03	1.06	31.08	1.11	31.73	1.19
4	41.15	3.51	43.37	3.61	32.50	2.71
5	47.11	1.23	46.28	1.38	37.22	2.62

Table 2.3 Eigenfrequencies [Hz] from experiment 3.

	Experiment 3					
Mode	Panel 1	Panel 2	Panel 3	Panel 4	Panel 5	Panel 6
1	110.76	99.72	97.31	123.08	94.92	108.35

2.3.2 Mode-shapes experiment 1 – specimen A

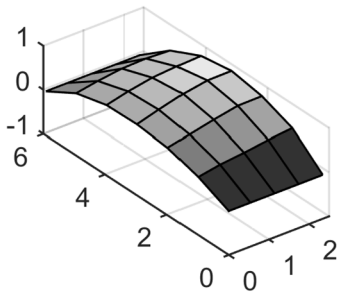

Mode 1 - 16.17 Hz

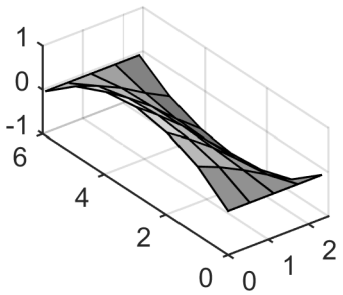

Mode 2 - 18.26 Hz

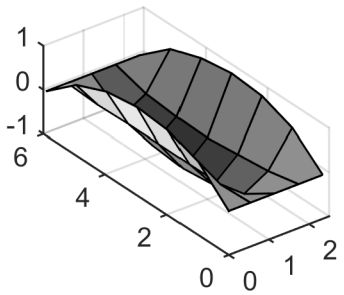

Mode 3 - 33.03 Hz

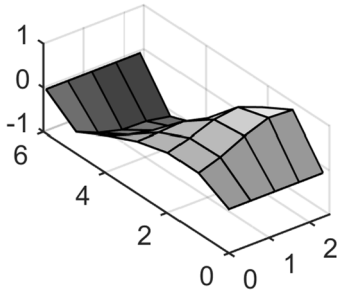

Mode 4 – 41.15 Hz

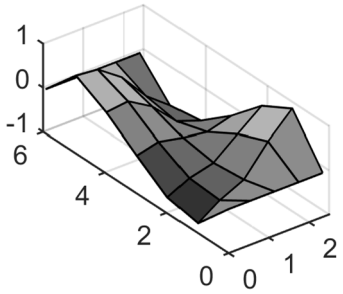

Mode 5 – 47.11 Hz

2.3.3 **Mode-shapes experiment 1 – specimen B**

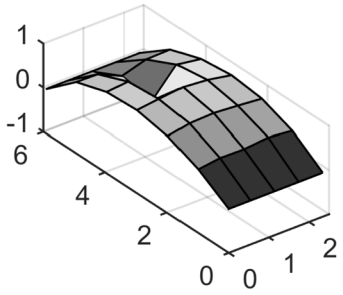

Mode 1- 16.32 Hz

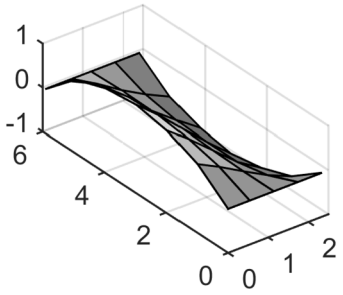

Mode 2 – 17.60 Hz

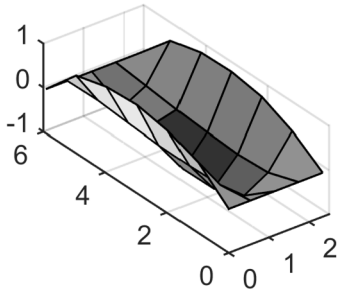

Mode 3 –31.08 Hz

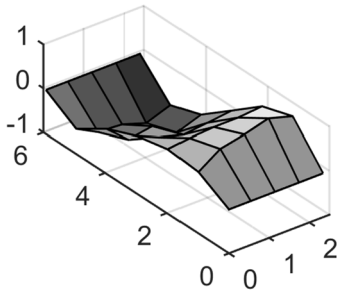

Mode 4 –43.37 Hz

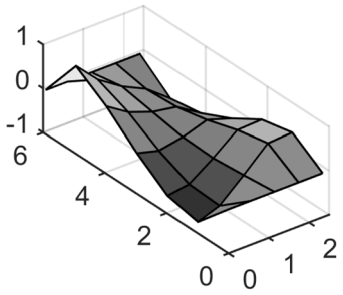

Mode 5 –46.28 Hz

2.3.4 **Mode-shapes experiment 2 – specimen A**

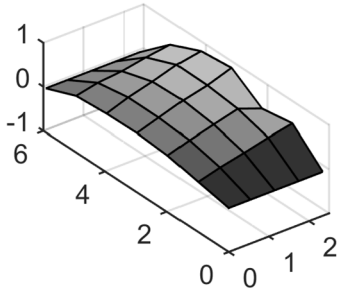

Mode 1 –14.42 Hz

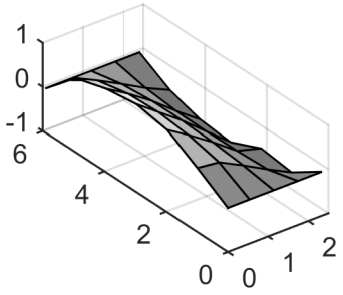

Mode 2 –15.86 Hz

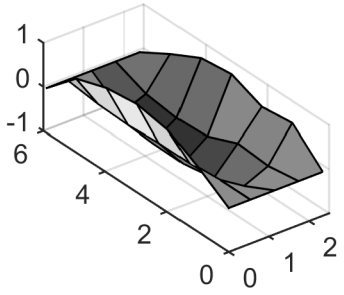

Mode 3 –31.73 Hz

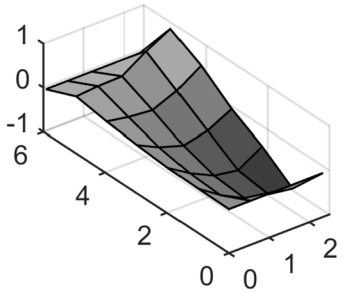

Mode 4 –32.50 Hz

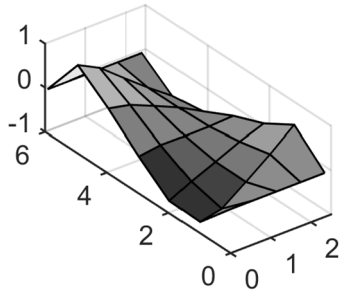

Mode 5 –37.22 Hz

2.4 Conclusions

The eigenfrequencies from the panels are present first at approximately 100 Hz, this rules out any panel modes in the range of interest, 0-40 Hz.

The first five mode-shapes from experiment 1 as presented in Chapter 2.3.2 and Chapter 0 are coherent with the modes expected prior to the experiment. Furthermore, the mode-shapes are fundamentally identical for specimen A and B. This shows that experiment 1 was successful for both specimens.

Experiment 2 exhibit similar mode-shapes as experiment 1 with the exception of mode 4 that is inverted and more asymmetric. However, in principle it is the second bending mode for a simply-supported beam which was expected. This shows that experiment 2 was successful.

The eigenfrequencies for all five modes was expected to be higher than measured – this indicates that the specimen might be less stiff than expected. The results from specimen A and B in experiment 1 are not exactly identical. This is probably due to variation in the material and manufacturing of the both specimen. Furthermore, it is very probable that the actual measurements were not performed with identical precision.

Experiment 2 exhibits considerably more damping for mode 1 and 2, this was expected and is also the main reason for using damping blocks at supports. However, it was not expected that the eigenfrequency would decrease for mode 1 to 5. This effect could be explained by the decreased stiffness at the supports due to the introduction of damping blocks. The boundary conditions introduced in this experiment were very simple and might not reflect the reality in-situ as wished. In-situ the pressure on the boundary conditions might be higher and this could change the behaviour of the damping material.

3 Static test

The purpose of the experiment is to determine the maximum deflection of both test specimens when subject to a 1 kN point load at mid-span.

3.1 Method

In order to perform the experiment the following equipment was used:

	Type	Product	Quantity
1	Deflection measuring gauge	Mako 0.001 mm	1
2	Hydraulic stand	-	1
3	Lead weight	40 kg	2
4	Concrete cube	100x100x100 mm^2	1

Furthermore, an overhead crane with straps was used to lower the weights.

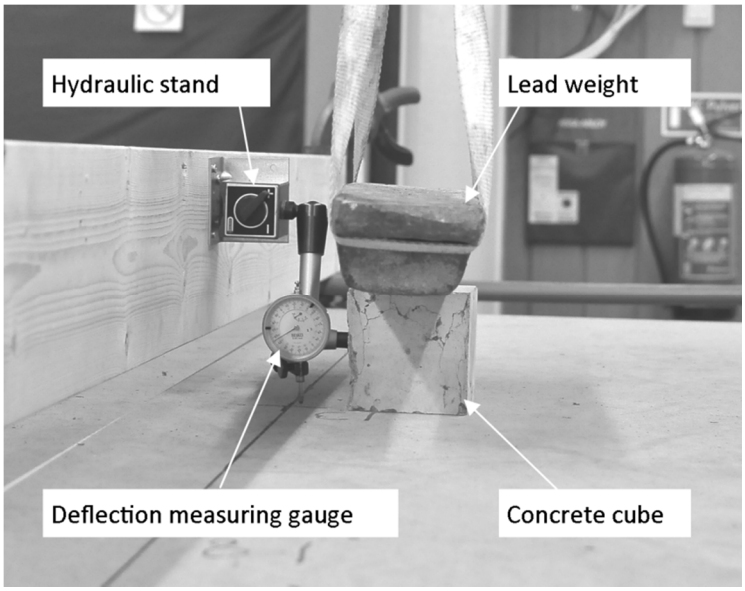

Figure 3.1 Set-up of static experiment.

The static deflection is measured at two positions for each specimen according to Figure 3.2.

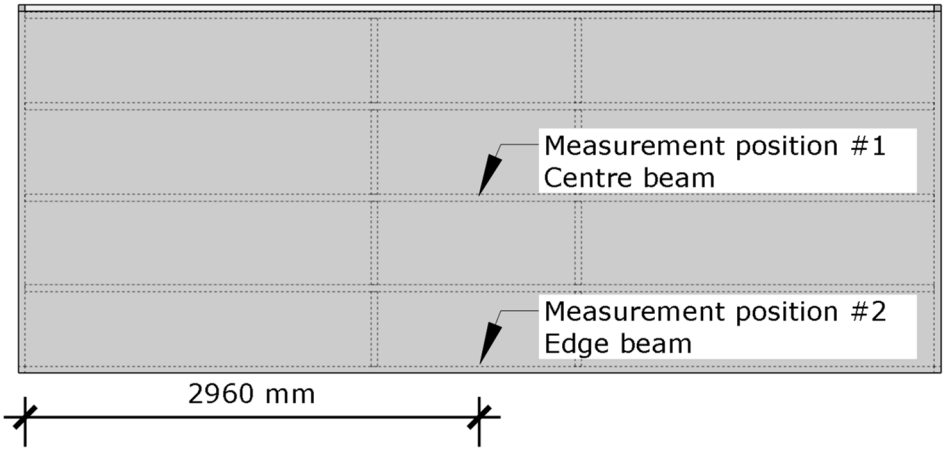

Figure 3.2 Measuring positions for static deflection.

The boundary conditions are simply supported with an effective span of 5920 mm.

The concrete block and the deflection measuring gauge are placed as close as possible at each respective measurement position. The concrete block is then loaded with one lead weight while the deflection is recorded. This is performed twice to check the coherence. The concrete block is then loaded with both lead weights and the deflection is recorded. This is also performed twice to check the coherence.

The results are then extrapolated to obtain the deflection at 1 kN load – assuming that the system is linear.

3.2 Results

Table 3.1 Deflection at measurements position 1 - centre beam.

	Deflection [mm]	
Load [kN]	Specimen A	Specimen B
1.000	0.49[3]	0.48[1]
0.850	0.42	0.41
0.423	0.15	0.16

Table 3.2 Deflection at measurement position 2 - edge beam.

	Deflection [mm]	
Load [kN]	Specimen A	Specimen B
1.000	1.25[1]	1.07[1]
0.850	1.06	0.91
0.423	0.51	0.41

[1] Extrapolated value based on 0.85 kN point load.

Appendix B – numerical modelling

The objects were modelled in Abaqus/CAE and the analysis performed was an Abaqus/Standard analysis. For the calculation of the eigenfrequencies linear perturbation was chosen. For stress and deflection calculations static analysis was used.

The elements of the models were chosen to be shell elements with elastic properties. These are plane stress elements, meaning that the stress normal to the plane in which the element is drawn is zero. The Lamina-function in Abaqus allows the orthotropic properties of wood to be modelled in an easy way. Young´s moduli parallel and transversal to the grains are defined as E1 or E2, depending on the orientation of the element. Poisson´s ratio, ν12, and the panel shear modulus, G12, correspond to the transverse contraction and shear rigidity in the plane of the shell element. The other shear moduli, G13 and G23, need to be defined for the calculation of shear deformation out of the plane of the shell element.

Abaqus defines the plane of the shell element as the local 1-2 plane. The default material orientation is defined by the global coordinate system. Local 1- and 2-direction correspond to global x- and y-direction. If the shell is placed so that just one of these global directions correspond to one local, the other direction, global z-direction, is given the remaining property. For example, if the shell element is placed in the global y-z-plane, local 2-direction corresponds to global y-direction. Since the global x-direction is perpendicular to the plane of the shell and cannot be given any properties, the 1-direction properties is given to the global z-direction.

The connections were modelled with full interaction, both between top plate and beams as well as between beams and blockings.

1 Modelling of the test specimen

The purpose of modelling the test object in an FE-software was to see how well the numerical calculations correspond to reality and to learn how to adjust the model so it corresponds better. A secondary purpose was to compare the analytical and numerical solutions.

1.1 Geometry of the specimen

The modelled geometry corresponds to the actual geometry of the test object, see Figure 2.1 in Appendix A.

1.2 Materials

Table 1.1 Stiffness properties used for the materials of the test specimen.

Material[1]	Properties	E/E1 [GPa]	E2 [GPa]	ν/ ν12	G12 [GPa]	G13 [GPa]	G23 [GPa]
Particleboard (P5)	Isotropic	1.8[2]		0.35[2]			
LVL (Kerto S) in **x**-z plane	Orthotropic/ Lamina	13.8	0.43	0.02	0.6	0.15	0.05
Structural timber (C24) in **y**-z plane	Orthotropic/ Lamina	0.37	11.0	0.03	0.3	0.03	0.69

Table 1.2 Mean values of the density for the materials of the test specimen.

Class	Density
P5	632.5 kg/m^3
KertoS	510 kg/m^3
C24	420 kg/m^3

The stiffness value for the chipboard, 1.8 GPa, is valid for the chipboard in tension and compression, according to the manufacturer. For bending, a higher value could be used. The chipboard in this experiment is in the compressive zone in the cross-section and the lower modes of the dynamic response also cause either compression or tension in the chipboard, not bending. Thus the lower values are used. For local action, like local deflection or dynamic response of the top plate the higher value could be used instead.

For Poisson´s ratio a value of 0.35 is used since this is recommended by scientists[2].

1.3 Boundary conditions

Boundary conditions were inserted at the bottom end node of each beam, representing the actual boundary condition with the beam screwed to a stud. At one side of the span displacement was prevented in all three directions. At the other side of the span

[1] The main grain direction is in bold type.
[2] Mail correspondence with Kirsi Jarnerö, scientist at SP Technical Research Institute of Sweden, 2015-04-17

displacement was prevented in y- and z-directions. If movement also had been prevented in x-direction the longitudinal modes would have been positively affected since this would make the connection semi-rigid.

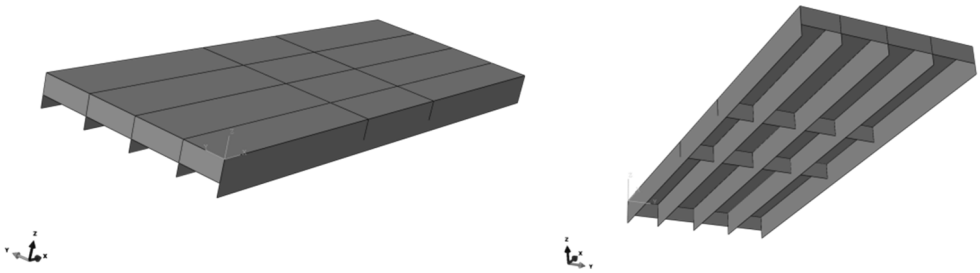

Figure 1.1 Views of the geometry of the FE-model.

1.4 Mesh and convergence study

The mesh elements were chosen to be dominated by quadrilateral elements, S4R. Five integration points were used over the thickness of each element.

A convergence study was performed to make sure that the element size would be small enough. The study was carried out in the following way:

1. A static analysis for the deflection under self-weight was performed. The element side was chosen relatively large.
2. The maximum deflection was noted.
3. A new analysis with the element side reduced to half was performed.
4. The maximum deflection was noted and compared to the previous one.

The process was repeated until the results converged.

1.5 Modification of FE-model

When the FE-model was compared to the experimental values it was noted a significant difference in eigenfrequency for the transversal modes. Probably because the connection between the blockings and the beams was modelled with full interaction. In reality this is hardly achieved. To make the modes correspond better to the experimental values two modifications of the FE-model were tested independently; the elastic modulus of the blockings in the model was reduced from 11.0 GPa to 1.65 GPa and spring elements with a stiffness of 10 MN/m were inserted between the blockings and the webs each 57 mm (see Figure 1.2)

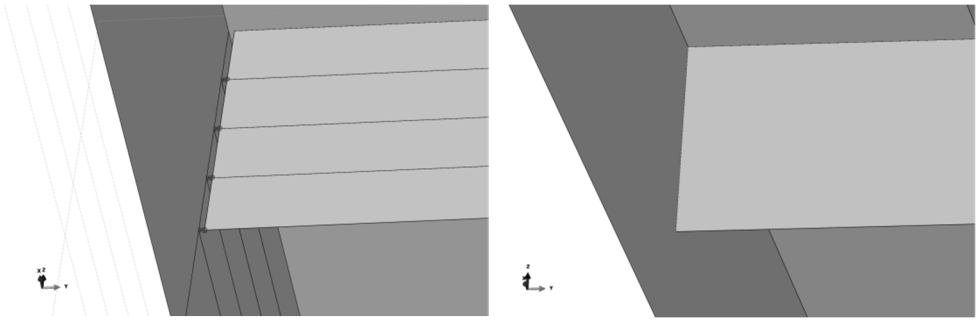

Figure 1.2 The connection between blocking and edge beam. To the left with spring elements and to the right with full composite action.

2 Modelling of the promising concept fat-beam

The promising concept fat-beam was modelled to see how shear deformations and holes in the web would affect the first eigenfrequency and how effectively the strongback would increase the transversal stiffness. A control of the deflection due to a 1 kN point load was made for comparison between analytical and numerical calculations.

The basis for the system would be floor elements with a span of 5.92 metres and a width of 2.4 metres. These elements would be possible to pre-fabricate and connect to each other at the building site, to increase the width.

2.1 Geometrical properties

The modelled geometry corresponds to the geometry of the test specimen described in Appendix 1. The element type used was shell elements. The material properties in Table 1.1 were used. The connections were modelled with full interaction and the boundary conditions inserted in a similar way as for the modelling of the test object, although the beams are wider giving some more nodes at each beam where translations are prevented.

The top plate right above each beam was given composite properties so that the timber stud and the plywood sheet could be inserted into the same element. The model was given a non-structural mass of 50 kg/m^2 of the top plate, to account for the gypsum boards needed for acoustic and fire safety reasons. The strongbacks would be connected to the top plate through screwing and gluing through the C14-stud. This is mirrored in the model by giving the strongback a 45 mm extension upwards, 220 mm wide, at the place where it crosses the beam (Figure 2.1). In this way it is connected to the top plate at the same place as the real connection is.

Figure 2.1 The part strongback for one floor element created for the FE-model.

In addition to the fat beam version of the Landvetter case study (H), another version (E) was modelled in three different ways, according to Table 2.1 and Table 2.2. Version E1 with one strongback at mid-span, versions E2 and E3 with three strongbacks each. The strongbacks have a distance of 1200 mm between each other. Versions three and four are simply supported along all four edges since they are meant to simulate the behaviour of a whole floor.

The point load for the deflection check was placed between two of the strongbacks, right above one of the middle beams. For version one, with only one strongback, the load is placed 0.75 metres away from the strongback. The point load was also placed at mid-span to check which case gave the largest deflection.

Table 2.1 Cross-section properties of the modelled fat-beam versions.

	Total construction height	Compression flange	Web	Tension flange
E	382 mm	Plywood (P30) $t_{top\ plate}$ = *24* mm	OSB/3 t_{web} = *9* mm h_{web} = *358* mm	Structural timber (C35) h_{C35} = *70* mm
F	382 mm	Plywood (P30) $t_{top\ plate}$ = *24* mm	OSB/3 t_{web} = *15* mm h_{web} = *358* mm	Structural timber (C35) h_{C35} = *70* mm
G	382 mm	Plywood (P30) $t_{top\ plate}$ = *24* mm	OSB/3 + steel t_{web} = *9+2* mm h_{web} = *358* mm	Structural timber (C35) h_{C35} = *70* mm
H	750 mm	Plywood (P30) $t_{top\ plate}$ = *48* mm	OSB/3 t_{web} = *12* mm h_{web} = *702* mm	Structural timber (C35) h_{C35} = *90* mm

Table 2.2 Geometry of the modelled fat beam concepts.

	Span x width	Boundary conditions	Number of strongbacks	Size of strongback
E1/F/G	5.92 x 2.4 m^2	Two simply supported, two free	1	220 x 45 mm^2
E2	5.92 x 2.4 m^2	Two simply supported, two free	3	220 x 45 mm^2
E3	5.92 x 7.2 m^2	Simply supported along all four edges	3	220 x 45 mm^2
H	9.6 x 16.2 m^2	Simply supported along all four edges	5	500 x 70 mm^2

2.2 Materials

Table 2.3 Stiffness properties used for the materials of the fat-beam.

Material[1]	Properties	E/E1 [GPa]	E2 [GPa]	ν/ ν12	G12 [GPa]	G13 [GPa]	G23 [GPa]
Steel (S275)	Isotropic	210		0.3			
Strucutral timber (C14) in **x**-y plane	Orthotropic/ Lamina	7.0	0.23	0.03	0.25	0.44	0.025
Structural timber (C35) in **x**-y plane	Orthotropic/ Lamina	13.0	0.43	0.03	0.4	0.81	0.04
Structural timber (C35) in **y**-z plane	Orthotropic/ Lamina	0.43	13	0.03	0.4	0.04	0.81
Plywood (P30) in **x**-y plane	Orthotropic/ Lamina	7.4	4.6	0.5	0.5	0.5	0.15
(OSB/3) in **x**-z plane	Orthotropic/ Lamina	4.93	1.98	0.25	1.08	0.9	0.05

[1] The main grain direction is in bold type.

Table 2.4 Mean values of the density for the materials of the fat-beam.

Class	Density
Steel	7400 kg/m^3
C14	350 kg/m^3
C35	480 kg/m^3
P30	460 kg/m^3
OSB/3	550 kg/m^3

3 Results and comments

The results from the dynamic analyses were evaluated graphically. The value for the deflection was obtained from the displacement of the node at the bottom of the beams right under the point load.

3.1 Convergence study

Based on the convergence study 0.05 metres was chosen as element side size since no major changes occur when decreasing the size, see Table 3.1.

Table 3.1 Maximum displacement in z-direction.

Element side [m]	0,2	0,1	0,05	0,025	0,0125
Displacement [mm]	-1,259	-1,056	-1,065	-1,08	-1,092
Difference		-19%	1%	1%	1%

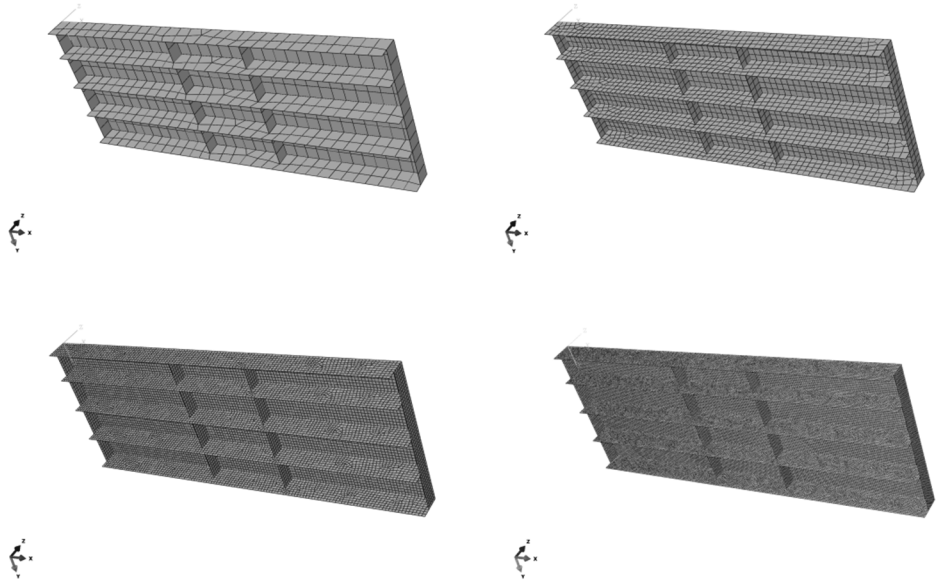

Figure 3.1 Pictures of the meshes; from top left to bottom right element side sizes 0.2, 0.1, 0.05 and 0.025.

3.2 Eigenfrequencies for the test specimen

From the FE-model the following eigenfrequencies were obtained corresponding to the eigenfrequencies of the test specimens, see Figure 3.2.

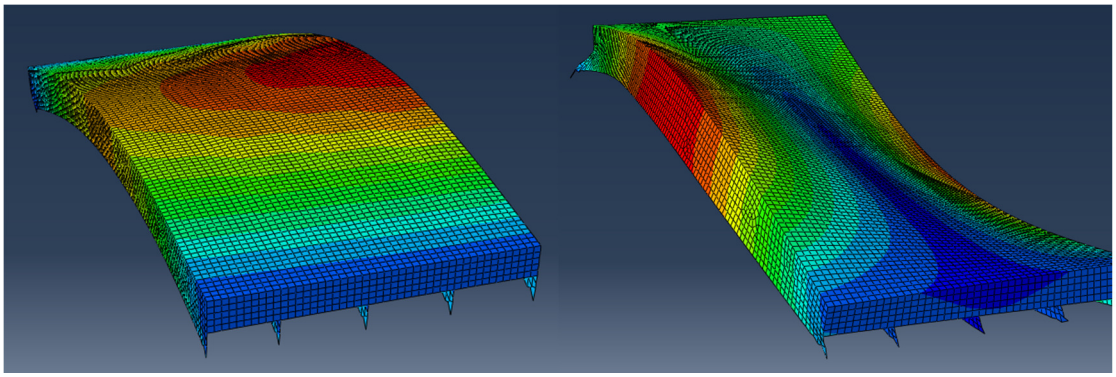

Mode 1 – 17.1 Hz

Mode 2 – 18.5 Hz

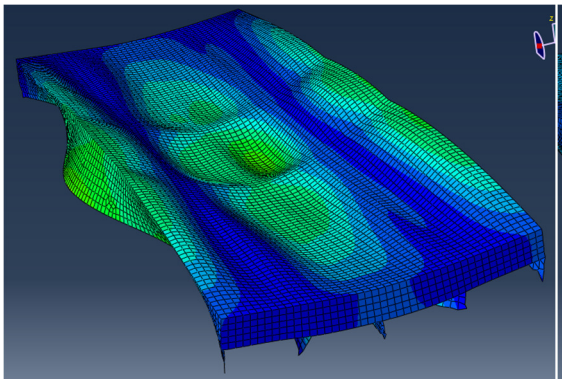

Mode 3 – 57.9 Hz

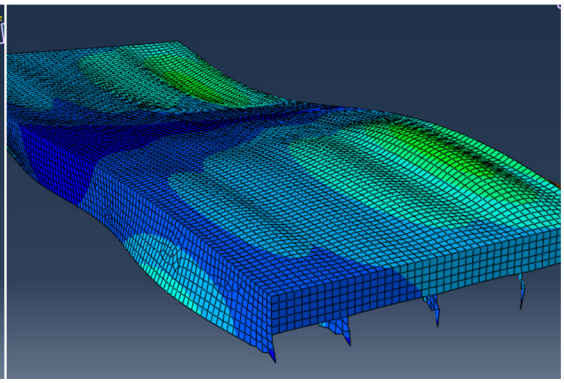

Mode 4 – 50.3 Hz

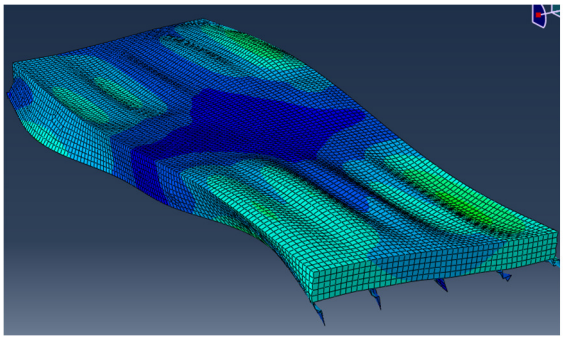

Mode 5 – 62.7 Hz

Figure 3.2 Mode shapes obtained from the numerical modelling.

For mode 1 the impact of the non-symmetry of the specimen can be clearly seen. The side with a lower amplitude has a lower c-c distance between the outermost beams, making it stiffer than the other side. When the stiffness of the blockings is reduced or springs are inserted in the connections the transversal modes are highly affected while the longitudinal modes remain unchanged as can be seen in Table 3.2. The deflection was also increased when the changes to the model are implemented, see Table 3.3.

Table 3.2 Comparison of eigenfrequencies between the different models.

Mode number	FE-model, full interaction	FE-model, reduced stiffness	FE-model, springs
1	17.1 Hz	17.1 Hz	17.1 Hz
2	18.5 Hz	18.5 Hz	18.5 Hz
3	57.9 Hz	37.8 Hz	32.4 Hz
4	50.3 Hz	50.1 Hz	49.5 Hz
5	62.7 Hz	62.4 Hz	61.3 Hz

Table 3.3 Comparison of deflection between the different models.

Deflection, 1kN point load	FE-model, full interaction	FE-model, reduced stiffness	FE-model, springs
Middle beam	0.43 mm	0.49 mm	0.58 mm
Edge beam	1.09 mm	1.14 mm	1.19 mm

The FE-model does calculate modes in all directions while the measurement used in the experiment only register acceleration in z-direction. A number of modes from the FE-results were therefore omitted since they show beams oscillating in the y-direction. For the same reason, that the model calculates modes in all directions, there are two closely situated modes that can come into question for being mode 3. One of them is, at 57.9 Hz, and can be seen in Figure 3.2 Mode shapes obtained from the numerical modelling.. The other one is at 46.4 Hz, and can be seen in Figure 3.3. The latter is closer, in Hz, to the one in the experiment but has much smaller relative amplitude, in z-direction, than the former one. The conclusion is that the mode on 46.4 Hz is a local mode of the beams and that the oscillations of the beams influence the rest of the structure making it look a little like mode 3.

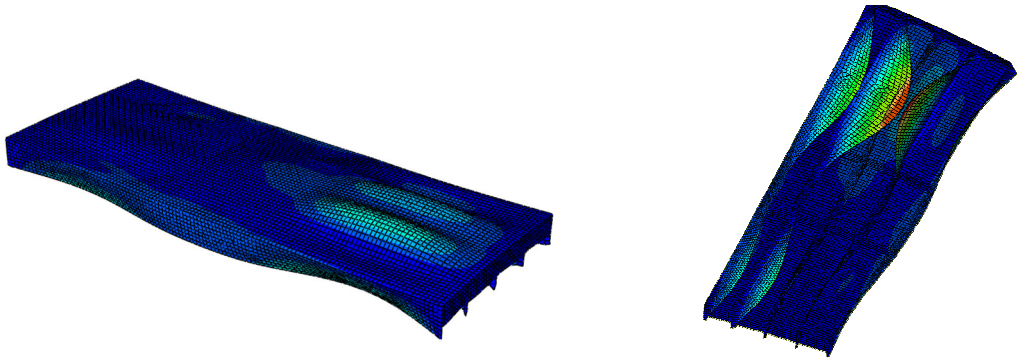

Figure 3.3 Mode shape connected to the oscillation of the beams in y-direction.

3.3 Results – Fat-beam

From the FE-analysis the following results were obtained for the promising concept fat-beam. It was concluded that the point load deflection gave the larger amplitude if placed between the strongbacks and not at mid-span.

Table 3.4 Numerical and analytical results of first eigenfrequency and deflection of fat-beam versions.

		E1	E2	E3	H
First eigen-frequency	Numerical	15.4 Hz	15.3 Hz	17.0 Hz	16.8 Hz
	Analytical	20.0 Hz	20.0 Hz	20.0 Hz	16.9 Hz
1 kN point load deflection	Numerical	0.30 mm	0.28 mm	0.19 mm	0.09 mm
	Analytical	0.74 mm	0.15 mm	0.15 mm	0.10 mm

Table 3.5 Numerical and analytical results of first eigenfrequency with changes in the properties of the web.

		E1	F	G
First eigen-frequency	Numerical	15.4 Hz	16.4 Hz	19.5 Hz
	Analytical	20.0 Hz	19.8 Hz	19.6 Hz

3.4 Discussion

The results from the modelling of the floor specimen for the experiment are thoroughly discussed in Chapter 3 of the main report. The results from the studied fat-beam versions are discussed in Chapter 6 of the main report.